



**Pacific Gas and
Electric Company**

Lawrence F. Womack
Vice President
Nuclear Services

Diablo Canyon Power Plant
P.O. Box 56
Avila Beach, CA 93424

805.545.4600
Fax: 805.545.4234

May 16, 2002

PG&E Letter DIL-02-005

U.S. Nuclear Regulatory Commission
ATTN: Document Control Desk
Washington, DC 20555-0001

Docket No. 72-26
Diablo Canyon Independent Spent Fuel Storage Installation
Submittal of Geoscience Calculation Packages

Dear Commissioners and Staff:

On December 21, 2001, Pacific Gas and Electric Company (PG&E) submitted an application to the Nuclear Regulatory Commission, in PG&E Letter DIL-01-002, requesting a site-specific license for an Independent Spent Fuel Storage Installation (ISFSI) at the Diablo Canyon Power Plant. The application included a Safety Analysis Report, Environmental Report, and other required documents in accordance with 10 CFR 72.

As requested by Mr. S. Baggett, 16 Geoscience calculations, performed in support of the Diablo Canyon ISFSI license application, are enclosed. These calculation packages are intended for use by the NRC staff in their review of the application.

If you have any questions regarding this matter, please contact Mr. Terence Grebel at (805) 595-6382.

Sincerely,

Lawrence F. Womack
Enclosure

gwh2

cc: Diablo Distribution
Ellis W. Merschoff
David L. Proulx
Girija S. Shukla
cc/enc: James R. Hall
John Stamatakis
David A. Repka

A member of the STARS (Strategic Teaming and Resource Sharing) Alliance
Callaway • Comanche Peak • Diablo Canyon • Palo Verde • South Texas Project • Wolf Creek

nmssol
public

LIST OF ATTACHED GEOSCIENCE CALCULATION PACKAGES

1. Development of Young's Modulus and Poisson's Ratios for DCPD ISFSI Based on Field Data
PGE Calculation 52.27.100.711, Revision 0
2. Development of Allowable Bearing Capacity for DCPD ISFSI Pad and CTF Stability Analyses
PGE Calculation 52.27.100.713, Revision 0
3. Methodology for Determining Sliding Resistance Along Base of DCPD ISFSI Pads
PGE Calculation 52.27.100.714, Revision 0
4. Determination of Pseudostatic Acceleration Coefficient for use in DCPD ISFSI Cutslope Stability Analyses
Calculation GEO.DCPD.01.05, Revision 2
5. Development of Coefficient of Subgrade Reaction for DCPD ISFSI Pad Stability Checks
PGE Calculation 52.27.100.717, Revision 0
6. Development of ISFSI Spectra
Calculation GEO.DCPD.01.11, Revision 1
7. Development of Fling Model for Diablo Canyon ISFSI
Calculation GEO.DCPD.01.12, Revision 1
8. Development of Spectrum Compatible Time Histories
PGE Calculation 52.27.100.723, Revision 0
9. Development of Time Histories with Fling
PGE Calculation 52.27.100.724, Revision 0
10. Development of Young's Modulus and Poisson's Ratio Values for DCPD ISFSI Based on Laboratory Data
PG&E Calculation 52.27.100.725, Revision 1
11. Development of Strength Envelopes for Non-jointed Rock at DCPD ISFSI Based on Laboratory Data
Calculation GEO.DCPD.01.16, Revision 1
12. Determination of Mean and Standard Deviation of Unconfined Compression Strengths for Hard Rock at DCPD ISFSI Based on Laboratory Tests
Calculation GEO.DCPD.01.17, Revision 2

13. Determination of Basic Friction Angle Along Rock Discontinuities at DCPD ISFSI
Based on Laboratory Tests
Calculation GEO.DCPD.01.18, Revision 2
14. Development of Strength Envelopes for Jointed Rock Mass at DCPD ISFSI Using
Hoek-Brown Equations
Calculation GEO.DCPD.01.19, Revision 1
15. Development of Strength Envelopes for Shallow Discontinuities at DCPD ISFSI
Using Barton Equations
Calculation GEO.DCPD.01.20, Revision 1
16. Development of Freefield Ground Motion Storage Cask Spectra and Time
Histories for the Used Fuel Storage Project
PGE Calculation 52.27.100.747, Revision 0

DIABLO CANYON

INDEPENDENT SPENT FUEL STORAGE INSTALLATION



CALCULATIONS



PACIFIC GAS AND ELECTRIC COMPANY

CF3.ID4
ATTACHMENT 7.2

TITLE: CALCULATION COVER SHEET

CALC No. 52.27.100.711, R0

RECORD OF REVISIONS

Rev No.	Status	Reason for Revision	Prepared By:	LBIE Screen	LBIE	Check Method*	LBIE Approval		Checked	Supervisor	Registered Engineer
		Remarks	Initials/ LAN ID/ Date	Yes/ No/ NA	Yes/ No/ NA		PSRC Mtg. No.	PSRC Mtg. Date	Initials/ LAN ID/ Date	Initials/ LAN ID/ Date	Signature/ LAN ID/ Date
0	F	Acceptance of Geosciences Calc. No. GEO.DCPP.01.01, Rev.2 Calc. is in support of 10CFR72, DCPD License Application (ISFSI Dry Cask) to the NRC prior to implementation. Note: Prepared per CF3.ID17 requirements	<i>11-7-01</i> NXJ1/ <i>11/7/01</i>	<input type="checkbox"/> Yes <input type="checkbox"/> No <input checked="" type="checkbox"/> NA	<input type="checkbox"/> Yes <input type="checkbox"/> No <input checked="" type="checkbox"/> NA	<input type="checkbox"/> A <input type="checkbox"/> B <input checked="" type="checkbox"/> C	N/A	N/A	<i>11-7-01</i> AE72 <i>11/6/01</i>	<i>11-7-01</i> LJS2 <i>11/9/01</i>	<i>11-7-01</i> LJS2 <i>11/9/01</i>
				<input type="checkbox"/> Yes <input type="checkbox"/> No <input type="checkbox"/> NA	<input type="checkbox"/> Yes <input type="checkbox"/> No <input type="checkbox"/> NA	<input type="checkbox"/> A <input type="checkbox"/> B <input type="checkbox"/> C					
				<input type="checkbox"/> Yes <input type="checkbox"/> No <input type="checkbox"/> NA	<input type="checkbox"/> Yes <input type="checkbox"/> No <input type="checkbox"/> NA	<input type="checkbox"/> A <input type="checkbox"/> B <input type="checkbox"/> C					

*Check Method: A: Detailed Check, B: Alternate Method (note added pages), C: Critical Point Check



SUBJECT Development of Young's Modulus and Poisson's Ratios for DCPD ISFSI Based on Field Data
(GEO.DCPP.01.01, Rev. 2)

MADE BY NXJ1 DATE 11/6/01 CHECKED BY AT DATE 11/6/01

Table of Contents:

Section	Type	Title	Page Numbers
1	Index	Cross-Index (For Information Only)	1 - 4
Attachments	"A"	Development of Young's Modulus and Poisson's Ratios for DCPD ISFSI Based on Field Data (GEO.DCPP.01.01 Rev. 2)	20



SUBJECT Development of Young's Modulus and Poisson's Ratios for DCPD ISFSI Based on Field Data
MADE BY NXJ1 DATE 11/6/01 CHECKED BY Aft2 DATE 11/6/01

1- Cross reference between Geo Sciences calculation Numbers and DCPD (Civil Group's) Calculation Numbers: This section is For Information Only.

Cross-Index

(For Information Only)

Item No.	Geosciences Dept. Calc. No.	Title	DCPD, Civil Calc. No.	Comments
1	GEO.DCPD.01.01	Development of Young's Modulus and Poisson's Ratios for DCPD ISFSI Based on Field Data	52.27.100.711	
2	GEO.DCPD.01.02	Determination of Probabilistically Reduced Peak Bedrock Accelerations for DCPD ISFSI Transporter Analyses	52.27.100.712	
3	GEO.DCPD.01.03	Development of Allowable Bearing Capacity for DCPD ISFSI Pad and CTF Stability Analyses	52.27.100.713	
4	GEO.DCPD.01.04	Methodology for Determining Sliding Resistance Along Base of DCPD ISFSI Pads	52.27.100.714	
5	GEO.DCPD.01.05	Determination of Pseudostatic Acceleration Coefficient for use in DCPD ISFSI Cutslope Stability Analyses	52.27.100.715	
6	GEO.DCPD.01.06	Development of Lateral Bearing Capacity for DCPD CTF Stability Analyses	52.27.100.716	
7	GEO.DCPD.01.07	Development of Coefficient of Subgrade Reaction for DCPD ISFSI Pad Stability Checks	52.27.100.717	
8	GEO.DCPD.01.08	Determination of Rock Anchor Design Parameters for DCPD ISFSI Cutslope	52.27.100.718	
9	GEO.DCPD.01.09	Determination of Applicability of Rock Elastic Stress-Strain Values to	52.27.100.719	Calculation to be replaced by letter



SUBJECT Development of Young's Modulus and Poisson's Ratios for DCPD ISFSI Based on Field Data
MADE BY NXJ1 DATE 11/6/01 CHECKED BY AFT2 DATE 11/6/01

Cross-Index

(For Information Only)

Item No.	Geosciences Dept. Calc. No.	Title	DCPD, Civil Calc. No.	Comments
		Stress-Strain Values to Calculated Strains Under DCPD ISFSI Pad		
10	GEO.DCPD.01.10	Determination of SSER 34 Long Period Spectral Values	52.27.100.720	
11	GEO.DCPD.01.11	Development of ISFSI Spectra	52.27.100.721	
12	GEO.DCPD.01.12	Development of Fling Model for Diablo Canyon ISFSI	52.27.100.722	
13	GEO.DCPD.01.13	Development of Spectrum Compatible Time Histories	52.27.100.723	
14	GEO.DCPD.01.14	Development of Time Histories with Fling	52.27.100.724	
15	GEO.DCPD.01.15	Development of Young's Modulus and Poisson's Ratio Values for DCPD ISFSI Based on Laboratory Data	52.27.100.725	
16	GEO.DCPD.01.16	Development of Strength Envelopes for Non-jointed Rock at DCPD ISFSI Based on Laboratory Data	52.27.100.726	
17	GEO.DCPD.01.17	Determination of Mean and Standard Deviation of Unconfined Compression Strengths for Hard Rock at DCPD ISFSI Based on Laboratory Tests	52.27.100.727	
18	GEO.DCPD.01.18	Determination of Basic Friction Angle Along Rock Discontinuities at DCPD ISFSI Based on Laboratory Tests	52.27.100.728	



SUBJECT Development of Young's Modulus and Poisson's Ratios for DCPD ISFSI Based on Field Data

MADE BY NXJ1 DATE 11/6/01 CHECKED BY MAF2 DATE 11/6/01

Cross-Index

(For Information Only)

Item No.	Geosciences Dept. Calc. No.	Title	DCPD, Civil Calc. No.	Comments
19	GEO.DCPD.01.19	Development of Strength Envelopes for Jointed Rock Mass at DCPD ISFSI Using Hoek-Brown Equations	52.27.100.729	
20	GEO.DCPD.01.20	Development of Strength Envelopes for Shallow Discontinuities at DCPD ISFSI Using Barton Equations	52.27.100.730	
21	GEO.DCPD.01.21	Analysis of Bedrock Stratigraphy and Geologic Structure at the DCPD ISFSI Site	52.27.100.731	
22	GEO.DCPD.01.22	Kinematic Stability Analysis for Cutslopes at DCPD ISFSI Site	52.27.100.732	
23	GEO.DCPD.01.23	Pseudostatic Wedge (SWEDGE) Analyses of DCPD ISFSI Cutslopes	52.27.100.733	
24	GEO.DCPD.01.24	Stability and Yield Acceleration Analysis of Cross-Section I-I'	52.27.100.734	
25	GEO.DCPD.01.25	Determination of Seismic Coefficient Time Histories for Potential Sliding Masses Along Cut Slope Behind ISFSI Pad	52.27.100.735	
26	GEO.DCPD.01.26	Determination of Potential Earthquake-Induced Displacements of Potential Sliding Masses on DCPD ISFSI Slope	52.27.100.736	
27	GEO.DCPD.01.27	Cold Machine Shop Retaining Wall Stability	52.27.100.737	
28	GEO.DCPD.01.28	Roadway Capacity with Transporter	52.27.100.738	



SUBJECT Development of Young's Modulus and Poisson's Ratios for DCPD ISFSI Based on Field Data
MADE BY NXJ1 DATE 11/6/01 CHECKED BY W. AFT2 DATE 11/6/01

Cross-Index

(For Information Only)

Item No.	Geosciences Dept. Calc. No.	Title	DCPD, Civil Calc. No.	Comments
29	GEO.DCPD.01.29	Determination of Seismic Coefficient Time Histories for Critical Slides on DCPD ISFSI Transport Route	52.27.100.739	
30	GEO.DCPD.01.30	Determination of Potential Earthquake-Induced Displacements of Critical Slides Along DCPD ISFSI Transport Route	52.27.100.740	
31	GEO.DCPD.01.31	Development of Strength Envelopes for Clay Beds	52.27.100.741	
32	GEO.DCPD.01.32	Verification of Computer Program SPCTLR.EXE	52.27.100.742	
33	GEO.DCPD.01.33	UTEXAS3 Computer Program Verification	52.27.100.743	
34	GEO.DCPD.01.34	Verification of Computer Code QUAD4M	52.27.100.744	
35	GEO.DCPD.01.35	Verification of Computer Program DEFORMP	52.27.100.745	
36	GEO.DCPD.01.36	Determination of Design Parameters for ISFSI Fill Slope	52.27.100.746	Calculation to be delayed – retaining wall to be shown on drawing
37	GEO.DCPD.01.37	Development of Freefield Ground Motion Storage Cask Spectra and Time Histories for the Used Fuel Storage Project	52.27.100.747	

PG&E
Geosciences Department
Departmental Calculation Procedure
Attachment 5.2

Number: GEO.001
Revision: 04
Page: 1 of 1

Title: Design Calculation Cover Sheet

PACIFIC GAS AND ELECTRIC COMPANY
GEOSCIENCES DEPARTMENT
CALCULATION DOCUMENT

Calc Number GEO.DCPP.01.01
Revision 2
Date 11/5/01
Calc Pages: ~~18~~
Verification Method: A
Verification Pages: 1

(SEE CALCULATION SHEET)
11/6/01
AT 11/6/01

TITLE: Development of Young's Modulus and Poisson's ratios for DCPD ISFSI based on field data

PREPARED BY:

Joseph Sun

DATE Nov. 5 '01

Joseph Sun

Printed Name

Geosciences

Organization

VERIFIED BY:

Robert K. White

DATE Nov. 5 '01

Robert K. White

Printed Name

Geosciences

Organization

APPROVED BY:

Lloyd S. Cluff

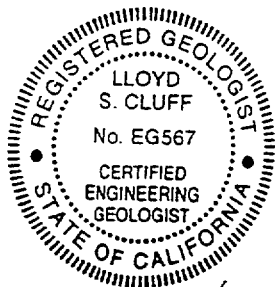
DATE Nov. 5 '01

Lloyd S. Cluff

Printed Name

Geosciences

Organization



Expires 12/31/02

**Development of Young's Modulus and Poisson's ratio for DCPD ISFSI based on
field data**

Calc Number GEO.DCDD.01.01

Record of Revisions

Rev. No.	Reason for Revision	Revision Date
1	Revised and added assumptions; revised and added inputs, references; revised conclusions to include reference to GEO.DCDD.01.15	10/15/01
2	Revised inputs and references; revised model depth referenced from 60 feet to 85 feet	11/5/01

DCPP ISFSI GEOTECHNICAL CALCULATION PACKAGE

Title: Development of Young's Modulus and Poisson's ratio for DCP
ISFSI based on field data

Calc Number: GEO.DCPP.01.01

Date: November 12, 2001

Revision: 2

Author: Joseph I. Sun

Verifier: Robert K. White

Purpose: As required by Geosciences Work Plan GEO 2001-03, Appendix A, determine values of Young's Modulus and Poisson's ratios for rock underlying the proposed DCP ISFSI pads from field measurements of rock elastic strains in borings. Values will be used by PG&E consultants in finite element analyses of pad response to earthquake loads.

- Assumptions:**
1. Bottom of mat excavation is estimated to be El. 302 ft (Klimczak, 10/5/01).
 2. Sandstone, dolomite and altered sandstone are expected to be encountered at bottom of excavation. This is based on Geosciences Calculation GEO.DCPP.01.21, Figure 21-41.
 3. In boring BA98-2, between depth interval of 13 to 15 feet, the boring log indicates the material to be altered (friable) sandstone (page 9, attached). However, because of core loss and higher shear wave velocities measured in this interval, the material in this depth interval is assumed to be unaltered and is not included in the calculation of Young's modulus for altered sandstone. This assumption is conservative because it minimizes the value of Young's modulus calculated for the altered sandstone.
 4. Wave velocity measurements made in BA98-3 correspond to the drill logs for BA98-2. This is a reasonable assumption because BA98-2 and BA98-3 were drilled next to each other.

- Input:**
1. GeoVision P-S suspension logging data of BA98-1, BA98-3 and BA98-4. (Tables 1 and 2, pp. 5 and 6, attached) from Witter, 11/5/01 (Data Report C).
 2. Boring log for BA98-2 that encountered altered sandstone between depth intervals of 5 feet to 15 feet (page 9, attached) from Witter, 11/5/01 (Data Report B).
 3. Unit weight of rock of 140 lb/ft³ used in the calculation was based on laboratory measurement of core samples as documented in Witter,

11/5/01 (Data Report I).

4. Finite element depth of 85 feet from Jahangir (6/5/01).

Methodology: Small-strain seismic velocity based Young's moduli and Poisson ratios were calculated using borehole suspension P-S logging data from borings BA98-3 (El. 322.8) and BA98-1/4 (El. 372.2' and 374.8') as listed in Tables 1 and 2 on pages 5 and 6 of this calculation package.

In the calculations, a unit weight of 140 pcf is used. The formulæ used in the calculations are based on page 140 and 141 of "Principles of Engineering Geology" by Robert B. Johnson and Jerome V. De Graff, 1988 (pages 10 and 11, attached), as follows:

Young's modulus: $k * \rho * V_s^2 * (3 * V_p^2 - 4 * V_s^2) / (V_p^2 - V_s^2)$
 Poisson's ratio: $(V_p^2 - 2 * V_s^2) / [2 * (V_p^2 - V_s^2)]$

in which ρ is the mass density, in our case, we used $140 / 62.4 \text{ g/cm}^3$. k is a unit dependent constant and is equal to 1000.6 when we use m/sec and g/cm^3 for velocities and mass density, respectively. V_s and V_p are shear and compression wave velocities from the suspension data.

Software: Only standard Excel mathematical and data plotting functions are used for this calculation.

Calculation: In the structural finite element analyses model, material at the base of the mat and to a depth of 85 feet (Elevs. 302 and El. 217, respectively) will be modeled as linear elastic material using the proposed Young modulus and Poisson's ratio, as indicated on page 16, attached. Based on the above understanding, Young's moduli and Poisson's ratios between the interval of El. 302 and El. 217 were calculated, plotted, and evaluated (Figures 1 and 2, pp. 7 and 8, attached). Within this interval, the Young's moduli varied between 0.4 to 3.5 ($\times 10^6$ psi) and does not show systematic dependency on depth. The majority of the data points fall between 0.8 to 2.0×10^6 psi (16th and 84th percentile) with a mean value of 1.33×10^6 psi. The mean value was calculated based on the average of individual measurements made in Borings BA98-3 and BA98-1/4 between El. 302 and 217. Similarly, the Poisson's ratio ranged between 0.17 to 0.45 with an average of 0.37. Within this depth interval, no altered sandstone was encountered in either of the borings.

Altered sandstone was encountered near the ground surface of boring BA98-2 (page 9 attached), adjacent to BA98-3. At the location of the boring, the altered sandstone strata are above El. 302 and thus will be removed as part of the pad excavation. However, a down dip projection of this stratum would indicate that this altered sandstone may exist

beneath the ISFSI pad. If the seismic wave velocity measurements for the near surface material in BA98-3 are indicative of the projected altered sandstone material exposed at the pad excavation, the Young modulus for the altered sandstone will likely range between 0.13 to 0.23 ($\times 10^6$ psi) with an estimated mean of 0.20×10^6 psi. Young's modulus for altered sandstone were calculated based on average shear wave and p-wave velocities measured in BA98-3. The Poisson's ratios ranged between 0.19 and 0.41 with an average value of 0.31.

Conclusions: On the above basis, the following conclusions are made:

- 1) Altered sandstone and dolomite both are expected to be present at the ISFSI pad excavation level of El. 302 ft.
- 2) The Young's moduli for the foundation material will likely range between 0.2×10^6 psi (corresponding to altered sandstone) to 2.0×10^6 psi (corresponding to upper range of dolomite). These values are by no means indicative of the absolute upper and lower bound values but rather suggest the likely range of variation.
- 3) The likely Poisson's ratios for the dolomite and altered sandstone are 0.37 and 0.31 respectively.
- 4) Both Young moduli and Poisson's ratios did not show a systematic dependency on depth.
- 5) A separate calculation, GEO.DCPP.01.15, describes elastic properties determined from core samples retrieved from borings made within the pad footprint area. For cemented sandstone and dolomite samples whose elastic properties are insensitive to in-situ stress, the lab-determined elastic properties are in good agreement with the wave velocity-based measurements developed in this calculation package. This demonstrates that the approach used in this calculation package is appropriate for the derivation of in-place elastic properties of these geo-materials. For friable sandstone samples, GEO.DCPP.01.15 concludes that the lab procedure is not appropriate for use in deriving elastic properties. On the above basis, it is recommended that values summarized from both calculations in GEO.DCPP.01.15 be reviewed by the pad designers to ensure that they do not control the design.

- References:**
- 1) Johnson, R.B. and De Graff, J. V., (1988), Principles of Engineering Geology, published by John Wiley & Sons, 497 pp.
 - 2) Witter (11/5/01): letter from Rob Witter to Rob White dated 11/5/01, entitled, "Completion of Data Reports," with enclosed:
Data Report B, Borings in ISFSI Site Area, Rev. 0;
Data Report C, 1998 Geophysical Investigations at the ISFSI Site Area, Rev. 0; and
Data Report I, Rock Laboratory Test Data, Rev. 0.

GEO.DCPP.01.01 Rev. 2
Page 4 of 18

- 3) Geosciences Work Plan GEO 2001-03, Development of Engineering Properties for ISFSI and CTF Foundation Design, ISFSI Slope Analyses, and ISFSI Cut and Fill Slope Reinforcement Design for The DCPD ISFSI Site, rev. 1.
 - 4) Geosciences Calculation GEO.DCPP.01.15, Development of Young's Modulus and Poisson's ratio values for DCPD ISFSI based on laboratory data, rev. 1.
 - 5) Geosciences Calculation GEO.DCPP.01.21, Analysis of Bedrock Stratigraphy and Geologic Structure at the DCPD ISFSI Site, rev. 0.
 - 6) Klimczak (10/5/01): letter from Richard Klimczak to William Page/Robert White, entitled "Transmittal of Requested Drawings and Re-Transmittal of Items Not Attached to 9/26/01 Letter," dated 10/5/01.
 - 7) Jahangir (6/5/01): letter from Nozar Jahangir to Rob White, entitled "PG&E Geosciences Work Plan GEO 2001-01, Transmittal of Reference Material," dated 6/5/01.
- Attachments:
- 1) Table 1, Young's Modulus and Poisson's Ratio for Boring BA98-3, pg. 5.
 - 2) Table 2, Young's Modulus and Poisson's Ratio Calculation from BA98-1/4, pg. 6.
 - 3) Figure 1, Young's Moduli vs. Elevation, pg. 7.
 - 4) Figure 2, Poisson's Ratios vs. Elevation, pg. 8.
 - 5) Boring log BA98-2, Depth Interval 0 to 15 feet, from Witter, 11/5/01, Data Report B, pg. 9.
 - 6) Dynamic elastic moduli equations, from Johnson and De Graff (1988), pp. 10 and 11.
 - 7) Letter from Richard Klimczak to William Page/Robert White, entitled "Transmittal of Requested Drawings and Re-Transmittal of Items Not Attached to 9/26/01 Letter," dated 10/5/01, pp. 12 and 13.
 - 8) Letter from Nozar Jahangir to Rob White, entitled "PG&E Geosciences Work Plan GEO 2001-01, Transmittal of Reference Material," dated 6/5/01, and cover page and page 12 of referenced Enercon calculation dated 6/25/01, pp. 14 through 16.
 - 9) Letter from Rob Witter to Rob White, entitled "Completion of Data Reports," dated 11/5/01 (without attachments), pp. 17 and 18.

GEO.DC.PP.01.01 Rev. 2
Page 5 of 10

DCPP DRY CASK SITING PROJECT
BORROW AREA HILLSIDE SITE BOREHOLE 8A 98-3
VELOCITY DATA ACQUIRED 6/8/98

Bottom of Excavation / Top of Foundation Section			
301.47	9197	1.33	0.34
299.83	8661	1.26	0.38
298.19	8432	1.22	0.37
296.55	8072	1.17	0.31
294.91	8107	1.18	0.32
293.27	5994	0.87	0.39
291.63	6685	0.97	0.17
289.99	4932	0.72	0.33
288.35	4631	0.67	0.38
286.71	8024	1.16	0.35
285.07	9098	1.32	0.30
283.43	5603	0.81	0.42
281.79	4911	0.71	0.41
280.15	6457	0.94	0.40
278.51	7161	1.04	0.38
276.87	7484	1.09	0.38
275.23	8046	1.17	0.34
273.59	16479	2.39	0.26
271.95	16888	2.45	0.31
270.31	8379	1.22	0.35
268.67	13691	1.99	0.25
267.03	17926	2.60	0.27
265.39	6485	0.94	0.40
263.74	8179	1.19	0.39
262.10	9551	1.38	0.33
260.46	18591	2.70	1.00
258.82	7803	1.13	0.42
257.18	6855	0.99	0.42
255.54	6498	0.94	0.40
253.90	6826	0.99	0.40
252.26	6861	0.99	0.39
250.62	6185	0.90	0.43
248.98	5106	0.74	0.44
247.34	9777	1.42	0.39
245.70	9700	1.41	0.42
244.06	9142	1.33	0.40
242.42	7429	1.08	0.40
240.78	5866	0.85	0.41
239.14	6545	0.95	0.40
237.50	9496	1.38	0.37
235.86	8094	1.17	0.40
234.22	5962	0.86	0.44
232.58	17827	2.58	0.29
230.94	16489	2.39	0.37
229.30	13393	1.94	0.40
227.66	7630	1.11	0.41
226.02	10224	1.48	0.30
224.37	4979	0.72	0.44
222.73	5655	0.82	0.44
221.09	8266	1.20	0.35
219.45	8391	1.22	0.43
217.81	9262	1.34	0.37
AVERAGE	8806	1.28	0.382

Bottom of Foundation Model

DCPP ISFSI

BA 98-4rev2.xls Sheet1

GEO.DCPP.01.01 Rev. 2
Page 6 of 18

TABLE 2 - YOUNG'S MODULUS AND POISSON'S RATIO CALCULATION FROM BA 98-1 & BA 98-4

DCPP DRY CASK SITING PROJECT
BORROW SITE BA 98-1 & BA 98-4
VELOCITY DATA ACQUIRED 6/8/98

R1-R2 ANALYSIS						k= 1001 rho (g/cm3)= 2.2			
DEPTH (FT)	Vs (FT/S)	Vp (FT/S)	Vs(m/se)	Vp (m/s)	El.	E (Mpa)	E (Mpsi)	Poisson	
					Bottom of Excavation / Top of Foundation				
BA 98-4	72.2	3185	10415	971	3175	302.62	6130	0.89	0.45
	73.8	3547	8634	1081	2632	300.98	7339	1.06	0.40
	75.5	4934	8412	1504	2564	299.34	12568	1.82	0.24
	77.1	3977	8412	1212	2564	297.70	8946	1.30	0.36
	78.7	2635	6309	803	1923	296.06	4039	0.59	0.39
	80.4	2891	4897	881	1493	294.42	4296	0.62	0.23
	82.0	2853	8867	870	2703	292.78	4896	0.71	0.44
	83.7	2635	6190	803	1887	291.14	4024	0.58	0.39
	85.3	3170	7906	966	2410	289.50	5886	0.85	0.40
	86.9	6190	10583	1887	3226	287.86	19820	2.87	0.24
	88.6	2828	6076	862	1852	286.22	4543	0.66	0.36
	90.2	3066	7542	935	2299	284.58	5494	0.80	0.40
	91.9	3547	7456	1081	2273	282.94	7104	1.03	0.35
	93.5	3170	8306	966	2532	281.30	5930	0.86	0.41
	95.1	3454	6835	1053	2083	279.66	6610	0.96	0.33
	96.8	2224	4721	678	1439	278.02	2801	0.41	0.36
	98.4	4434	8989	1351	2740	276.37	10981	1.59	0.34
	100.1	4206	8634	1282	2632	274.73	9921	1.44	0.34
	101.7	3666	7812	1117	2381	273.09	7616	1.10	0.36
	103.4	3110	8634	948	2632	271.45	5750	0.83	0.43
	105.0	3281	8634	1000	2632	269.81	6356	0.92	0.42
	106.6	4494	9650	1370	2941	268.17	11471	1.66	0.36
	108.3	5378	11313	1639	3448	266.53	16338	2.37	0.35
	109.9	6020	12381	1835	3774	264.89	20334	2.95	0.35
	111.6	5292	10757	1613	3279	263.25	15656	2.27	0.34
	113.2	4026	8867	1227	2703	261.61	9262	1.34	0.37
	114.8	4345	9510	1325	2899	259.97	10776	1.56	0.37
	116.5	5249	10757	1600	3279	258.33	15445	2.24	0.34
	118.1	6020	10415	1835	3175	256.69	18883	2.74	0.25
	119.8	6628	12619	2020	3846	255.05	23995	3.48	0.31
	121.4	3686	9374	1124	2857	253.41	7984	1.16	0.41
	123.0	2969	7812	905	2381	251.77	5205	0.75	0.42
	124.7	3793	8634	1156	2632	250.13	8284	1.20	0.38
	126.3	3977	8634	1212	2632	248.49	9007	1.31	0.37
	128.0	3860	8002	1176	2439	246.85	8379	1.22	0.35
	129.6	3793	7906	1156	2410	245.21	8104	1.18	0.35
	131.2	4345	10253	1325	3125	243.57	10953	1.59	0.39
	132.2	4494	9650	1370	2941	242.58	11471	1.66	0.36
BA 98-1	147.6	3686	8412	1124	2564	224.56	7829	1.14	0.38
	149.3	3977	8867	1212	2703	222.92	9065	1.31	0.37
	150.9	4654	9650	1418	2941	221.28	12181	1.77	0.35
	152.6	4345	7720	1325	2353	219.64	9988	1.45	0.27
Bottom of Analytical Section					AVERAGE	9563	1.39	0.36	

Foundation Material Modeled In Pad Stability Analysis

Young's Moduli vs. Elevation

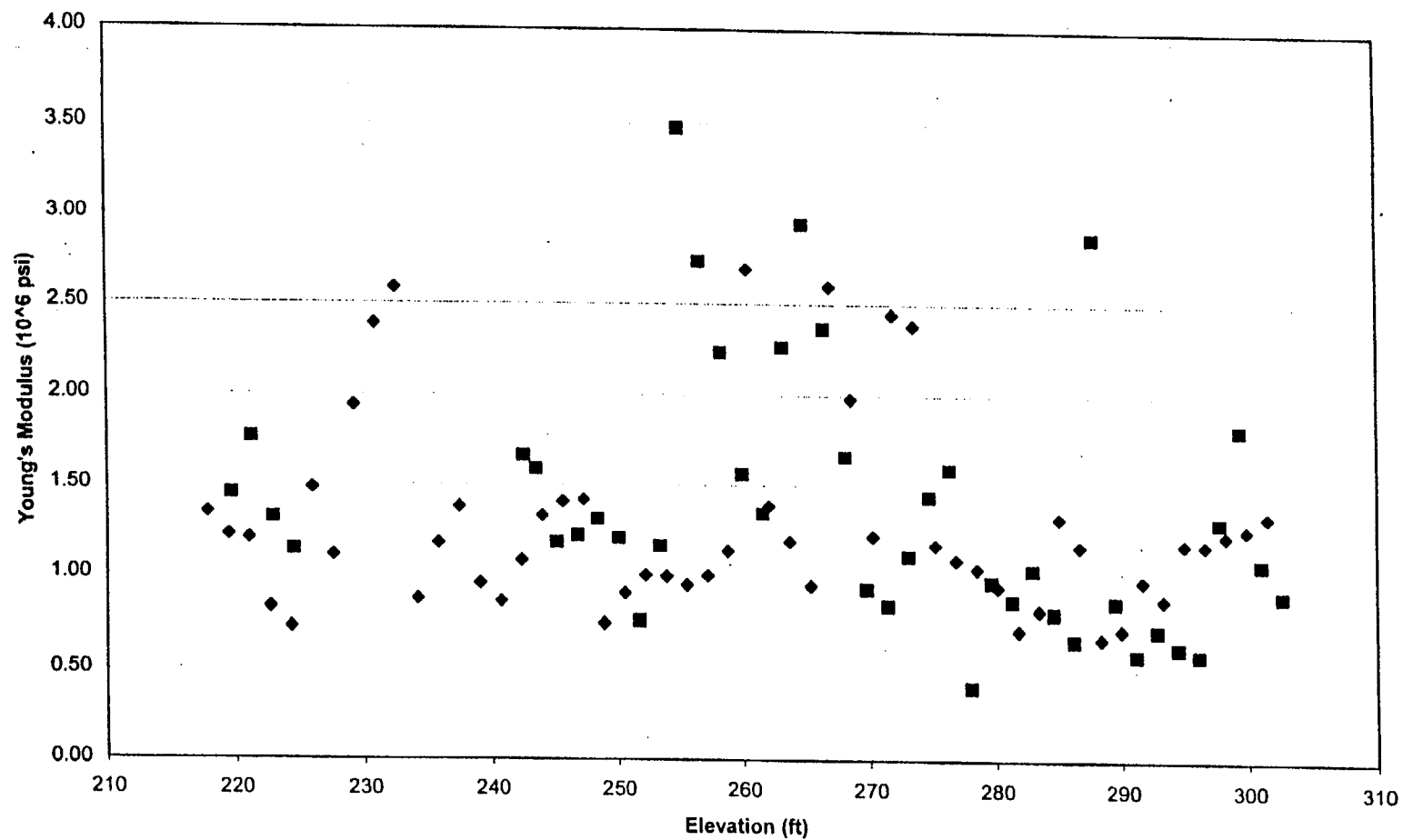


Figure 1 Variation of Young's Moduli with Elevation at ISFSI

Poisson's Ratios vs Elevation

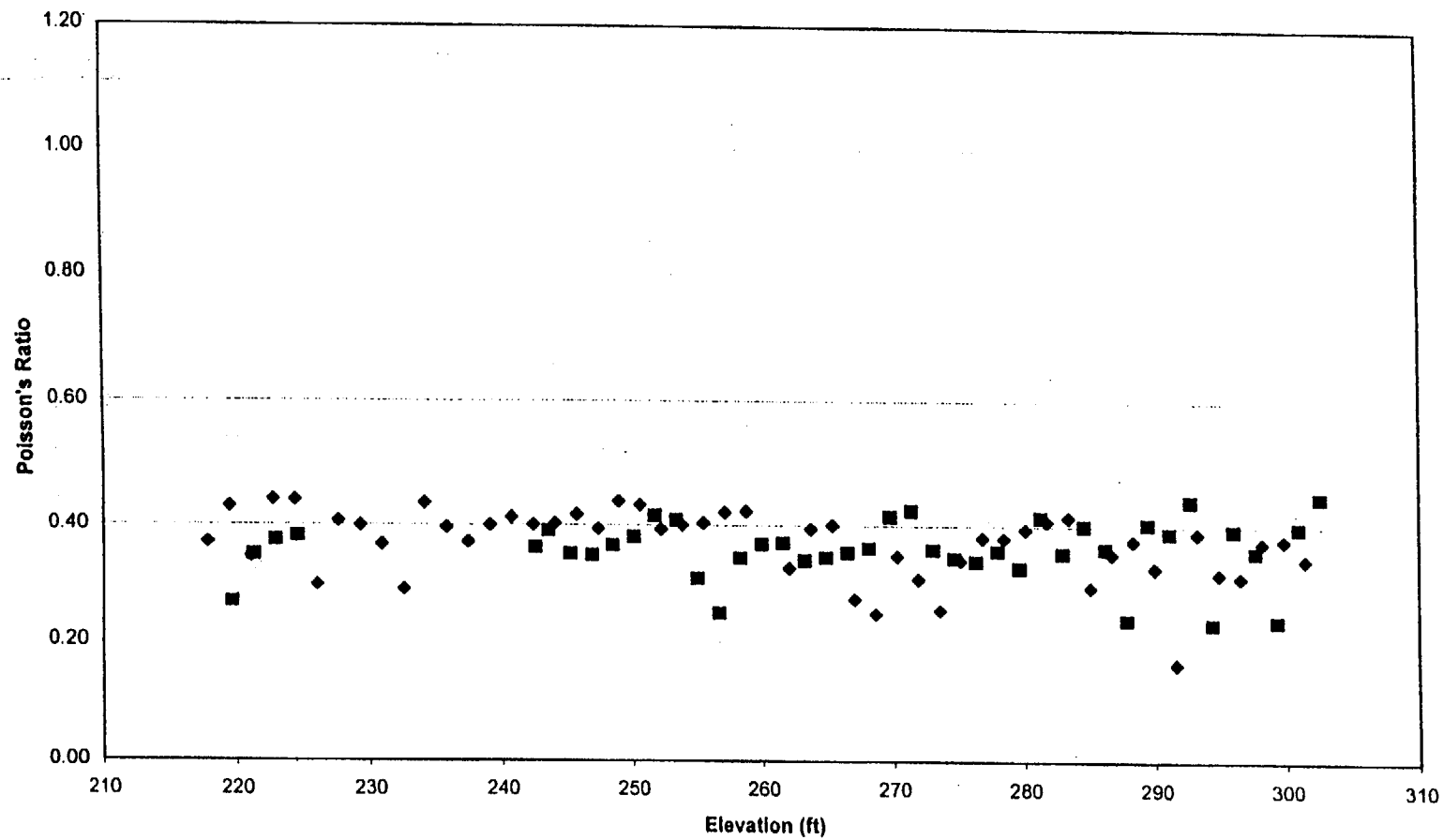


Figure 2 Variation of Poisson's Ratios with Elevation at ISFSI

Renamed 31:510 for consistency. GEDC000001.01 Rev 1993A-2/;

49 (93BA-2) 5/31 Felt like zone calls 26- 5/2/3

Σελίδα 59 από 62 ΣΑΚ-102 5/25/93

Page 1 of 12

2nd + 9.5'

Depth (feet)

Log

Drill Rate (min/ft)

Run No.

Recovery/Cut

% Recovery

RDD

Weathering

Fracture Spacing

Strength

Lithologic Description

Discontinuities

Description of Discontinuities

Remarks

0

1

2

3

4

5

6

7

8

9

10

11

12

13

14

15

16

17

18

19

20

21

22

23

24

25

26

27

28

29

30

31

32

33

34

35

36

37

38

39

40

41

42

43

44

45

46

47

48

49

50

51

52

53

54

55

56

57

58

59

60

61

62

63

64

65

66

67

68

69

70

71

72

73

74

75

76

77

78

79

80

81

82

83

84

85

86

87

88

89

90

91

92

93

94

95

96

97

98

99

100

101

102

103

104

105

106

107

108

109

110

111

112

113

114

115

116

117

118

119

120

121

122

123

124

125

126

127

128

129

130

131

132

133

134

135

136

137

138

139

140

141

142

143

144

145

146

147

148

149

150

151

152

153

154

155

156

157

158

159

160

161

162

163

164

165

166

167

168

169

170

171

172

173

174

175

176

177

178

179

180

181

182

183

184

185

186

187

188

189

190

191

192

193

194

195

196

197

198

199

200

201

202

203

204

205

206

207

208

209

210

211

212

213

214

215

216

217

218

219

220

221

222

223

224

225

226

227

228

229

230

231

232

233

234

235

236

237

238

239

240

241

242

243

244

245

246

247

248

249

250

251

252

253

254

255

256

257

258

259

260

261

262

263

264

265

266

267

268

269

270

271

272

273

274

275

276

277

278

279

280

281

282

283

284

285

286

287

288

289

290

291

292

293

294

295

296

297

298

299

300

301

302

303

304

305

306

307

308

309

310

311

312

313

314

315

316

317

318

319

320

321

322

323

324

325

326

327

328

329

330

331

332

333

334

335

336

337

338

339

340

341

342

343

344

345

346

347

348

349

350

351

352

353

354

355

356

357

358

359

360

361

362

363

364

365

366

367

368

369

370

371

372

373

374

375

376

377

378

379

380

381

382

383

384

385

386

387

388

389

390

391

392

393

394

395

396

397

398

399

400

401

402

403

404

405

406

407

408

409

410

411

412

413

414

415

416

417

418

419

420

421

422

423

424

425

426

427

428

429

430

431

432

433

434

435

436

437

438

439

440

441

442

443

444

445

446

447

448

44

page 9 of 18

Weathering: F-Fresh, SW-Slight, MW-Moderate, HW-Highly, CW-Completely, and RS-Residual soil. Fracture Spacing: VW-Very Wide (>3'), W-Wide (1'-3'), Mo-Moderate (0.5'-1'), C-Close (0.1'-0.5'), and VC-Very Close (<0.1'). Strength: AS-Extremely Strong, R3-Very Strong, R4-Strong, R3-Medium Strong, R2-Weak, R1-Very Weak, and R0-Extremely Weak. Lithologic Description: Rock type, color, texture, grain size, etc. Discontinuities: Be-Bedding, Fa-Fault, Fo-Foliation, Jo-Joint, Me-Mechanical break, Sh-Shear, and Ve-Vein. Joint descriptions: Dip, Surface shape (Pl-Planar, St-Stepped, or Wa-Wavy), Roughness (S-Smooth, SI-Slightly Rough, R-Rough, and VR-Very Rough), Aperture (F-Filled, Mo-Mealed, O-Open and TI-Tight), type of infilling, slickensides, etc.

GES.DCRR.01.01 Rev 2

PRINCIPLES OF ENGINEERING GEOLOGY

Robert B. Johnson

Jerome V. DeGraff



JOHN WILEY & SONS

New York Chichester Brisbane Toronto Singapore

page 10 of 18

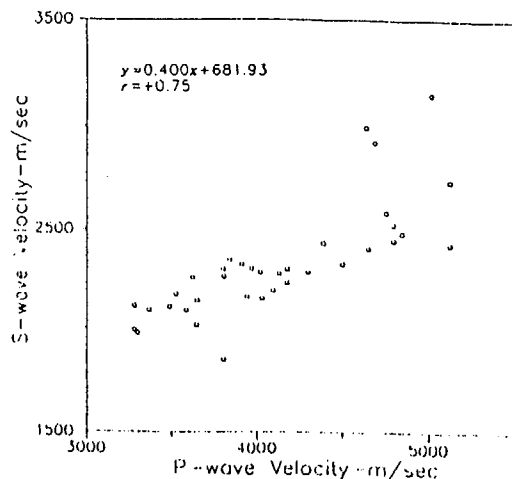


Figure 4.9 Plot of compressional (p-) wave velocity versus shear (s-) wave velocity. (From Jesch et al., 1979)

calculating E_d (Figure 4.10). By comparison, Poisson's ratio shows no well-defined linear relationships with either V_p or V_s (Figure 4.12).

Influence of Confinement on Strength and Elastic Moduli

The geotechnical properties of rocks obtained during uniaxial, or unconfined, testing are numerically unlike *in situ* rock properties. In the latter case, the rock is subjected to confining stresses along the other two orthog-

Modulus	Equation
Young's modulus = $E_d = k\rho V_p^2 \frac{(3V_p^2 - 4V_s^2)}{(V_p^2 - V_s^2)}$	
Poisson's ratio = $\nu_d = \frac{V_p^2 - 2V_s^2}{2(V_p^2 - V_s^2)}$	
Shear modulus = G_d or $\mu = \rho V_s^2$	

Where:

ρ = mass density (rho)

V_p = P or compressional wave propagation velocity

V_s = S or shear wave propagation velocity

k = constant, depending on units used

Figure 4.10 Dynamic elastic moduli equations.

MODULE 4.2

Calculation of dynamic elastic moduli from test data.

Sample data

Pikes Peak granite, Rampart Range, Douglas County, Colorado, NX (2 1/4 in. or 54 mm diameter) core

Core length = 0.123 m

Bulk density = 2.643 g/cm³

P-wave travel time through core

$$= 2.880 \times 10^{-3} \text{ sec}$$

S-wave travel time through core

$$= 5.426 \times 10^{-3} \text{ sec}$$

Velocity calculations

P-wave, $V_p = .123 \text{ m} / 2.880$

$$\times 10^{-3} \text{ sec} = 4,270.8 \text{ m/sec}$$

S-wave, $V_s = .123 \text{ m} / 5.426$

$$\times 10^{-3} \text{ sec} = 2,266.9 \text{ m/sec}$$

Young's Modulus, E_d , calculation (see Figure 4.10)

Value of k (conversion of bulk to mass density and Pa) = 1,000.6

$$E_d = (1,000.6) (2.643) (2,266.9^2) / ((3)$$

$$(4,270.8^2) - (4) (2,266.9^2)) /$$

$$(4,270.8^2 - 2,266.9^2) = 35.44 \times 10^9$$

$$\text{Pa} = 35.44 \text{ GPa}$$

Poisson's Ratio, ν_d , calculation (see Figure 4.10)

$$\nu_d = ((4,270.8^2) - (2) (2,266.9^2)) / ((2) (4,270.8^2 - 2,266.9^2)) = .304$$

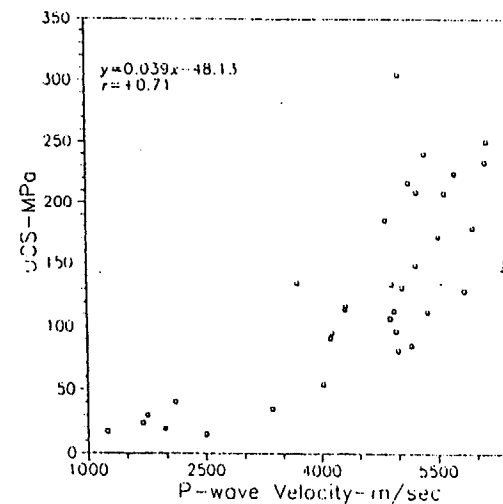


Figure 4.11 Plot of compressional (p-) wave velocity versus uniaxial compressive strength (UCS). (Adapted from D'Andrea et al., 1965).

GES.DUP.01.01 Rev. 2

Oct 09 01 03:52p

PG&E Used Fuel Storage

(805) 595-6402

P. 2

GEO. DUFF. 01.01 Rev. 2

Date: October 5, 2001

File #: 72.10.05

To: William Page / Robert K. White
PG&E Geosciences Dept

From: Richard L. Klimczak, Project Engineer

Subject: Diablo Canyon Units 1 and 2
Transmittal of Requested Drawings and Re-Transmittal of Items Not
Attached to 9/26/01 Letter**Pacific Gas and
Electric Company**

Dear Bill,

Reference your 10/4/01 e-mail "Maps Still Needed."

Drawing Fig. 2.1-2

We are transmitting herewith paper and electronic "For Information Only" copies of Fig. 2.1-2, dated 10/5/01, to replace the drawing transmitted by our letter dated 9/27/01. The attached drawing identifies the subject road as the Patton Cove Bypass.

Requested Drawings

Attached are full copies of the EDMS drawings tabulated on the second page of this memo. Electronic copies are provided in a CD ROM, "UFSP GEO Site & Topo Dwgs.", 10/5/01.

Four Survey Runs and Profiles

As we agreed, and you noted in another e-mail later on 10/4/01, profiles for survey information for Sections D-D', E-E', F-F' and I-I' are to be plotted by Geosciences' consultants using appropriate software.

Transmittal Letter to Robert K. White, "Transmittal of Survey Points for Four Cross-Sections", dated 9/26/01

Transmitted herewith are paper and electronic copies of items missing from the subject transmittal related to field surveys performed by Fleming Surveys, Inc., at the request of Bill Page and including:

Oct 09 01 03:53p

PG&E Used Fuel Storage

(805) 595-6402

p. 3

GEO. DCP. 01.01 Rev. 2

- 1) Diablo-pnts.xls: The Points Lists submitted by Pacific Engineering for four topographic profile lines D-D', E-E', F-F' and I-I'.
- 2) CYN-r14.dwg: A sketch prepared by Pacific Engineering showing in plan the routes of the four field survey lines and can serve as a guide to the relative locations of the tabulated data.

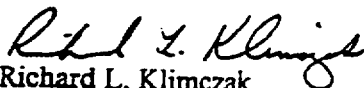
Per your request, the survey routes shown on this sketch will be re-transmitted at a later date after it has been plotted on plant 20-scale drawings.

The last sentence of the subject 9/26/01 letter should read "Please confirm that documents transmitted with this letter are the same as those sent to you by FAX and e-mail as mentioned herein. This transmittal is per requirements of DCPD Procedures CF3.ID17."

Also included in the CD is an electronic copy of engineering drawing PGE-004-54-001, Rev. 0. A hard copy was transmitted on 9/27/01. The elevation at the bottom of the ISFSI slab is 302 ft.

This transmittal is per requirements of DCPD Procedure CF3.ID17.

If you have questions please contact me at (805) 595-6320 or A. Tafoya at (805) 595-6392.



Richard L. Klimczak

Project Engineer

Diablo Canyon Used Fuel Storage Project

cc:	LJStrickland	SLO B3	w/o
	BHPatton	SLO BB	w/o
	AFTafoya	SLO B10	w/o
	CEHartz	SLO B0	w/o
	WPage	245 Market N4C, 422B	w/o
	RKWhite	245 Market N4C, 418B	w/o
	JISun	245 Market N4C	w/o
	JCYo:mg	245 Market N4C, 413C	w/o
	DCPD Chronological File		
	DCPD RMS	DCPD 119/1	
	DCPD File No. 72.10.05		

Date: June 5, 2001

GEO. DUMP. 01. 01 Rev. 2
File #: 72.10.05 : _____

To: PG&E GEOSCIENCES DEPARTMENT

From: NUCLEAR SERVICES - USED FUEL STORAGE PROGRAM

Subject: PG&E Geosciences Work Plan GEO 2001-01, Transmittal of Reference Material



ROB WHITE

Rob,

The purpose of this document, is for coordination of the ISFSI seismic calculation (provided by Enercon to PG&E) with Geosciences department, insofar as the appropriate use of the Rock properties are concerned (e.g. "E", Poisson...). The purpose of the coordination is primarily to;

- 1) General familiarity with the use of the information provided by Geosciences in this FEA.
- 2) Review & approval of the underlying Rock Stresses and displacements under Gravity and dynamic load conditions. This is to satisfy the section 6.4.3.6 of the design spec. (10012-N-NPG) regarding the "Soil Elastic Settlement Loads".
- 3) Review of the rock shear strains, as these values were determined to be important to the development and use of appropriate "E" values.

Please call me if you have any questions. 805-595-6374

Sincerely,

A handwritten signature in cursive script, appearing to read 'Nozar Jahangir'.


Nozar Jahangir
ISFSI Pad Design Technical Coordinator
Diablo Canyon Used Fuel Storage Project

Enclosure: CD

NXJahangir:kmn

cc: RL Klimczak
LJ Strickland
AF Tafoya
DCPP RMS
DCPP File No. 72.10.05

GEO. DEPT. 01.01 Rev. 2

 ENERCON SERVICES, INC.	ENGINEERING CALCULATION COVER SHEET	Calc. No. PGE-009-CALC-003
		Rev. 0
		Sheet 1 of 50
Title: ISFSI Cask Storage Pad Seismic Analysis		Client: PG&E
		Job No. PGE-009
Purpose Of Calculation: The purpose of this calculation is to compute the size and thickness of the ISFSI Cask Storage Pads and to compute the moments within the storage pad for the controlling seismic load combinations specified for the site. Analyses are in compliance with the seismic load combinations, as set forth, in References 2, 3, 8 and 9 for load combinations, which involve Hosgri and Long-Term Seismic Program earthquakes. The ISFSI Facility will contain (7) pads, which will support (20) HI-Storm Storage Casks per pad. The storage casks are arranged in a 5 x 4 array and are located on 17'-0" centers. The results of the analyses indicate that a pad, 105'-0" (N-S direction) x 68'-0" (E-W direction) x 7'-6" thick (nominal), is acceptable for the storage casks and the seismic loads. This Calculation does <u>not</u> consider load combinations for the sequencing of cask placements and load conditions other than seismic (e.g., curing temperatures and shrinkage). The sequencing of cask placements will be designed, so that, the pad size stated above is acceptable. The results from this Calculation will be used in Calculation No. PGE-009-CALC-007 to evaluate the concrete per the design codes and to determine the size of steel reinforcement. NOTE: This Calculation is furnished as part of PG&E Contract No. 4600010841, Change Order No. 001		
Scope Of Revision: N/A		
Revision Impact On Results: N/A		
<input checked="" type="checkbox"/> Safety Related <input type="checkbox"/> Non-Safety Related <input type="checkbox"/> Preliminary Calculation <input checked="" type="checkbox"/> Final		
Approvals (Print Name and Sign)		
Originator	S.C. TUMMINELLI	Date
Reviewer		Date
Verification Engineer	K.L. WHITMORE	Date
Approver	R.F. EVERS	Date



ENERCON SERVICES, INC.

GEO. DCP. 01.01 Rev. 2

JOB. NO.	PGE-009	SHEET	12	OF	50
PROJECT	DCPP ISFSI	DATE	May 25, 2001		
SUBJECT	ISFSI Cask Storage Pad Seismic Analysis				
CLIENT	PG&E-DCPP	ORIGINATOR	S. C. Tumminelli		
REVIEWER	K. L. Whitmore	APPROVED	R. F. Evers		
CALCULATION NO.	PGE-009-CALC-003	REVISION	0		

Rock Elements

The rock is modeled with Element Type #2. Element Type #2 is also the ANSYS SOLID45 8-noded structural solid element. As with the use of this element for the pad, no special features of this element were invoked for the rock. The rock is designated Material Type 2 and is assumed to be homogeneous. Young's Modulus for this element type is varied to simulate two different types of rock. One rock is described as soft with $E = 0.2 \times 10^6$ psi, while the other rock is described as hard with $E = 2.0 \times 10^6$ psi (Ref. 5). Poisson's ratio is 0.35 for both of these models. The soft rock Poisson's ratio from Ref. 5 is 0.336 for the soft rock and 0.367 for the hard rock. The value selected for analysis is within 5% of both of these values and is, therefore, a valid value to use for analysis. The third model has very hard rock with a Young's Modulus $E = 4.9 \times 10^6$ psi and a Poisson's ratio of 0.24 (Ref. 11).

* The rock portion of the model is wide and thick to insure that the rock extends a sufficient distance from the pad so that the boundary conditions of the rock do not affect the stiffness of the rock beneath the pad. It is 158 feet in the X direction, 175 feet in the Z, and is 85 feet thick, see Figure 7 below. The pad is located in the center of the rock surface. The boundary conditions for the rock model are that all three degrees of freedom are fixed on the sides and on the bottom of the rock. These are applied as loads in the ANSYS system and will be discussed again below. The completed model with the material numbers identified for the various materials is shown in Figures 11 and 12 below.

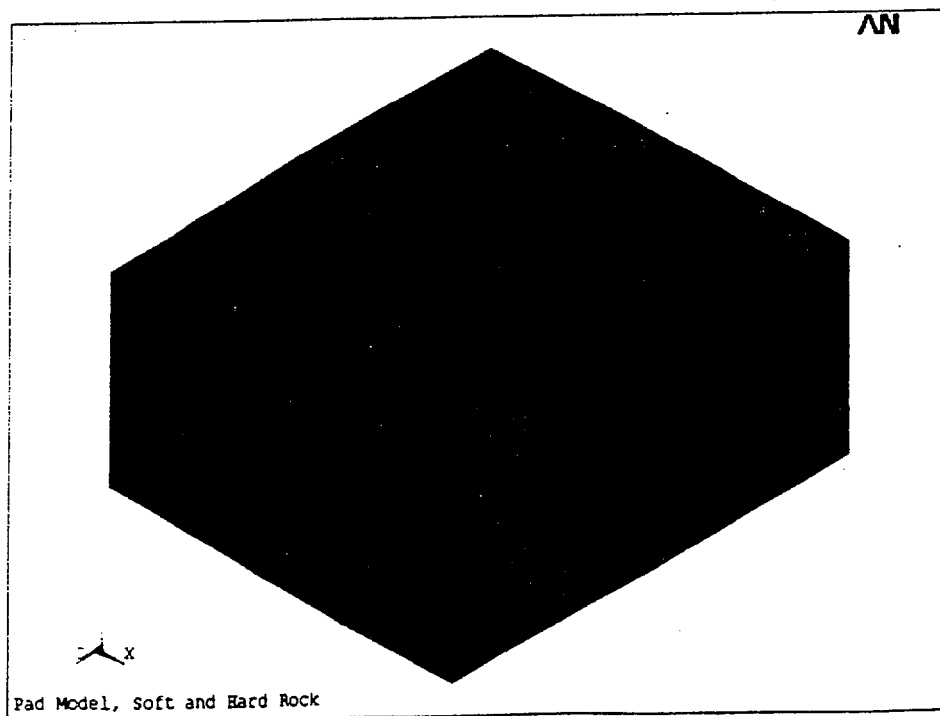
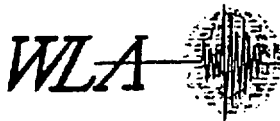


Figure 7 – Isometric view of the rock



GEO. DATA 01.01 Rev. 2
William Lettis & Associates, Inc.

1777 Botelho Drive, Suite 262, Walnut Creek, California 94596
Voice: (925) 256-6070 FAX: (925) 256-6076

Mr. Robert White
Geosciences Department
Pacific Gas & Electric Company
245 Market Street, Rm. 421-N4C
San Francisco, CA 94105

November 5, 2001

Re: Completion of Data Reports (formerly appendices)

Dear Rob:

This letter transmits to Geosciences the following Diablo Canyon ISFSI Data Reports (formerly called appendices) that were prepared under the WLA Work Plan, Additional Geologic Mapping, Exploratory Drilling, and Completion of Kinematic Analyses for the Diablo Canyon Power Plant Independent Spent Fuel Storage Installation Site, Rev. 2 (11/28/00) using data collected under that Work Plan and a second WLA Work Plan, Additional Exploratory Drilling and Geologic Mapping for the ISFSI Site, Rev. 1 (9/21/01).

Diablo Canyon ISFSI Data Report A - Geologic Mapping in the Plant Site and ISFSI Site Areas, Rev. 0, November 5, 2001, November 5, 2001, prepared by J. Bachhuber, 42 p.

Diablo Canyon ISFSI Data Report B - Borings in ISFSI Site Area, Rev. 0, November 5, 2001, prepared by J. Bachhuber, 244 p.

Diablo Canyon ISFSI Data Report C - 1998 Geophysical Investigations at the ISFSI Site Area, (Agabian Associates and GeoVision), Rev. 0, November 5, 2001, prepared by J. Bachhuber, 84 p.

Diablo Canyon ISFSI Data Report D - Trenches in the ISFSI Site Area, Rev. 0, November 5, 2001, prepared by J. Bachhuber, 66 p.

Diablo Canyon ISFSI Data Report E - Borehole Geophysical Data (NORCAL Geophysical Consultants, Inc.), Rev. 0, November 5, 2001, prepared by C. Brankman, 303 p.

Diablo Canyon ISFSI Data Report F - Field Discontinuity Measurements, Rev. 0, November 5, 2001, prepared by J. Bachhuber and C. Brankman, 85 p.

Diablo Canyon ISFSI Data Report G - Soil Laboratory Test Data (Cooper Testing Laboratory), Rev. 0, November 5, 2001, prepared by J. Sun, 63 p.

Diablo Canyon ISFSI Data Report H - Rock Strength Data and GSI Sheets, Rev. 0, November 5, 2001, prepared by J. Bachhuber, 37 p.

GEO.DC.PP.01.02
Rev. 2

WLA

Diablo Canyon ISFSI Data Report I - Rock Laboratory Test Data (GeoTest Unlimited), Rev. 0, November 5, 2001, prepared by J. Sun, 203 p.

Diablo Canyon ISFSI Data Report J - Petrographic Analysis and X-Ray Diffraction of Rock Samples (Spectrum Petrographics, Inc.), Rev. 0, November 5, 2001, prepared by J. Bachhuber, 204 p.

Diablo Canyon ISFSI Data Report K - Petrographic and X-Ray Diffraction Analyses of Clay Beds (Schwein/Christensen Laboratories, Inc.), Rev. 0, November 5, 2001, prepared by J. Bachhuber, 36 p.

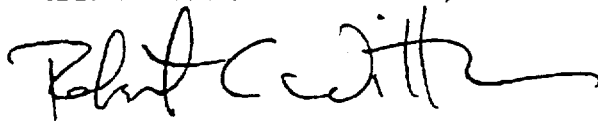
In addition to the revisions of those reports required under the various Work Plans, Mr. Scott Lindvall, the WLA ITR for the ISFSI project, has performed independent technical reviews of the Diablo Canyon ISFSI Data Reports as part of his review of Calculation Package GEO.DC.PP.01.21, Analysis of Bedrock Stratigraphy and Geologic Structure at the DCPD ISFSI Site. He finds that the reports clearly and accurately compile and organize the data.

Mr. Albert Tafoya from the Diablo Canyon ISFSI Project Office in San Luis Obispo, Mr. Dale Marcum, NQS Technical Oversight for the project, and William Page of your office provided comments on the August versions of the Diablo Canyon ISFSI Data Reports (formerly called appendices) and their comments have been addressed.

These reports are submitted to you as per the PG&E Geosciences Department Calculation Procedure GEO.001, Rev. 04 (10/10/01).

We look forward to any comments you may have.

Sincerely,
WILLIAM LETTIS & ASSOCIATES, INC.



Robert C. Witter
Project Manager

CC: William Page

Index No. 402 _____
Binder No. _____

TITLE: CALCULATION COVER SHEET

Unit(s): 1 & 2 File No.: 52.27

Responsible Group: Civil Calculation No.: 52.27.100.713

No. of Pages 3 Cover pages + Index (4 pages) + Design Calculation YES [x] NO []
1 Attachment (32 pages)

System No.	42C	Quality Classification	Q (Safety-Related)
------------	-----	------------------------	--------------------

Structure, System or Component: Independent Spent Fuel Storage Facility

Subject: Development of Allowable Bearing Capacity for DCPD ISFSI Pad and CTF Stability Analyses (Ref. GEO.DCPD.01.03)

Electronic calculation YES [] NO [x]

Computer Model	Computer ID	Program Location	Date of Last Change

Registered Engineer Stamp: Complete A or B

A. Insert PE Stamp or Seal Below

B. Insert stamp directing to the PE stamp or seal

**REGISTERED ENGINEERS'
STAMPS AND EXPIRATION DATES
ARE SHOWN ON DWG 063618**

Expiration Date:

NOTE 1: Update DCI promptly after approval.

NOTE 2: Forward electronic calculation file to CCTG for uploading to EDMS.

CF3.ID4
ATTACHMENT 7.2

TITLE: CALCULATION COVER SHEET

CALC No. 52.27.100.713, R0

RECORD OF REVISIONS

Rev No.	Status	Reason for Revision	Prepared By:	LBIE Screen	LBIE	Check Method*	LBIE Approval		Checked	Supervisor	Registered Engineer
		Remarks	Initials/ LAN ID/ Date	Yes/ No/ NA	Yes/ No/ NA		PSRC Mtg. No.	PSRC Mtg. Date	Initials/ LAN ID/ Date	Initials/ LAN ID/ Date	Signature/ LAN ID/ Date
0	F	Acceptance of Geosciences Calc. No. GEO.DCPP.01.03, Rev. 1 Calc. is in support of 10CFR72 DCP License Application (ISFSI Dry Cask) to the NRC prior to implementation. Note: Prepared per CF3.ID17 requirements	<i>ALP</i> /NXJ1 11/6/01	<input type="checkbox"/> Yes <input type="checkbox"/> No <input checked="" type="checkbox"/> NA	<input type="checkbox"/> Yes <input type="checkbox"/> No <input checked="" type="checkbox"/> NA	<input type="checkbox"/> A <input type="checkbox"/> B <input checked="" type="checkbox"/> C	N/A	N/A	<i>AT</i> AE72 11/6/01	<i>LSJ</i> LSJ2 11/9/01	<i>LSJ</i> LSJ2 11/9/01
				<input type="checkbox"/> Yes <input type="checkbox"/> No <input type="checkbox"/> NA	<input type="checkbox"/> Yes <input type="checkbox"/> No <input type="checkbox"/> NA	<input type="checkbox"/> A <input type="checkbox"/> B <input type="checkbox"/> C					
				<input type="checkbox"/> Yes <input type="checkbox"/> No <input type="checkbox"/> NA	<input type="checkbox"/> Yes <input type="checkbox"/> No <input type="checkbox"/> NA	<input type="checkbox"/> A <input type="checkbox"/> B <input type="checkbox"/> C					

*Check Method: A: Detailed Check, B: Alternate Method (note added pages), C: Critical Point Check



SUBJECT _Development of Allowable Bearing Capacity for DCPD ISFSI Pad and CTF Stability Analyses (GEO Sciences # GEO.DCPP.01.03)

MADE BY NXJ1 DATE 11/6/01 CHECKED BY AT DATE 11/6/01

Table of Contents:

Section	Type	Title	No. of Pages
1	Index	Cross-Index (For Information Only)	1 - 4
Attachments	"A"	Development of Allowable Bearing Capacity for DCPD ISFSI Pad and CTF Stability Analyses (GEO Sciences # GEO.DCPP.01.03 Rev. 1)	32



SUBJECT Development of Allowable Bearing Capacity for DCPD ISFSI Pad and CTF Stability Analyses
MADE BY NXJ1 DATE 11/6/01 CHECKED BY KT DATE 11/6/01

1- Cross reference between Geo Sciences calculation Numbers and DCPD (Civil Group's) Calculation Numbers: This section is For Information Only.

Cross-Index

(For Information Only)

Item No.	Geosciences Dept. Calc. No.	Title	DCPD, Civil Calc. No.	Comments
1	GEO.DCPD.01.01	Development of Young's Modulus and Poisson's Ratios for DCPD ISFSI Based on Field Data	52.27.100.711	
2	GEO.DCPD.01.02	Determination of Probabilistically Reduced Peak Bedrock Accelerations for DCPD ISFSI Transporter Analyses	52.27.100.712	
3	GEO.DCPD.01.03	Development of Allowable Bearing Capacity for DCPD ISFSI Pad and CTF Stability Analyses	52.27.100.713	
4	GEO.DCPD.01.04	Methodology for Determining Sliding Resistance Along Base of DCPD ISFSI Pads	52.27.100.714	
5	GEO.DCPD.01.05	Determination of Pseudostatic Acceleration Coefficient for use in DCPD ISFSI Cutslope Stability Analyses	52.27.100.715	
6	GEO.DCPD.01.06	Development of Lateral Bearing Capacity for DCPD CTF Stability Analyses	52.27.100.716	
7	GEO.DCPD.01.07	Development of Coefficient of Subgrade Reaction for DCPD ISFSI Pad Stability Checks	52.27.100.717	
8	GEO.DCPD.01.08	Determination of Rock Anchor Design Parameters for DCPD ISFSI Cutslope	52.27.100.718	
9	GEO.DCPD.01.09	Determination of Applicability of Rock Elastic Stress-Strain Values to	52.27.100.719	Calculation to be replaced by letter



SUBJECT Development of Allowable Bearing Capacity for DCPD ISFSI Pad and CTF Stability Analyses
MADE BY NXJ1 DATE 11/6/01 CHECKED BY MT DATE 11/6/01

Cross-Index

(For Information Only)

Item No.	Geosciences Dept. Calc. No.	Title	DCPD, Civil Calc. No.	Comments
		Stress-Strain Values to Calculated Strains Under DCPD ISFSI Pad		
10	GEO.DCPD.01.10	Determination of SSER 34 Long Period Spectral Values	52.27.100.720	
11	GEO.DCPD.01.11	Development of ISFSI Spectra	52.27.100.721	
12	GEO.DCPD.01.12	Development of Fling Model for Diablo Canyon ISFSI	52.27.100.722	
13	GEO.DCPD.01.13	Development of Spectrum Compatible Time Histories	52.27.100.723	
14	GEO.DCPD.01.14	Development of Time Histories with Fling	52.27.100.724	
15	GEO.DCPD.01.15	Development of Young's Modulus and Poisson's Ratio Values for DCPD ISFSI Based on Laboratory Data	52.27.100.725	
16	GEO.DCPD.01.16	Development of Strength Envelopes for Non-jointed Rock at DCPD ISFSI Based on Laboratory Data	52.27.100.726	
17	GEO.DCPD.01.17	Determination of Mean and Standard Deviation of Unconfined Compression Strengths for Hard Rock at DCPD ISFSI Based on Laboratory Tests	52.27.100.727	
18	GEO.DCPD.01.18	Determination of Basic Friction Angle Along Rock Discontinuities at DCPD ISFSI Based on Laboratory Tests	52.27.100.728	



SUBJECT Development of Allowable Bearing Capacity for DCPD ISFSI Pad and CTF Stability Analyses
MADE BY NXJ1 DATE 11/6/01 CHECKED BY [Signature] DATE 11/6/01

Cross-Index

(For Information Only)

Item No.	Geosciences Dept. Calc. No.	Title	DCPD, Civil Calc. No.	Comments
19	GEO.DCPD.01.19	Development of Strength Envelopes for Jointed Rock Mass at DCPD ISFSI Using Hoek-Brown Equations	52.27.100.729	
20	GEO.DCPD.01.20	Development of Strength Envelopes for Shallow Discontinuities at DCPD ISFSI Using Barton Equations	52.27.100.730	
21	GEO.DCPD.01.21	Analysis of Bedrock Stratigraphy and Geologic Structure at the DCPD ISFSI Site	52.27.100.731	
22	GEO.DCPD.01.22	Kinematic Stability Analysis for Cutslopes at DCPD ISFSI Site	52.27.100.732	
23	GEO.DCPD.01.23	Pseudostatic Wedge (SWEDGE) Analyses of DCPD ISFSI Cutslopes	52.27.100.733	
24	GEO.DCPD.01.24	Stability and Yield Acceleration Analysis of Cross-Section I-I'	52.27.100.734	
25	GEO.DCPD.01.25	Determination of Seismic Coefficient Time Histories for Potential Sliding Masses Along Cut Slope Behind ISFSI Pad	52.27.100.735	
26	GEO.DCPD.01.26	Determination of Potential Earthquake-Induced Displacements of Potential Sliding Masses on DCPD ISFSI Slope	52.27.100.736	
27	GEO.DCPD.01.27	Cold Machine Shop Retaining Wall Stability	52.27.100.737	
28	GEO.DCPD.01.28	Roadway Capacity with Transporter	52.27.100.738	



SUBJECT Development of Allowable Bearing Capacity for DCPD ISFSI Pad and CTF Stability Analyses
MADE BY NXJ1 DATE 11/6/01 CHECKED BY K1 DATE 11/6/01

Cross-Index

(For Information Only)

Item No.	Geosciences Dept. Calc. No.	Title	DCPD, Civil Calc. No.	Comments
29	GEO.DCPD.01.29	Determination of Seismic Coefficient Time Histories for Critical Slides on DCPD ISFSI Transport Route	52.27.100.739	
30	GEO.DCPD.01.30	Determination of Potential Earthquake-Induced Displacements of Critical Slides Along DCPD ISFSI Transport Route	52.27.100.740	
31	GEO.DCPD.01.31	Development of Strength Envelopes for Clay Beds	52.27.100.741	
32	GEO.DCPD.01.32	Verification of Computer Program SPCTLR.EXE	52.27.100.742	
33	GEO.DCPD.01.33	UTEXAS3 Computer Program Verification	52.27.100.743	
34	GEO.DCPD.01.34	Verification of Computer Code QUAD4M	52.27.100.744	
35	GEO.DCPD.01.35	Verification of Computer Program DEFORMP	52.27.100.745	
36	GEO.DCPD.01.36	Determination of Design Parameters for ISFSI Fill Slope	52.27.100.746	Calculation to be delayed – retaining wall to be shown on drawing
37	GEO.DCPD.01.37	Development of Freefield Ground Motion Storage Cask Spectra and Time Histories for the Used Fuel Storage Project	52.27.100.747	

PG&E
Geosciences Department
Departmental Calculation Procedure
Attachment 5.2

Number: GEO.001
Revision: 04
Page: 1 of 1

Title: Design Calculation Cover Sheet

PACIFIC GAS AND ELECTRIC COMPANY
GEOSCIENCES DEPARTMENT
CALCULATION DOCUMENT

Calc Number GEO.DCPP.01.03
Revision 1
Date 11/5/01
Calc Pages: 30
Verification Method: A
Verification Pages: 1

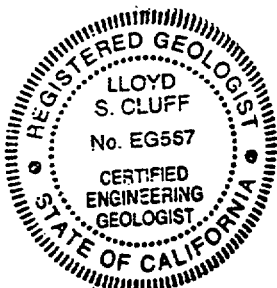
(SEE GEO SCIENCES
ORIGINAL FILES)
REV 11/6/01
M 11/6/01

TITLE: Development of allowable bearing capacity for DCPD ISFSI pad and CTF
stability analyses

PREPARED BY: Robert K White DATE 11/5/01
Robert K White Geosciences
Printed Name Organization

VERIFIED BY: Joseph Sun DATE 11/5/01
Joseph Sun Geosciences
Printed Name Organization

APPROVED BY: Lloyd Cluff DATE 11/5/01
Lloyd Cluff Geoscience
Printed Name Organization



Expires 12/31/02

Development of allowable bearing capacity for DCPD ISFSI pad and CTF stability
analyses
Calc Number GEO.DCPD.01.03

Record of Revisions

Rev. No.	Reason for Revision	Revision Date
1	revised Appendix B and I reference to Data Report B and I	11/5/01

DCPP ISFSI GEOTECHNICAL CALCULATION PACKAGE

Title: Development of allowable bearing capacity for DCPD ISFSI pad and CTF stability analyses
Calc Number: GEO.DCPP.01.03
Revision: Rev. 1
Date: November 5 2001
Author: Robert K. White
Verifier: Joseph I. Sun

PURPOSE

As required by Geosciences Work Plan GEO 2001-03, Appendix B, determine static and dynamic bearing capacity of rock underlying the proposed DCPD ISFSI concrete pads and CTF site. Bearing capacity values will be used by PG&E consultants in assessing factor of safety against bearing capacity failure given static and dynamic loads.

ASSUMPTIONS

1. Rock characteristics beneath ISFSI pads and CTF are adequately defined for purposes of determining bearing capacity by the series of borings performed between 1998 and 2001 within ISFSI pad and CTF footprint and by strength envelopes derived from field and lab data. This is a realistic assumption because the field and lab data and associated rock strength characteristics have been extensively documented in Geosciences calculation packages GEO.DCPP.01.16 through GEO.DCPP.01.21 and related Data Reports referenced in those calculations.
2. Locations, dimensions, and elevations of ISFSI pads and CTF are as defined in Klimczak, 9/27/01 (Drawing PGE-009-SK-001, page 11, attached) and in relation to borings, as indicated in Fig. 21-4, GEO.DCPP.01.21.
3. Pads are not embedded on at least one side during a substantial period of time prior to additional pads being constructed adjacent. This is a conservative assumption, as the assumed lack of embedment reduces the allowable bearing capacity in the rock when modeled as a cohesionless material.
4. Groundwater is much lower than base of pads, based on field measurements as documented in Klimczak, 10/19/01, page 16, attached, in borings as shown in Figure 21-3 of GEO.DCPP.01.21.

Calc. Number: GEO.DCPP.01.03 Rev. 1

DESIGN INPUTS

1. Rock Quality Designation (RQD) as tabulated in Table 1, from borings within ISFSI and CTF footprints per boring logs in Witter, 11/5/01, Data Report B.
2. Rock mass types beneath footprint as presented in Figure 21-41 from Geosciences calculation GEO.DCPP.01.21.
3. Rock friction angle of 50 degrees for dolomite, sandstone, and friable sandstone beneath footprint, from Geosciences calculations GEO.DCPP.01.16 and GEO.DCPP.01.19.
4. Rock unit weight of 140 pcf for rock mass beneath footprint, from Witter, 11/5/01, Data Report I.
5. Elevation of base of ISFSI pads of 302, from Klimczak, 10/5/01, page 14, attached. Elevation of base of CTF of 282, from Klimczak, 10/17/01, page 18, attached, for elevation of ground surface at 306 for boring CTF-A, and Klimczak, 9/27/01 (Drawing UFSP-SK-00, page 12, attached) for 24-foot depth of CTF.

METHODOLOGY

1. Determine average RQD for depth below pad equal to proposed foundation width from each boring beneath pads, or to maximum depth of borings if less than foundation width.
2. Determine average RQD for depth below pad equal to $\frac{1}{4}$ proposed foundation width.
3. Using whichever average value of RQD is less, obtain allowable (static) contact pressure beneath pads from Table 22.2, pg. 362, of Peck and others (1974), which limits settlement to 0.5 inch or less.
4. Using the friction angle defined for the underlying rock mass and the general bearing equation and associated bearing capacity factors from pp. 26 to 28 of U.S. Army Corps of Engineers (1993), calculate ultimate bearing capacity beneath pads. Reduce ultimate by factor of 3 for allowable static capacity.
5. Compare value of allowable contact pressure from RQDs with allowable bearing capacity from strength envelope and select minimum value for analyses. Increase static value by $\frac{1}{3}$ for dynamic analyses per Section 1612.3.2 of ICBO (1997).
6. Perform similar assessment of RQD for CTF site, and compare with average RQD value to determine applicability of value derived for ISFSI pads at CTF site.

Calc. Number: GEO.DCPP.01.03 Rev. 1

SOFTWARE

No software is used to perform calculations.

ANALYSIS

A plan view of the ISFSI pad footprint is provided in Klimczak, 9/29/01, Drawing PGE-009-SK-001, page 11, attached. Planned pad width of 68 feet is shown on the plan view on page 11. The planned pad base elevation is 302 feet from Klimczak, 10/5/01, page 14, attached. Boring log designations, elevations, total depths, and date borings begun, all from the boring logs in Witter, 11/5/01, Data Report B, are tabulated in Table 1 (page 7). Elevations from boring logs were approximated at time of borings, but are within 2 feet of surveyed elevations (Klimczak, 10/17/01, page 18), which is acceptable for this engineering purpose. Values of RQD were obtained from the boring logs and are also tabulated in Table 1, as well as average values of RQD calculated for depths equal to $\frac{1}{4}$ of the pad width (conservatively, say 20 feet, based on pad width of 68 feet from page 11), and to depths of full pad width or to bottom of hole if less.

The minimum average RQD for the elevation interval between 300 and 280 feet from the values tabulated on page 7 is 19 (boring 01-C). The minimum average RQD for the elevation interval between 300 and 255 feet is 18 (boring 01-D). It should be noted that three of the four borings with significantly lower RQD (A, C, and D) were drilled by the same rig and crew (based on the boring logs), whereas borings with significantly higher RQD (B, E, and G) were drilled by an alternate rig and crew. (Boring 98BA-2 was drilled by a third rig and crew.) This suggests that the variations in RQD for these borings may be more a function of drilling expertise than actual variations in rock quality. Nevertheless, for analysis purposes, the lowest RQD values will be used. Interpolating between values of allowable contact pressure listed in Table 22.2 from Peck and others (1974), page 20, attached, for an RQD of 18, the allowable contact pressure equals 24 tsf; say, 20 tsf.

Values of RQD were also obtained from the boring at the CTF site and are tabulated in Table 2. The minimum RQD value of 30 is still well above the minimum average obtained in the ISFSI pad footprint. Therefore, the allowable contact pressure of 20 tsf determined at the pads is also applicable, though conservative, at the CTF site.

Calc. Number: GEO.DCPP.01.03 Rev. 1

To determine the ultimate bearing capacity, the rock types underlying the pads are determined from Figure 21-41 (from GEO.DCPP.01.21) to be dolomite, sandstone, and friable sandstone. These rock types are all determined to have about the same friction angle of 50 degrees with no cohesion (from GEO.DCPP.01.16 and GEO.DCPP.01.19) for potential large-scale (100 feet or longer) failure surfaces passing simultaneously through numerous discontinuities and intact portions of rock, which would be the case for a bearing capacity type failure under the large pads proposed. The analysis uses formulas and tables from U.S. Army Corps of Engineers (1993), pp. 21 through 25, attached.

Ultimate bearing capacity, q_u , is defined by:

$$q_u = \frac{1}{2} B \gamma_h N_\gamma, \text{ (equation 4-1, pg. 22, attached**)}$$

where: B = footing width, (68 feet from page 11 attached, but no greater than 6 feet, per page 25 attached)

γ_h = unit weight, (140 pcf, or 0.07 tcf, per Witter, 11/5/01, Data Report I)

N_γ = bearing capacity factor for soil weight in the failure wedge (minimum value from Table 4-4 is 568.56 for $\phi = 50$ degrees, from page 24 attached)

** Note: N_c and N_q terms are zero since assuming no cohesion and no surcharge from embedment.

Inserting these values into the equation obtains:

$$q_u = \frac{1}{2} (6) (0.07) (568) = 119 \text{ tsf}$$

The allowable bearing capacity is obtained by:

$$q_a = q_u / SF = 119 / 3 = 40 \text{ tsf.}$$

By comparison, the allowable contact pressure of 20 tsf is less than the allowable bearing capacity of 40 tsf, so the former governs. The allowable capacity is for static loading. During earthquake loading, the allowable capacity can be increased by 33% to 26 tsf, per ICBO (1997), Section 1612.3.2, page 28, attached.

RESULTS

The allowable bearing capacity of the rock underlying the proposed ISFSI pad base under static loading is 20 tsf, based on RQD data from borings obtained in the pad footprint. The allowable capacity can be increased to 26 tsf, for earthquake loading.

Calc. Number: GEO.DCPP.01.03 Rev. 1

CONCLUSION

Allowable static and dynamic bearing capacities have been developed for the DCPD ISFSI concrete pads, for use by others in assessing factors of safety against excessive settlement or bearing failure. These values are also applicable, though conservative, at the CTF site.

REFERENCES

1. Geosciences Calculation GEO.DCPP.01.16, Development of strength envelopes for non-jointed rock at DCPD ISFSI based on laboratory data, rev. 1.
2. Geosciences Calculation GEO.DCPP.01.19, Development of strength envelopes for jointed rock mass at DCPD ISFSI using Hoek-Brown equations, rev. 1.
3. Geosciences Calculation GEO.DCPP.01.21, Analysis of Bedrock Stratigraphy and Geologic Structure at the DCPD ISFSI Site, rev. 0.
4. Witter (11/5/01): letter from Rob Witter to Rob White, entitled "Completion of Data Reports," dated 11/5/01, and accompanying Data Report B, Borings in ISFSI Site Area, rev. 0.
5. Witter (11/5/01): letter from Rob Witter to Rob White, entitled "Completion of Data Reports," dated 11/5/01, and accompanying Data Report I, Rock Laboratory Test Data, rev. 0.
6. Peck, R.B., Hanson, W.E., and Thornburn, T.H. (1974), Foundation Engineering.
7. U.S. Army Corps of Engineers (1993), Bearing Capacity of Soils, manual EM 1110-1-1905, published by ASCE as Technical Engineering and Design Guide No. 7.
8. ICBO (1997), Uniform Building Code, International Conference of Building Officials, USA.
9. Klimczak (9/27/01): letter from Richard Klimczak to Robert White, entitled "Transmittal of ISFSI Site and Vicinity Plans for the DCPD Used Fuel Storage Project," dated 9/27/01.
10. Klimczak (10/5/01): letter from Richard Klimczak to William Page/Robert White, entitled "Transmittal of Requested Drawings and Re-Transmittal of Items Not Attached to 9/26/01 Letter," dated 10/5/01.
11. Klimczak (10/19/01): letter from Richard Klimczak to Robert White, entitled "Transmittal of January 2001 Ground Water Level Measurements at the ISFSI Site and Parking Lot 7," dated 10/19/01.

Calc. Number: GEO.DCPP.01.03 Rev. 1

12. Klimczak (10/17/01): letter from Richard Klimczak to Robert White, entitled "Transmittal of Field Survey Points for ISFSI Site," dated 10/17/01.
13. Geosciences Work Plan GEO 2001-03, Development of Engineering Properties for ISFSI and CTF Foundation Design, ISFSI Slope Analyses, and ISFSI Cut and Fill Slope Reinforcement Design for The DCPD ISFSI Site, rev. 1.

ATTACHMENTS

1. Table 1, RQD from borings in proposed ISFSI pad footprint and averages for various intervals, page 7.
2. Table 2, RQD from borings in proposed CTF footprint, page 8.
3. Klimczak (9/27/01): letter from Richard Klimczak to Robert White, entitled "Transmittal of ISFSI Site and Vicinity Plans for the DCPD Used Fuel Storage Project," dated 9/27/01, and Drawings PGE-009-SK-001 and UFSP-SK-00, pages 9 to 12.
4. Klimczak (10/5/01): letter from Richard Klimczak to William Page/Robert White, entitled "Transmittal of Requested Drawings and Re-Transmittal of Items Not Attached to 9/26/01 Letter," dated 10/5/01, pages 13 to 14.
5. Klimczak (10/19/01): letter from Richard Klimczak to Robert White, entitled "Transmittal of January 2001 Ground Water Level Measurements at the ISFSI Site and Parking Lot 7," dated 10/19/01, pages 15 to 16.
6. Klimczak (10/17/01): letter from Richard Klimczak to Robert White, entitled "Transmittal of Field Survey Points for ISFSI Site," dated 10/17/01 and table 42301.doc, pages 17 to 18.
7. Peck, R.B., Hanson, W.E., and Thornburn, T.H. (1974), Foundation Engineering, cover sheet and page 362, pages 19 to 20.
8. U.S. Army Corps of Engineers (1993), Bearing Capacity of Soils, manual EM 1110-1-1905, published by ASCE as Technical Engineering and Design Guide No. 7, cover sheet and pages 26, 27, 30, and 34, pages 21 to 25.
9. ICBO (1997), Uniform Building Code, International Conference of Building Officials, USA, cover sheet and pages 2-4 and 2-5, pages 26 to 28.
10. Witter (11/5/01): letter from Rob Witter to Rob White, entitled "Completion of Data Reports," dated 11/5/01 (without attachments), pages 29 to 30.

RQD from borings in proposed ISFSI pad footprint and averages for various intervals

Boring	01-A		01-B		01-C		01-D		01-E		01-G		98BA-2	
Elevation	305		320		323		326		339		315		330	
Total Depth	72		72		67		69		81		76		165	
Log Date	04/19/2001		04/21/2001		04/22/2001		04/17/2001		04/19/2001		04/17/2001		05/27/1998	
Depth Interval	Run	RQD	Run	RQD	Run	RQD	Run	RQD	Run	RQD	Run	RQD	Run	RQD
300-295	2	14	5	64	4	30	7,8	30	8	45	5	62	7	22
295-290	3	19	6	40	5	0	9,10	23	9	16	6	84	8	20
290-285	4	23	7	68	6	34	11	25	10	84	7	87	9	10
285-280	5	47	8	40	7	12	12	9	11	66	8	78	10	36
280-275	6,7	28	9	34	8,9	13	13,14,15	10	12	76	9	78	11	0
275-270	8	48	10	28	10	7	16	15	13	80	10	83	12	36
270-265	9,10	40	11	62	11	27	17	9	14	90	11	5	13	16
265-260	11	26	12	48	12	62	18	20	15	88	12	20	14	50
260-255	12	52	13	56	13	10	19,20	22	16	88	13	30	15	52
255-250	13	44	14	48							14,14a	48	16	26
250-245	14	66									15	66	17	34
245-240	15	56									16	30	18	24
240-235	16	16											19	38
235-230													20	74
230-225													21	66
225-220													22	0
	Average		Average		Average		Average		Average		Average		Average	
300-280	26		53		19		22		53		78		22	
280-BOH	42		46		24		15		84		45		35	
300-BOH	37		49		22		18		70		56		32	

TABLE 1

RQD from boring in proposed CTF footprint

Boring	CTF-A	
Elevation	306	
Total Depth	59	
Log Date	04/18/2001	
	Run	RQD
Depth Interval		
284-279	6	86
279-274	7	66
274-269	8	30
269-264	9	48
264-259	10	64
259-255	11	52
255-253	12	35
253-248	13	84

TABLE 2

GEO.DCPP.01.03 Rev.1

Memorandum

Date: September 27, 2001 File #: 72.10.05
To: Robert K. White Phone: (415) 973-0544
PG&E Geosciences Dept
From: Richard L. Klimczak, Project Engineer
Subject: Diablo Canyon Units 1 and 2
Transmittal of ISFSI Site and Vicinity Plans for the DCPP Used Fuel
Storage Project

**Pacific Gas and
Electric Company**

Dear Rob,

Attached are copies of three site plan drawings and a sketch of the cask transfer facility.

PG&E Drawing 471124 is a plant site plot plan. Fig. 2.1-2 is a site plan showing the ISFSI and Transport Route. UFSP-SK-004 is a sketch of the Cask Transfer Facility.

PGE-009-SK-001 is the ISFSI site plot plan showing the cask storage pads, Cask Transfer Facility and the near vicinity of the ISFSI site. The drawing was prepared by Enercon Services Inc. Per Holtec calculation HI-2012618, Rev. 3, the weight of each loaded cask is 360,000 pounds.

This transmittal is per requirements of DCPP Procedure CF3.ID17.

If you have comments or questions please contact me at (805) 595-6320 or A. Tafoya at (805) 595-6392.

Richard L. Klimczak
Project Engineer
Diablo Canyon Used Fuel Storage Project

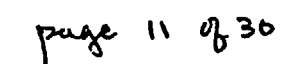
Attachments: Dwg 471124, Fig. 2.1-2, PGE-009-SK-001, UFSP-SK-004

cc: LJStrickland	SLO B3	w/o	WPage	245 Market N4C 418B	w/o
BHPatton	SLO BB	w/o	DCPP RMS	DCPP 119/1	
NJahangir	DCPP 201/112	w/o	DCPP Chronological File		
AFTafoya	SLO B10		DCPP File No.72.10.05		

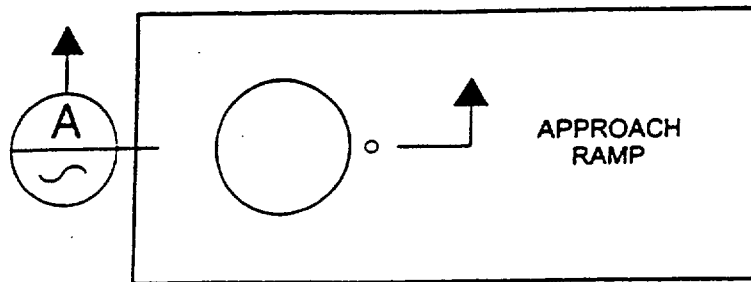
page 9 of 30

GEO. DCEP 01.03 Rev. 1

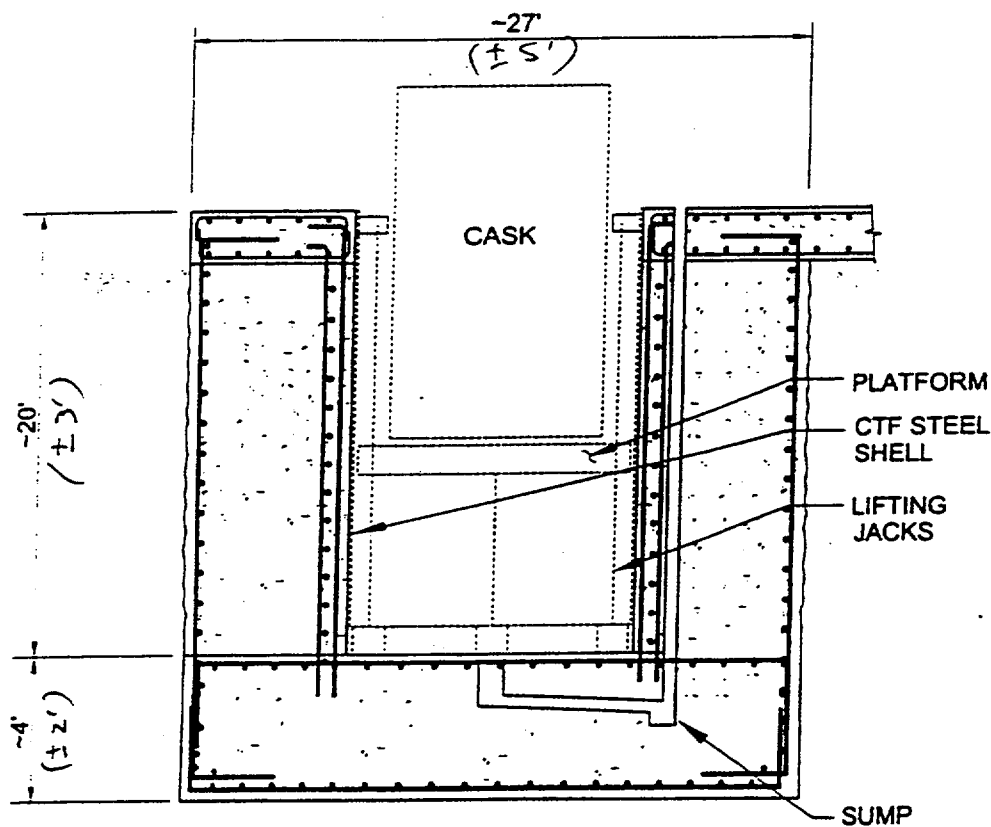
<u>DWG. NO.</u>	<u>REVISION</u>	<u>TITLE</u>
471124	1	Plot Plan
Fig. 2.1-2	D	Plan Drawing of the ISFSI Site
PGE-009-SK-001	0	Site Plot Plan, ISFSI Cask Storage Pad, Cask Transfer Facility
UFSP-SK-004	A	Cask Transfer Facility Structure (Schematic)



GEO.DCCP.01.03 Rev. 1

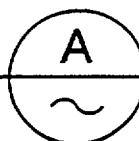


PLAN



SECTION

N.T.S.



NOTE: DIMENSIONS SHOWN ARE APPROXIMATE.

BY: A. TADYAC, JR. 7/27/01

CHK: N. JAHNGIR 9/27/01

UNIT

CASK TRANSFER FACILITY STRUCTURE
(SCHEMATIC)

DIABLO CANYON POWER PLANT

PG&E CO.

SHEET 1 OF 1 SHEETS

DRAWING NUMBER

UFSP-SK-00

REV.

A

Oct 09 01 03:52p

PG&E Used Fuel Storage

(805) 595-6402

P. 2

GEO.DC.PP.01.03 Rev. 1

Date: October 5, 2001 File #: 72.10.05
To: William Page / Robert K. White
PG&E Geosciences Dept
From: Richard L. Klimczak, Project Engineer
Subject: Diablo Canyon Units 1 and 2
Transmittal of Requested Drawings and Re-Transmittal of Items Not
Attached to 9/26/01 Letter



**Pacific Gas and
Electric Company**

Dear Bill,

Reference your 10/4/01 e-mail "Maps Still Needed."

Drawing Fig. 2.1-2

We are transmitting herewith paper and electronic "For Information Only" copies of Fig. 2.1-2, dated 10/5/01, to replace the drawing transmitted by our letter dated 9/27/01. The attached drawing identifies the subject road as the Patton Cove Bypass.

Requested Drawings

Attached are full copies of the EDMS drawings tabulated on the second page of this memo. Electronic copies are provided in a CD ROM, "UFSP GEO Site & Topo Dwgs.", 10/5/01.

Four Survey Runs and Profiles

As we agreed, and you noted in another e-mail later on 10/4/01, profiles for survey information for Sections D-D', E-E', F-F' and I-I' are to be plotted by Geosciences' consultants using appropriate software.

Transmittal Letter to Robert K. White, "Transmittal of Survey Points for Four Cross-Sections", dated 9/26/01

Transmitted herewith are paper and electronic copies of items missing from the subject transmittal related to field surveys performed by Fleming Surveys, Inc., at the request of Bill Page and including:

Oct 09 01 03:53p

PGL&E Used Fuel Storage

(805) 595-6402

p. 3

GEO.DC.PP.01.03 Rev. 1

- 1) Diablo-pnts.xls: The Points Lists submitted by Pacific Engineering for four topographic profile lines D-D', E-E', F-F' and I-I'.
- 2) CYN-r14.dwg: A sketch prepared by Pacific Engineering showing in plan the routes of the four field survey lines and can serve as a guide to the relative locations of the tabulated data.

Per your request, the survey routes shown on this sketch will be re-transmitted at a later date after it has been plotted on plant 20-scale drawings.

The last sentence of the subject 9/26/01 letter should read "Please confirm that documents transmitted with this letter are the same as those sent to you by FAX and e-mail as mentioned herein. This transmittal is per requirements of DCPD Procedures CF3.ID17."

Also included in the CD is an electronic copy of engineering drawing PGE-004-54-001, Rev. 0. A hard copy was transmitted on 9/27/01. The elevation at the bottom of the ISFSI slab is 302 ft.

This transmittal is per requirements of DCPD Procedure CF3.ID17.

If you have questions please contact me at (805) 595-6320 or A. Tafoya at (805) 595-6392.

Richard L. Klimczak

Richard L. Klimczak

Project Engineer

Diablo Canyon Used Fuel Storage Project

cc:	LJStrickland	SLO B3	w/o
	BHPatton	SLO BB	w/o
	AFTafoya	SLO B10	w/o
	CEHartz	SLO B0	w/o
	WPage	245 Market N4C, 422B	w/o
	RKWhite	245 Market N4C, 418B	w/o
	JISun	245 Market N4C	w/o
	JCYoung	245 Market N4C, 413C	w/o
	DCPD Chronological File		
	DCPD RMS	DCPD 119/1	
	DCPD File No. 72.10.05		

Memorandum

Geo.DC.PP.01.03 Rev. 1

Date: October 19, 2001 File #: 72.10.05 : 19
To: Robert K. White
From: Richard L. Klimczak, Project Engineer
Subject: Diablo Canyon Units 1 and 2
Transmittal of January 2001 Ground Water Level Measurements at the ISFSI Site



**Pacific Gas and
Electric Company**

Dear Rob,

Attached is a copy of the one page TES Report No. 420DC-01.70 as revised on 10/16/01 to add ground water level measurements performed by TES, on January 23, 2001. A report of measurements taken October 4, 2001 were previously transmitted to you on October 10, 2001.

The water levels were measured inside boreholes 98BA-1 and 98BA-3 at the ISFSI site.

The record of January 2001 measurements was requested in AR A0541736.

This transmittal is per requirements of DCPD Procedure CF3.ID17.

Please let me, or A. Tafoya, know if you have any questions.

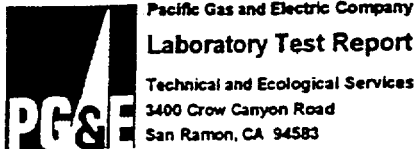
Richard L. Klimczak
Project Engineer
Diablo Canyon Used Fuel Storage Project

cc: LJStrickland SLO B3
BHPatton SLO BB
AFTafoya SLO B10
CEHartz SLO B0
WPage 245 Market N4C, 422B
JISun 245 Market N4C, 422A
JYoung 245 Market N4C, 413C
DCPD Chronological File
DCPD RMS DCPD 119/1
DCPD File No. 72.10.05

Report issued: October 8, 2001
Report Revised: October 16, 2001

Report 420DC-01.70

GEO.DC-P. 01.03 Rev. 1

**SUBJECT: DIABLO CANYON POWER PLANT - ISFSI Water Level Readings**

On October 4, 2001 water level readings were taken at the ISFSI site and the Lot 7 site. A Solinst Model 101-300 P3 Serial # 20436 water level indicator was used for all readings and is in good working order. The water level indicator is graduated in hundredths of a foot. All piezometer caps were in place before readings and replaced after readings. All water level readings are from the top of the standpipe. The readings are as follows:

<u>Bore Hole #</u>	<u>Water Level</u>
ISFSI Site	
98 BA-1	235.60'
98 BA-3	217.76'
Lot 7 Site	
DCSF 96-1(WLA-1)	18.22'(Bottom at 32.00')
DCSF 96-6(WLA-6)	Dry(Bottom at 23.68')

Read on January 23, 2001

ISFSI Site	
98 BA-1	205.90'
98 BA-3	199.76'

All readings were performed with the same water level indicator. The January 23, 2001 readings were the first set of readings for the ISFSI site by TES. The first readings for the Lot #7 site by TES was October 4, 2001.

Distribution: Steve Flaten
Al Tafoya
Jon Schletz
Robert White

Date: 10/16/01

Tested By:

Douglas S. Watson

Approved By:

Anton Pirtz

page 12 of 30

GEO.DC.PP.01.03 Rev. 1

Date: October 17, 2001
 To: Robert K. White
 PG&E Geosciences Department
 From: Richard L. Klimczak, Project Engineer
 Subject: Diablo Canyon Units 1 and 2
 Transmittal of Field Survey Points for ISFSI Site

File #: 72.10.05 : 18



**Pacific Gas and
Electric Company**

Dear Rob,

Attached are a transmittal letter, hard copy and CD of files containing data points from several field surveys performed by Fleming Surveying at the ISFSI Site.

Item	ASCII File	Date of Field Work	Brief Description
1	--	--	Transmittal of Files, Fleming Surveys, Inc., dated 10/12/01
2	71498.asc	7/14/98	"Topo" of hillside
3	61600.asc	6/16/00	Trenches
4	122000.asc	12/20/00	Added trenches
5	42301.asc	4/23/01	Bores
6	9601.asc	9/6/01 & 9/7/01	Cross sections

This transmittal is per requirements of DCPD Procedure CF3.ID17.

If you have questions please contact me at (805) 595-6321 or A. Tafoya at (805) 595-6392.

Richard L. Klimczak
 Project Engineer
 Diablo Canyon Used Fuel Storage Project

cc: LJStrickland SLO B3 w/o
 BHPatton SLO BB w/o
 AFTafoya SLO B10
 WPage 245 Market N4C, 422B w/o
 JCYoung 245 Market N4C, 413C w/o
 DCPD Chronological File
 DCPD RMS DCPD 119/1
 DCPD File No. 72.10.05

GEO.DC.PP.01.03 Rev. 1

42301.ASC

167,60266.255870722170000,10873.532097572580000,306.106000000000000,BORECTFA
168,60158.251874317640000,10908.356706366500000,305.736000000000000,BORE01A
169,60092.640256130250000,10990.101588700710000,318.864000000000000,BORE01B
170,60134.829073928110000,11101.535504892410000,323.002000000000000,BORE01C
171,60141.845489351130000,11193.118651396620000,325.249000000000000,BORE01D
172,60208.271361286180000,11378.710508145980000,316.781000000000000,BORE01G
173,60120.334498442410000,11384.969447848240000,337.654000000000000,BORE01E
174,59999.083641240850000,11044.959746739750000,346.623000000000000,BORE01H
175,59913.901425639340000,10999.219236574050000,359.590000000000000,TOPOPOINT
176,59867.342311764190000,10903.296215978570000,351.277000000000000,TOPOPOINT
177,59751.500807354660000,10945.125520074330000,386.709000000000000,TOPOPOINT
178,59772.282250623520000,10996.760863567540000,395.397000000000000,TOPOPOINT
179,59883.340643193420000,11138.866600062560000,390.640000000000000,BORE01F
180,59600.079729418060000,10978.622866559040000,422.734000000000000,SWITCHBACK
181,59687.510623138450000,11077.878168247440000,436.729000000000000,STAKE
182,59736.749714209490000,11207.759577677340000,447.883000000000000,EDGE OF ROAD
183,59760.650965863450000,11309.800475156600000,456.028000000000000,ROAD INTERSECTION
184,59669.034334645950000,11275.445757615080000,481.180000000000000,EDGE OF ROAD
185,59575.148433126000000,11296.412361436070000,511.876000000000000,BORETEMP MARKER
186,59490.267235867700000,11193.389709358980000,510.514000000000000,SWITCHBACK
187,59460.578072059810000,11313.467682311510000,551.698000000000000,EDGE OF ROAD
188,59463.889559621200000,11407.904095284100000,566.954999999999900,BORE01TEMP

GEO.DC.PP.01.03 Rev.1

Foundation Engineering

SECOND EDITION

RALPH B. PECK

Professor of Foundation Engineering
University of Illinois at Urbana-Champaign

WALTER E. HANSON

Consulting Engineer and Senior Partner
Hanson Engineers Incorporated, Springfield, Illinois

THOMAS H. THORNBURN

Professor of Civil Engineering
University of Illinois at Urbana-Champaign

JOHN WILEY & SONS

New York • Chichester • Brisbane • Toronto • Singapore

page 19 of 30

GEO.DC.PP.01.03 Rev. 1

362

22/Foundations on Rock

Table 22.1 Allowable Pressures on Rock (Tons/Sq Ft) Abstracts from Various Building Codes^a

Material	Code ^b			
	A	B	C	D
Massive crystalline bedrock including granite, diorite, gneiss, traprock, hard limestone, and dolomite	100	100	$0.2q_u^c$	10
Foliated rocks such as schist or slate in sound condition	40	40	$0.2q_u$	4
Bedded limestone in sound condition	40	15	$0.2q_u$	4
Sedimentary rock, including hard shales and sandstones	25	15	$0.2q_u$	3
Soft or broken bedrock (excluding shale), and soft limestone	10		$0.2q_u$	
Soft shale	4		$0.2q_u$	

Note: The New York City (1970) code refers specifically to the geological formations in the locality and to their condition. For example, 60 tons/sq ft are allowed on *hard sound rock*, defined as follows: "Includes crystalline rocks such as Fordham gneiss, Ravenswood gneiss, Palisades diabase, Manhattan schist. Characteristics are: the rock rings when struck with a pick or bar; does not disintegrate after exposure to air or water; breaks with sharp fresh fracture; cracks are unweathered and less than $\frac{3}{8}$ in. wide, generally no closer than 3 ft apart; core recovery with a double tube, diamond core barrel is generally 86 per cent or greater for each 5 ft run." Such provisions, based on local experience and conditions, represent excellent practice.

^a Values do not include increases allowed for embedment.

^b A = BOCA (1968); B = National Building Code (1967); C = Uniform Building Code (1964); D = Los Angeles (1959).

^c q_u = unconfined compressive strength.

the design is based on these values, the settlement of the foundation should not exceed 0.5 in., even for large loaded areas.

The RQD for use in Table 22.2 should be the average within a depth below foundation level equal to the width of the foundation, provided the RQD is fairly uniform within that depth. If the upper part of the rock, within a depth of about $B/4$, is of lower quality, the value for this part should be used or the inferior rock should be removed. Since the values in Table 22.2 are based on limiting the settlement, they should not be increased if the foundation is embedded into the rock. Although some building codes arbitrarily allow substantial increases in contact pressure if a pier is drilled into the rock two or three diameters, or allow increases attributed to the development of side friction between the embedded portions of the piers and the rock, such

Table 22.2 Allowable Contact Pressure q_a on Jointed Rock

RQD	q_a^a (tons/sq ft)	q_a^a (lb/sq in)
100	300	4170
90	200	2780
75	120	1660
50	65	970
25	30	410
0	10	140

^a If tabulated value of q_a exceeds unconfined compressive strength q_u of intact samples of the rock, as it might in the case of some clay shales, for instance, take $q_a = q_u$.

allowances are usually based on the incorrect premise that the capacity of the piers is governed by the bearing capacity rather than the compressibility of the rock.

ROB WHITE

GEO.DCOP.01.03 Rev.1

**TECHNICAL ENGINEERING AND DESIGN GUIDES
AS ADAPTED FROM THE
US ARMY CORPS OF ENGINEERS, No. 7**

BEARING CAPACITY OF SOILS



Published by
ASCE Press
American Society of Civil Engineers
345 East 47th Street
New York, New York 10017-2398

GEO.DC.PP.01.03 Rev. 1

BEARING CAPACITY OF SOILS

26

CHAPTER 4

SHALLOW FOUNDATIONS

4-1. Basic Considerations

Shallow foundations may consist of spread footings supporting isolated columns, combined footings for supporting loads from several columns, strip footings for supporting walls, and mats for supporting the entire structure.

A. SIGNIFICANCE AND USE. These foundations may be used where there is a suitable bearing stratum near the ground surface and settlement from compression or consolidation of underlying soil is acceptable. Potential heave of expansive foundation soils should also be acceptable. Deep foundations should be considered if a suitable shallow bearing stratum is not present or if the shallow bearing stratum is underlain by weak, compressible soil.

B. SETTLEMENT LIMITATIONS. Settlement limitation requirements in most cases control the pressure which can be applied to the soil by the footing. Acceptable limits for total downward settlement or heave are often 1 to 2 inches or less. Refer to EM 1110-1-1904 for evaluation of settlement or heave.

1. Total Settlement. Total settlement should be limited to avoid damage with connections in structures to outside utilities, to maintain adequate drainage and serviceability, and to maintain adequate freeboard of embankments. A typical allowable settlement for structures is 1 inch.

2. Differential Settlement. Differential settlement nearly always occurs with total settlement and must be limited to avoid cracking and other damage in structures. A typical allowable differential/span length ratio Δ/L for steel and concrete frame structures is 1/500 where Δ is the differential movement within span length L .

C. BEARING CAPACITY. The ultimate bearing capacity should be evaluated using results from a detailed in situ and laboratory study with suitable theoretical analyses given in 4-2. Design and allowable bearing capacities are subsequently determined according to Table 1-1.

4-2. Solution of Bearing Capacity

Shallow foundations such as footings or mats may undergo either a general or local shear failure. Local shear occurs in loose sands which undergo large strains without complete failure. Local shear may also occur for foundations in sensitive soils with high ratios of peak to residual strength. The failure pattern for general shear is modeled by Figure 1-3. Solutions of the general equation are provided using the Terzaghi, Meyerhof, Hansen and Vesic models. Each of these models have different capabilities for considering foundation geometry and soil conditions. Two or more models should be used for each design case when practical to increase confidence in the bearing capacity analyses.

A. GENERAL EQUATION. The ultimate bearing capacity of the foundation shown in Figure 1-6 can be determined using the general bearing capacity Equation 1-1

$$q_u = cN_c \zeta_c + \frac{1}{2} B' \gamma'_s N_\gamma \zeta_\gamma + \sigma'_0 N_q \zeta_q \quad (4-1)$$

where

q_u = ultimate bearing capacity, ksf

c = unit soil cohesion, ksf

B' = minimum effective width of foundation $B - 2e_s$, ft

e_s = eccentricity parallel with foundation width B , M_b/Q , ft

M_b = bending moment parallel with width B , kips-ft

Q = vertical load applied on foundation, kips

γ'_s = effective unit weight beneath foundation base within the failure zone, kips/ft³ [1-6]

σ'_0 = effective soil or surcharge pressure at the foundation depth D , $\gamma'_0 \cdot D$, ksf

γ'_0 = effective unit weight of soil from ground surface to foundation depth, kips/ft³

D = foundation depth, ft

SHALLOW FOUNDATIONS

Table 4-1. Terzaghi dimensionless bearing capacity factors (after Bowles 1988)

ϕ'	N_q	N_c	N_γ	ϕ'	N_q	N_c	N_γ
28	17.81	31.61	15.7	0	1.00	5.70	0.0
30	22.46	37.16	19.7	2	1.22	6.30	0.2
32	28.52	44.04	27.9	4	1.49	6.97	0.4
34	36.50	52.64	36.0	6	1.81	7.73	0.6
35	41.44	57.75	42.4	8	2.21	8.60	0.9
36	47.16	63.53	52.0	10	2.69	9.60	1.2
38	61.55	77.50	80.0	12	3.29	10.76	1.7
40	81.27	95.66	100.4	14	4.02	12.11	2.3
42	108.75	119.67	180.0	16	4.92	13.68	3.0
44	147.74	151.95	257.0	18	6.04	15.52	3.9
45	173.29	172.29	297.5	20	7.44	17.69	4.9
46	204.19	196.22	420.0	22	9.19	20.27	5.8
48	287.85	258.29	780.1	24	11.40	23.36	7.8
50	415.15	347.51	1153.2	26	14.21	27.09	11.7

N_c, N_q, N_γ = dimensionless bearing capacity factors of cohesion c , soil weight in the failure wedge, and surcharge q terms

$\zeta_c, \zeta_\gamma, \zeta_q$ = dimensionless correction factors of cohesion c , soil weight in the failure wedge, and surcharge q accounting for foundation geometry and soil type

1. Net Bearing Capacity. The net ultimate bearing capacity q'_u is the maximum pressure that may be applied to the base of the foundation without undergoing a shear failure that is in addition to the overburden pressure at depth D .

$$q'_u = q_u - \gamma_D \cdot D \quad (4-2)$$

2. Bearing Capacity Factors. The dimensionless bearing capacity factors N_c , N_q , and N_γ are functions of the effective friction angle ϕ' and depend on the model selected for solution of Equation 4-1.

3. Correction Factors. The dimensionless correction factors ζ consider a variety of options for modeling actual soil and foundation conditions and depend on the model selected for solution of the ultimate bearing capacity. These options are foundation shape with eccentricity, inclined loading, foundation depth, foundation base on a slope, and a tilted foundation base.

B. TERZAGHI MODEL. An early approximate solution to bearing capacity was defined as general shear failure (Terzaghi 1943). The Terzaghi model is applicable to level strip footings placed on or near

a level ground surface where foundation depth D is less than the minimum width B . Assumptions include use of a surface footing on soil at plastic equilibrium and a failure surface similar to Figure 1-3a. Shear resistance of soil above the base of an embedded foundation is not included in the solution.

1. Bearing Capacity Factors. The Terzaghi bearing capacity factors N_c and N_q for general shear are shown in Table 4-1 and may be calculated by

$$N_c = (N_q - 1) \cot \phi' \quad (4-3a)$$

$$N_q = \frac{e^{(270 - \phi')/180) \tan \phi'}}{2 \cos^2(45 + \phi'/2)} \quad (4-3b)$$

Factor N_γ depends largely on the assumption of the angle ψ in Figure 1-3a. N_γ varies from minimum values using Hansen's solution to maximum values using the original Terzaghi solution. N_γ , shown in Table 4-1, was backfigured from the original Terzaghi values assuming $\psi = \phi'$ (Bowles 1988).

2. Correction Factors. The Terzaghi correction factors ζ_c and ζ_γ consider foundation shape only and are given in Table 4-2. $\zeta_q = 1.0$ (Bowles 1988).

C. MEYERHOF MODEL. This solution considers correction factors for eccentricity, load inclination, and foundation depth. The influence of the shear strength of soil above the base of the foundation is considered in this solution. Therefore, beneficial effects of the foundation depth can be included in the analysis. Assumptions include use of a shape factor ζ_q

GEO.DC.PP.01.03 Rev.1

BEARING CAPACITY OF SOILS

30

Table 4-4. Meyerhof, Hansen, and Vesic dimensionless bearing capacity Factors

ϕ	N_c	N_c	N_q	N_q		
				Meyerhof	Hansen	Vesic
0	1.00	5.14	1.00	0.00	0.00	0.00
2	1.07	5.63	1.20	0.01	0.01	0.15
4	1.15	6.18	1.43	0.04	0.05	0.34
6	1.23	6.81	1.72	0.11	0.11	0.57
8	1.32	7.53	2.06	0.21	0.22	0.86
10	1.42	8.34	2.47	0.37	0.39	1.22
12	1.52	9.28	2.97	0.60	0.63	1.69
14	1.64	10.37	3.59	0.92	0.97	2.29
16	1.76	11.63	4.34	1.37	1.43	3.06
18	1.89	13.10	5.26	2.00	2.08	4.07
20	2.04	14.83	6.40	2.87	2.95	5.39
22	2.20	16.88	7.82	4.07	4.13	7.13
24	2.37	19.32	9.60	5.72	5.75	9.44
26	2.56	22.25	11.85	8.00	7.94	12.54
28	2.77	25.80	14.72	11.19	10.94	16.72
30	3.00	30.14	18.40	15.67	15.07	22.40
32	3.25	35.49	23.18	22.02	20.79	30.21
34	3.54	42.16	29.44	31.15	28.77	41.06
36	3.85	50.59	37.75	44.43	40.05	56.31
38	4.20	61.35	48.93	64.07	56.17	78.02
40	4.60	75.31	64.19	93.69	79.54	109.41
42	5.04	93.71	85.37	139.32	113.95	155.54
44	5.55	118.37	115.31	211.41	165.58	224.63
46	6.13	152.10	158.50	328.73	244.64	330.33
48	6.79	199.26	222.30	526.44	368.88	495.99
50	7.55	266.88	319.05	873.84	568.56	762.85

1. Restrictions. Foundation shape with eccentricity ζ_{ci} , ζ_{yi} , and ζ_{qi} and inclined loading ζ_{ci} , ζ_{yi} , and ζ_{qi} correction factors may not be used simultaneously. Correction factors not used are unity.

2. Eccentricity. Influence of bending moments is evaluated as in the Meyerhof model.

3. Inclined loads. The B component in Equation 4-1 should be width B if horizontal load T is parallel with B or should be W if T is parallel with length W .

E. VESIC MODEL. Table 4-6 illustrates the Vesic dimensionless bearing capacity and correction factors for solution of Equation 4-1.

1. Bearing Capacity Factors. N_c and N_q are identical with Meyerhof's and Hansen's factors. N_q was taken from an analysis by Caquot and Kerisel (1953) using $\psi = 45 + \phi/2$.

2. Local Shear. A conservative estimate of N_q may be given by

$$N_q = (1 + \tan\phi') \cdot e^{\tan\phi'} \cdot \tan^2 \left[45 + \frac{\phi'}{2} \right] \quad (4-9)$$

Equation 4-9 assumes a local shear failure and leads to a lower bound estimate of q_u . N_q from Equation 4-9 may also be used to calculate N_c and N_q by the equations given in Table 4-6.

F. COMPUTER SOLUTIONS. by computer programs provide effective methods of estimating ultimate and allowable bearing capacities.

1. Program CBEAR. Program CBEAR (Mosher and Pace 1982) can be used to calculate the bearing capacity of shallow strip, rectangular, square, or circular footings on one or two soil layers. This program uses the Meyerhof and Vesic bearing capacity factors and correction factors.

GEO.DC.PP.01.03 Rev. 1

BEARING CAPACITY OF SOILS

34

K_{ps} = punching shear coefficient, Figure 4-2a, 4-2b, and 4-2c

ϕ_{sand} = angle of internal friction of upper dense sand, degrees

S_s = shape factor

q_u = ultimate bearing capacity of upper dense sand, ksf

The punching shear coefficient k_{ps} can be found from the charts in Figure 4-2 using the undrained shear strength of the lower soft clay and a punching shear parameter C_{ps} . C_{ps} , ratio of ζ/ϕ_{sand} where ζ is the average mobilized angle of shearing resistance on the assumed failure plane, is found from Figure 4-2d using ϕ_{sand} and the bearing capacity ratio R_{bc} . $R_{bc} = 0.5\gamma_{sand}BN_u/(C_uN_d)$. B is the diameter of a circular footing or width of a wall footing. The shape factor S_s , which varies from 1.1 to 1.27, may be assumed unity for conservative design.

3. Stiff Over Soft Clay. Punching shear failure is assumed for stiff over soft clay.

a. $D = 0.0$. The ultimate bearing capacity can be calculated for a footing on the ground surface by (Brown and Meyerhof 1969)

Wall Footing:

$$q_u = C_{u,upper}N_{cw,0} \quad (4-11a)$$

Circular Footing:

$$N_{cw,0} = 1.5 \frac{H_i}{B_{dia}} + 5.14 \frac{C_{u,lower}}{C_{u,upper}} \leq 5.14 \quad (4-11b)$$

$$q_u = C_{u,upper}N_{cw,0} \quad (4-11c)$$

$$N_{cc,0} = 3.0 \frac{H_i}{B_{dia}} + 6.05 \frac{C_{u,lower}}{C_{u,upper}} \leq 6.05 \quad (4-11d)$$

where

$C_{u,upper}$ = undrained shear strength of the stiff upper clay, ksf

$C_{u,lower}$ = undrained shear strength of the soft lower clay, ksf

$N_{cw,0}$ = bearing capacity factor of the wall footing

$N_{cc,0}$ = bearing capacity factor of the circular footing

B_{dia} = diameter of circular footing, ft

A rectangular footing may be converted to a circular footing by $B_{dia} = 2(BW/\pi)^{1/2}$ where B = width and W

= length of the footing. Factors $N_{cw,0}$ and $N_{cc,0}$ will overestimate bearing capacity by about 10 percent if $C_{u,lower}/C_{u,upper} \geq 0.7$. Refer to Brown and Meyerhof (1969) for charts of $N_{cw,0}$ and $N_{cc,0}$.

b. $D > 0.0$. The ultimate bearing capacity can be calculated for a footing placed at depth D by

Wall Footing:

$$q_u = C_{u,upper}N_{cw,D} + \gamma D \quad (4-12a)$$

Circular Footing:

$$q_u = C_{u,upper}N_{cc,D} + \gamma D \quad (4-12b)$$

where

$N_{cw,D}$ = bearing capacity factor of wall footing with $D > 0.0$

$N_{cc,D}$ = bearing capacity factor of rectangular footing with $D > 0.0$

$$= N_{cw,0}[1 + 0.2(B/W)]$$

γ = wet unit soil weight of upper soil, kips/ft³

D = depth of footing, ft

$N_{cw,D}$ may be found using Table nd $N_{cw,0}$ from Equation 4-11b. Refer to Department of the Navy (1982) for charts that can be used to calculate bearing capacities in two layer soils.

4. Computer Analysis. The bearing capacity of multilayer soils may be estimated from computer solutions using program CBEAR (Mosher and Pace 1982). Program UTEXAS2 (Edris 1987) calculates FS for wall footings and embankments, which have not been validated with field experience. UTEXAS2 is recommended as a supplement to CBEAR until FS have been validated.

H. CORRECTION FOR LARGE FOOTINGS AND MATS. Bearing capacity, obtained using Equation 4-1 and the bearing capacity factors, gives capacities that are too large for widths $B > 6$ ft. This is apparently because the $0.5 \cdot B' \gamma' N_{cw,0}$ term becomes too large (DeBeer 1965; Vesic 1969).

1. Settlement usually controls the design and loading of large dimensioned structures because the foundation soil is stressed by the applied loads to deep depths.

2. Bearing capacity may be corrected for large footings or mats by multiplying the surcharge

Kent Fene'

GEO.P.C.P.P.01.03 Rev.1

1997

**UNIFORM
BUILDING
CODE™**

VOLUME 2

**STRUCTURAL ENGINEERING DESIGN
PROVISIONS**



CHAP. 16, DIV. I
1611.5
1612.3.2

1997 UNIFORM BUILDING CODE

GEO. D. CPT. 01.03 Rev. 1

walls under a load of 5 psf (0.24 kN/m²) shall not exceed $\frac{1}{240}$ of the span for walls with brittle finishes and $\frac{1}{120}$ of the span for walls with flexible finishes. See Table 16-O for earthquake design requirements where such requirements are more restrictive.

EXCEPTION: Flexible, folding or portable partitions are not required to meet the load and deflection criteria but must be anchored to the supporting structure to meet the provisions of this code.

1611.6 Retaining Walls. Retaining walls shall be designed to resist loads due to the lateral pressure of retained material in accordance with accepted engineering practice. Walls retaining drained soil, where the surface of the retained soil is level, shall be designed for a load, H , equivalent to that exerted by a fluid weighing not less than 30 psf per foot of depth (4.71 kN/m²/m) and having a depth equal to that of the retained soil. Any surcharge shall be in addition to the equivalent fluid pressure.

Retaining walls shall be designed to resist sliding by at least 1.5 times the lateral force and overturning by at least 1.5 times the overturning moment, using allowable stress design loads.

1611.7 Water Accumulation. All roofs shall be designed with sufficient slope or camber to ensure adequate drainage after the long-term deflection from dead load or shall be designed to resist ponding load, P , combined in accordance with Section 1612.2 or 1612.3. Ponding load shall include water accumulation from any source, including snow, due to deflection. See Section 1506 and Table 16-C, Footnote 3, for drainage slope. See Section 1615 for deflection criteria.

1611.8 Hydrostatic Uplift. All foundations, slabs and other footings subjected to water pressure shall be designed to resist a uniformly distributed uplift load, F , equal to the full hydrostatic pressure.

1611.9 Flood-resistant Construction. For flood-resistant construction requirements, where specifically adopted, see Appendix Chapter 16, Division IV.

1611.10 Heliport and Helistop Landing Areas. In addition to other design requirements of this chapter, heliport and helistop landing or touchdown areas shall be designed for the following loads, combined in accordance with Section 1612.2 or 1612.3:

1. Dead load plus actual weight of the helicopter.
2. Dead load plus a single concentrated impact load, L , covering 1 square foot (0.093 m²) of 0.75 times the fully loaded weight of the helicopter if it is equipped with hydraulic-type shock absorbers, or 1.5 times the fully loaded weight of the helicopter if it is equipped with a rigid or skid-type landing gear.
3. The dead load plus a uniform live load, L , of 100 psf (4.8 kN/m²). The required live load may be reduced in accordance with Section 1607.5 or 1607.6.

1611.11 Prefabricated Construction.

1611.11.1 Connections. Every device used to connect prefabricated assemblies shall be designed as required by this code and shall be capable of developing the strength of the members connected, except in the case of members forming part of a structural frame designed as specified in this chapter. Connections shall be capable of withstanding uplift forces as specified in this chapter.

1611.11.2 Pipes and conduit. In structural design, due allowance shall be made for any material to be removed for the installation of pipes, conduits or other equipment.

1611.11.3 Tests and inspections. See Section 1704 for requirements for tests and inspections of prefabricated construction.

SECTION 1612 — COMBINATIONS OF LOADS

1612.1 General. Buildings and other structures and all portions thereof shall be designed to resist the load combinations specified in Section 1612.2 or 1612.3 and, where required by Chapter 16, Division IV, or Chapters 18 through 23, the special seismic load combinations of Section 1612.4.

The most critical effect can occur when one or more of the contributing loads are not acting. All applicable loads shall be considered, including both earthquake and wind, in accordance with the specified load combinations.

1612.2 Load Combinations Using Strength Design or Load and Resistance Factor Design.

1612.2.1 Basic load combinations. Where Load and Resistance Factor Design (Strength Design) is used, structures and all portions thereof shall resist the most critical effects from the following combinations of factored loads:

$$1.4D \quad (12-1)$$

$$1.2D + 1.6L + 0.5(L_r \text{ or } S) \quad (12-2)$$

$$1.2D + 1.6(L_r \text{ or } S) + (f_1 L \text{ or } 0.8W) \quad (12-3)$$

$$1.2D + 1.3W + f_1 L + 0.5(L_r \text{ or } S) \quad (12-4)$$

$$1.2D + 1.0E + (f_1 L + f_2 S) \quad (12-5)$$

$$0.9D \pm (1.0E \text{ or } 1.3W) \quad (12-6)$$

WHERE:

- f_1 = 1.0 for floors in places of public assembly, for live loads in excess of 100 psf (4.9 kN/m²), and for garage live load.
= 0.5 for other live loads.
- f_2 = 0.7 for roof configurations (such as saw tooth) that do not shed snow off the structure.
= 0.2 for other roof configurations.

EXCEPTIONS: 1. Factored load combinations for concrete per Section 1909.2 where load combinations do not include seismic forces.

2. Factored load combinations of this section multiplied by 1.1 for concrete and masonry where load combinations include seismic forces.

3. Where other factored load combinations are specifically required by the provisions of this code.

1612.2.2 Other loads. Where F , H , P or T are to be considered in design, each applicable load shall be added to the above combinations factored as follows: 1.3F, 1.6H, 1.2P and 1.2T.

1612.3 Load Combinations Using Allowable Stress Design.

1612.3.1 Basic load combinations. Where allowable stress design (working stress design) is used, structures and all portions thereof shall resist the most critical effects resulting from the following combinations of loads:

$$D \quad (12-7)$$

$$D + L + (L_r \text{ or } S) \quad (12-8)$$

$$D + \left(W \text{ or } \frac{E}{1.4} \right) \quad (12-9)$$

$$0.9D \pm \frac{E}{1.4} \quad (12-10)$$

$$D + 0.75 \left[L + (L_r \text{ or } S) + \left(W \text{ or } \frac{E}{1.4} \right) \right] \quad (12-11)$$

No increase in allowable stresses shall be used with these load combinations except as specifically permitted by Section 1809.2.

1612.3.2 Alternate basic load combinations. In lieu of the basic load combinations specified in Section 1612.3.1, structures and

1997 UNIFORM BUILDING CODE

GEO.DCPP-01.03 Rev. 1

portions thereof shall be permitted to be designed for the most critical effects resulting from the following load combinations. When using these alternate basic load combinations, a one-third increase shall be permitted in allowable stresses for all combinations, including W or E .

$$D + L + (L_r \text{ or } S) \quad (12-12)$$

$$D + L + \left(W \text{ or } \frac{E}{1.4} \right) \quad (12-13)$$

$$D + L + W + \frac{S}{2} \quad (12-14)$$

$$D + L + S + \frac{W}{2} \quad (12-15)$$

$$D + L + S + \frac{E}{1.4} \quad (12-16)$$

EXCEPTIONS: 1. Crane hook loads need not be combined with roof live load or with more than three fourths of the snow load or one half of the wind load.

2. Design snow loads of 30 psf (1.44 kN/m²) or less need not be combined with seismic loads. Where design snow loads exceed 30 psf (1.44 kN/m²), the design snow load shall be included with seismic loads, but may be reduced up to 75 percent where consideration of siting, configuration and load duration warrant when approved by the building official.

1612.3.3 Other loads. Where F , H , P or T are to be considered in design, each applicable load shall be added to the combinations specified in Sections 1612.3.1 and 1612.3.2. When using the alternate load combinations specified in Section 1612.3.2, a one-third

increase shall be permitted in allowable stresses for all combinations including W or E .

1612.4 Special Seismic Load Combinations. For both Allowable Stress Design and Strength Design, the following special load combinations for seismic design shall be used as specifically required by Chapter 16, Division IV, or by Chapters 18 through 23:

$$1.2D + f_1L + 1.0E_m \quad (12-17)$$

$$0.9D \pm 1.0E_m \quad (12-18)$$

WHERE:

f_1 = 1.0 for floors in places of public assembly, for live loads in excess of 100 psf (4.79 kN/m²), and for garage live load.

= 0.5 for other live loads.

SECTION 1613 — DEFLECTION

The deflection of any structural member shall not exceed the values set forth in Table 16-D, based on the factors set forth in Table 16-E. The deflection criteria representing the most restrictive condition shall apply. Deflection criteria for materials not specified shall be developed in a manner consistent with the provisions of this section. See Section 1611.7 for camber requirements. Span tables for light wood-frame construction as specified in Chapter 23, Division VII, shall conform to the design criteria contained therein. For concrete, see Section 1909.5.2.6; for aluminum, see Section 2003; for glazing framing, see Section 2404.2.

$$U = 0.90 \pm E/1.4$$

GEO.DC.PP.01.03 Rev 1

WLA



William Lettis & Associates, Inc.

1777 Rotelho Drive, Suite 262, Walnut Creek, California 94596
Voice: (925) 256-6070 FAX: (925) 256-6076

Mr. Robert White
Geosciences Department
Pacific Gas & Electric Company
245 Market Street, Rm. 421-N4C
San Francisco, CA 94105

November 5, 2001

Re: Completion of Data Reports (formerly appendices)

Dear Rob:

This letter transmits to Geosciences the following Diablo Canyon ISFSI Data Reports (formerly called appendices) that were prepared under the WLA Work Plan, Additional Geologic Mapping, Exploratory Drilling, and Completion of Kinematic Analyses for the Diablo Canyon Power Plant Independent Spent Fuel Storage Installation Site, Rev. 2 (11/28/00) using data collected under that Work Plan and a second WLA Work Plan, Additional Exploratory Drilling and Geologic Mapping for the ISFSI Site, Rev. 1 (9/21/01).

Diablo Canyon ISFSI Data Report A - Geologic Mapping in the Plant Site and ISFSI Site Areas, Rev. 0, November 5, 2001, November 5, 2001, prepared by J. Bachhuber, 42 p.

Diablo Canyon ISFSI Data Report B - Borings in ISFSI Site Area, Rev. 0, November 5, 2001, prepared by J. Bachhuber, 244 p.

Diablo Canyon ISFSI Data Report C - 1998 Geophysical Investigations at the ISFSI Site Area, (Agabian Associates and GeoVision), Rev. 0, November 5, 2001, prepared by J. Bachhuber, 84 p.

Diablo Canyon ISFSI Data Report D - Trenches in the ISFSI Site Area, Rev. 0, November 5, 2001, prepared by J. Bachhuber, 66 p.

Diablo Canyon ISFSI Data Report E - Borehole Geophysical Data (NORCAL Geophysical Consultants, Inc.), Rev. 0, November 5, 2001, prepared by C. Brankman, 303 p.

Diablo Canyon ISFSI Data Report F - Field Discontinuity Measurements, Rev. 0, November 5, 2001, prepared by J. Bachhuber and C. Brankman, 85 p.

Diablo Canyon ISFSI Data Report G - Soil Laboratory Test Data (Cooper Testing Laboratory), Rev. 0, November 5, 2001, prepared by J. Sun, 63 p.

Diablo Canyon ISFSI Data Report H - Rock Strength Data and GSI Sheets, Rev. 0, November 5, 2001, prepared by J. Bachhuber, 37 p.

Page 29 of 30

GEO.DCPP.01.03 KQV.1

WLA

Diablo Canyon ISFSI Data Report J - Rock Laboratory Test Data (GeoTest Unlimited), Rev. 0, November 5, 2001, prepared by J. Sun, 203 p.

Diablo Canyon ISFSI Data Report J - Petrographic Analysis and X-Ray Diffraction of Rock Samples (Spectrum Petrographics, Inc.), Rev. 0, November 5, 2001, prepared by J. Bachhuber, 204 p.

Diablo Canyon ISFSI Data Report K - Petrographic and X-Ray Diffraction Analyses of Clay Beds (Schwein/Christensen Laboratories, Inc.), Rev. 0, November 5, 2001, prepared by J. Bachhuber, 36 p.

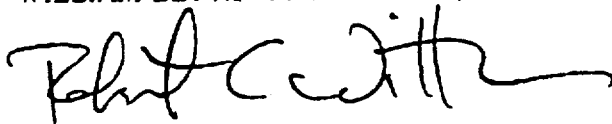
In addition to the revisions of those reports required under the various Work Plans, Mr. Scott Lindvall, the WLA ITR for the ISFSI project, has performed independent technical reviews of the Diablo Canyon ISFSI Data Reports as part of his review of Calculation Package GEO.DCPP.01.21, Analysis of Bedrock Stratigraphy and Geologic Structure at the DCPD ISFSI Site. He finds that the reports clearly and accurately compile and organize the data.

Mr. Albert Tafoya from the Diablo Canyon ISFSI Project Office in San Luis Obispo, Mr. Dale Marcum, NQS Technical Oversight for the project, and William Page of your office provided comments on the August versions of the Diablo Canyon ISFSI Data Reports (formerly called appendices) and their comments have been addressed.

These reports are submitted to you as per the PG&E Geosciences Department Calculation Procedure GEO.001, Rev. 04 (10/10/01).

We look forward to any comments you may have.

Sincerely,
WILLIAM LETTIS & ASSOCIATES, INC.



Robert C. Witter
Project Manager

CC: William Page

CF3.ID4
ATTACHMENT 7.2

TITLE: CALCULATION COVER SHEET

CALC No. 52.27.100.714, R0

RECORD OF REVISIONS

Rev No.	Status	Reason for Revision	Prepared By:	LBIE Screen	LBIE	Check Method*	LBIE Approval		Checked	Supervisor	Registered Engineer
			Initials/ LAN ID/ Date	Yes/ No/ NA	Yes/ No/ NA		PSRC Mtg. No.	PSRC Mtg. Date	Initials/ LAN ID/ Date	Initials/ LAN ID/ Date	Signature/ LAN ID/ Date
0	F	Acceptance of Geosciences Calc. No. GEO.DCPP.01.04, Rev.1 Calc. is in support of 10CFR72, DCPD License Application (ISFSI Dry Cask) to the NRC prior to implementation. Note: Prepared per CF3.ID17 requirements	N.J. NXJ1/ 12/6/01	<input type="checkbox"/> Yes <input type="checkbox"/> No <input checked="" type="checkbox"/> NA	<input type="checkbox"/> Yes <input type="checkbox"/> No <input checked="" type="checkbox"/> NA	<input type="checkbox"/> A <input type="checkbox"/> B <input checked="" type="checkbox"/> C	N/A	N/A	N 45-72 11/6/01	LJS LJS2 11/9/01	LJS LJS2 11/9/01
				<input type="checkbox"/> Yes <input type="checkbox"/> No <input type="checkbox"/> NA	<input type="checkbox"/> Yes <input type="checkbox"/> No <input type="checkbox"/> NA	<input type="checkbox"/> A <input type="checkbox"/> B <input type="checkbox"/> C					
				<input type="checkbox"/> Yes <input type="checkbox"/> No <input type="checkbox"/> NA	<input type="checkbox"/> Yes <input type="checkbox"/> No <input type="checkbox"/> NA	<input type="checkbox"/> A <input type="checkbox"/> B <input type="checkbox"/> C					

*Check Method: A: Detailed Check, B: Alternate Method (note added pages), C: Critical Point Check



CALC. NO. 52.27.100.714
REV. NO. 0
SHEET NO. 3 of 3

SUBJECT Methodology for Determining Sliding Resistance Along Base of DCPD ISFSI Pads

MADE BY NXJ1 DATE 11/6/01 CHECKED BY K1 DATE 11/6/01

Table of Contents:

Section	Type	Title	Page Numbers
1	Index	Cross-Index (For Information Only)	1 - 4
Attachments	"A"	Methodology for Determining Sliding Resistance Along Base of DCPD ISFSI Pads (GEO.DCPD.01.04 Rev. 1)	20



SUBJECT Methodology for Determining Sliding Resistance Along Base of DCPD ISFSI Pads
MADE BY NXJ1 DATE 11/6/01 CHECKED BY M1 AFT2 DATE 11/6/01

1- Cross reference between Geo Sciences calculation Numbers and DCPD (Civil Group's) Calculation Numbers: This section is For Information Only.

Cross-Index

(For Information Only)

Item No.	Geosciences Dept. Calc. No.	Title	DCPD, Civil Calc. No.	Comments
1	GEO.DCPD.01.01	Development of Young's Modulus and Poisson's Ratios for DCPD ISFSI Based on Field Data	52.27.100.711	
2	GEO.DCPD.01.02	Determination of Probabilistically Reduced Peak Bedrock Accelerations for DCPD ISFSI Transporter Analyses	52.27.100.712	
3	GEO.DCPD.01.03	Development of Allowable Bearing Capacity for DCPD ISFSI Pad and CTF Stability Analyses	52.27.100.713	
4	GEO.DCPD.01.04	Methodology for Determining Sliding Resistance Along Base of DCPD ISFSI Pads	52.27.100.714	
5	GEO.DCPD.01.05	Determination of Pseudostatic Acceleration Coefficient for use in DCPD ISFSI Cutslope Stability Analyses	52.27.100.715	
6	GEO.DCPD.01.06	Development of Lateral Bearing Capacity for DCPD CTF Stability Analyses	52.27.100.716	
7	GEO.DCPD.01.07	Development of Coefficient of Subgrade Reaction for DCPD ISFSI Pad Stability Checks	52.27.100.717	
8	GEO.DCPD.01.08	Determination of Rock Anchor Design Parameters for DCPD ISFSI Cutslope	52.27.100.718	
9	GEO.DCPD.01.09	Determination of Applicability of Rock Elastic Stress-Strain Values to	52.27.100.719	Calculation to be replaced by letter



SUBJECT Methodology for Determining Sliding Resistance Along Base of DCPD ISFSI Pads
MADE BY NXJ1 DATE 11/6/01 CHECKED BY K1 AFT2 DATE 11/6/01

Cross-Index

(For Information Only)

Item No.	Geosciences Dept. Calc. No.	Title	DCPD, Civil Calc. No.	Comments
		Stress-Strain Values to Calculated Strains Under DCPD ISFSI Pad		
10	GEO.DCPD.01.10	Determination of SSER 34 Long Period Spectral Values	52.27.100.720	
11	GEO.DCPD.01.11	Development of ISFSI Spectra	52.27.100.721	
12	GEO.DCPD.01.12	Development of Fling Model for Diablo Canyon ISFSI	52.27.100.722	
13	GEO.DCPD.01.13	Development of Spectrum Compatible Time Histories	52.27.100.723	
14	GEO.DCPD.01.14	Development of Time Histories with Fling	52.27.100.724	
15	GEO.DCPD.01.15	Development of Young's Modulus and Poisson's Ratio Values for DCPD ISFSI Based on Laboratory Data	52.27.100.725	
16	GEO.DCPD.01.16	Development of Strength Envelopes for Non-jointed Rock at DCPD ISFSI Based on Laboratory Data	52.27.100.726	
17	GEO.DCPD.01.17	Determination of Mean and Standard Deviation of Unconfined Compression Strengths for Hard Rock at DCPD ISFSI Based on Laboratory Tests	52.27.100.727	
18	GEO.DCPD.01.18	Determination of Basic Friction Angle Along Rock Discontinuities at DCPD ISFSI Based on Laboratory Tests	52.27.100.728	



SUBJECT Methodology for Determining Sliding Resistance Along Base of DCPD ISFSI Pads

MADE BY NXJ1 DATE 11/6/01 CHECKED BY M. AFT2 DATE 11/6/01

Cross-Index

(For Information Only)

Item No.	Geosciences Dept. Calc. No.	Title	DCPD, Civil Calc. No.	Comments
19	GEO.DCPD.01.19	Development of Strength Envelopes for Jointed Rock Mass at DCPD ISFSI Using Hoek-Brown Equations	52.27.100.729	
20	GEO.DCPD.01.20	Development of Strength Envelopes for Shallow Discontinuities at DCPD ISFSI Using Barton Equations	52.27.100.730	
21	GEO.DCPD.01.21	Analysis of Bedrock Stratigraphy and Geologic Structure at the DCPD ISFSI Site	52.27.100.731	
22	GEO.DCPD.01.22	Kinematic Stability Analysis for Cutslopes at DCPD ISFSI Site	52.27.100.732	
23	GEO.DCPD.01.23	Pseudostatic Wedge (SWEDGE) Analyses of DCPD ISFSI Cutslopes	52.27.100.733	
24	GEO.DCPD.01.24	Stability and Yield Acceleration Analysis of Cross-Section I-I'	52.27.100.734	
25	GEO.DCPD.01.25	Determination of Seismic Coefficient Time Histories for Potential Sliding Masses Along Cut Slope Behind ISFSI Pad	52.27.100.735	
26	GEO.DCPD.01.26	Determination of Potential Earthquake-Induced Displacements of Potential Sliding Masses on DCPD ISFSI Slope	52.27.100.736	
27	GEO.DCPD.01.27	Cold Machine Shop Retaining Wall Stability	52.27.100.737	
28	GEO.DCPD.01.28	Roadway Capacity with Transporter	52.27.100.738	



SUBJECT Methodology for Determining Sliding Resistance Along Base of DCPD ISFSI Pads
MADE BY NXJ1 DATE 11/6/01 CHECKED BY K AFT2 DATE 11/6/01

Cross-Index

(For Information Only)

Item No.	Geosciences Dept. Calc. No.	Title	DCPD, Civil Calc. No.	Comments
29	GEO.DCPD.01.29	Determination of Seismic Coefficient Time Histories for Critical Slides on DCPD ISFSI Transport Route	52.27.100.739	
30	GEO.DCPD.01.30	Determination of Potential Earthquake-Induced Displacements of Critical Slides Along DCPD ISFSI Transport Route	52.27.100.740	
31	GEO.DCPD.01.31	Development of Strength Envelopes for Clay Beds	52.27.100.741	
32	GEO.DCPD.01.32	Verification of Computer Program SPCTLR.EXE	52.27.100.742	
33	GEO.DCPD.01.33	UTEXAS3 Computer Program Verification	52.27.100.743	
34	GEO.DCPD.01.34	Verification of Computer Code QUAD4M	52.27.100.744	
35	GEO.DCPD.01.35	Verification of Computer Program DEFORMP	52.27.100.745	
36	GEO.DCPD.01.36	Determination of Design Parameters for ISFSI Fill Slope	52.27.100.746	Calculation to be delayed – retaining wall to be shown on drawing
37	GEO.DCPD.01.37	Development of Freefield Ground Motion Storage Cask Spectra and Time Histories for the Used Fuel Storage Project	52.27.100.747	

PG&E
Geosciences Department
Departmental Calculation Procedure
Attachment 5.2

Number: GEO.001
Revision: 04
Page: 1 of 1

Title: Design Calculation Cover Sheet

PACIFIC GAS AND ELECTRIC COMPANY
GEOSCIENCES DEPARTMENT
CALCULATION DOCUMENT

Calc Number GEO.DCPP.01.04
Revision 1
Date 11/5/01
Calc Pages: 18
Verification Method: A
Verification Pages:

(SEE GEO SCIENCES
ORIGINAL FILES)
ATTN 11/6/01
AT 4/6/01

TITLE: Methodology for determining sliding resistance along the base of DCPD ISFSI
pads

PREPARED BY:

Robert K White

DATE

11/5/01

Robert K White
Printed Name

Geosciences
Organization

VERIFIED BY:

Joseph S. Cluff

DATE

11/5/01

Joseph S. Cluff
Printed Name

Geosciences
Organization

APPROVED BY:

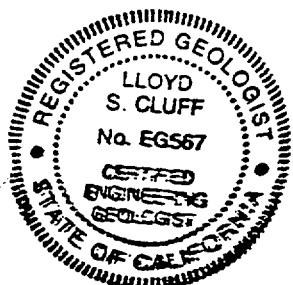
Lloyd S. Cluff

DATE

11/5/01

Lloyd S. Cluff
Printed Name

Geosciences
Organization



Methodology for determining sliding resistance along the base of DCPD ISFSI pads
Calc Number GEO.DCPD.01.04

Record of Revisions

Rev. No.	Reason for Revision	Revision Date
1	revised Appendix I reference to Data Report I; deleted Appendix F reference; added text regarding enveloping values in Analysis; added text regarding backfill recommendations in Analysis and Results	11/5/01

DCPP ISFSI GEOTECHNICAL CALCULATION PACKAGE

Title: Methodology for determining sliding resistance along the base of DCP
ISFSI pads
Calc Number: GEO.DCPP.01.04
Revision: Rev. 1
Author: Robert K. White
Date: November 5, 2001
Verifier: Joseph I. Sun

PURPOSE

As required by Geosciences Work Plan GEO 2001-03, Appendix C, this calculation package documents the criteria for evaluating resistance to sliding beneath the concrete DCP ISFSI pads due to lateral forces generated by an earthquake. In particular, the frictional component of the sliding resistance at the base of the pads is developed based on the range of friction angles expected to be encountered within the rock at the ISFSI site. This sliding resistance will be used in pad stability analyses to be performed by others.

ASSUMPTIONS

1. Pad concrete base-to-rock interface is very rough and tight (concrete is poured on cleaned rough excavated rock surface), such that the weaker sliding surface is in the rock below the interface rather than at the interface. This is a reasonable assumption as described in Bowles (1988), page 551 (page 13, attached), and Peck and others (1974), pg. 426, (page 15, attached).
2. Potential lateral sliding beneath the pads will occur along bedding planes and through intact rock in jointed dolomite, sandstone, and localized areas of weaker, friable rock (Figure 21-41 from GEO.DCPP.01.21). The location and extent of the potential failure will depend on the properties of the bedding planes and the relative proportion and strengths of the unaltered rock and the friable rock beneath any particular pad at the ISFSI site. These are reasonable assumptions because the distribution of rock and

DCPP ISFSI

Calc. Number: GEO.DCPP.01.04 Rev. 1

discontinuities and their related properties at pad grade are relatively well understood, as described in GEO.DCPP.01.21.

3. The maximum extent of potential lateral sliding along a single bedding plane, or a close set there of, is over an area at most half the area of a pad (pad area 68 by 105 feet per Klimczak, 9/27/01 (Drawing PGE-009-SK-001, page 11, attached)). The rest of the potential sliding area will occur through the fractured rock mass or the friable rock. This is a conservative assumption because:
 - a. Bedding is not horizontal, but is variably inclined beneath the pads.
 - b. Field observations show that bedding planes and subhorizontal joints are generally tightly bonded and extend only up to a few tens of feet; clay beds, however, can be longer, depending on their thickness.
 - c. The lateral continuity of bedding is disrupted by the jointed and faulted nature of the rock mass; typical fracture spacing is about $\frac{1}{2}$ to 4 feet. (References: GEO.DCPP.01.21.)
4. Clay beds beneath the pads are limited to two areas (Figure 21-41 from GEO.DCPP.01.21). The clay beds are inclined, so are likely to be partially exposed during excavation for the pad subgrade. The total area of these clay beds within five feet of the pad subgrade is roughly equal to one pad area.
5. Bedding plane and rock mass strength properties beneath a pad can be proportioned to provide a representative strength value for simultaneous sliding through both. This is a reasonable assumption because the strength properties for bedding planes and rock mass are well documented (GEO.DCPP.01.19 and GEO.DPP.01.20) and because the total resistance along a failure plane is by definition the sum of the individual resistances along the plane relatively proportioned to their length along the plane.
6. The entire site is excavated but only one or two pads at a time are constructed, thereby leaving at least one edge of the nearly eight-foot-thick pad partially or nearly completely exposed (unembedded). Thus, no passive resistance to sliding on pad edges is assumed. Conservatively, the very minor contribution to resistance to sliding on pad sides is also ignored. Also, the pads are not assumed to interact or be connected in any way so as to reduce or eliminate potential sliding. These

DCPP ISFSI

Calc. Number: GEO.DCPP.01.04 Rev. 1

assumptions may be either conservative or realistic, depending upon the final pad design construction sequence.

DESIGN INPUTS

1. Friction angle for sandstone and dolomite rock mass of 50 degrees, from Geosciences calculation package GEO.DCPP.01.19.
2. Friction angle of 50 degrees for non-jointed (altered) rock from Geosciences calculation package GEO.DCPP.01.16.
3. Friction angle of 31 degrees for sandstone bedding planes, 21 degrees for clay coated sandstone bedding planes, 33 degrees for dolomite bedding planes, and 18 degrees for clay coated dolomite bedding planes, all from Geosciences calculation package GEO.DCPP.01.20, Figures 20-3 and 20-6.
4. Drained strength friction angle of 22 degrees and undrained strength friction angle of either 29 degrees and 0 psf cohesion or 15 degrees and 800 psf cohesion (whichever is lower for a given normal stress) for clay beds from Geosciences calculation package GEO.DCPP.01.31.
5. Rock unit weight of 140 pcf for rock mass beneath pads, from Witter, 11/5/01, Data Report I.
6. Pad dimensions of 68 x 105 feet from Klimczak, 9/27/01 (Drawing PGE-009-SK-001, page 11, attached).

METHODOLOGY

1. Summarize the failure envelopes for the various rock types underlying the ISFSI site given the potential range of failure mechanisms. Select the most representative failure envelope, or a representative range of envelopes, for further development of sliding resistance beneath the pads.
2. Develop the sliding resistance beneath the pads as a function of the failure envelope and pad variables for use in sliding analyses by others.
3. Determine depth of removal required for clay beds beneath the pads to prevent preferential sliding along clay beds.

DCPP ISFSI

Calc. Number: GEO.DCPP.01.04 Rev. 1

SOFTWARE

No software is used to perform calculations.

ANALYSIS

1. The failure envelopes of the various types of rock underlying the ISFSI site are summarized as follows:

At the scale of potentially very large sliding surfaces (with dimensions of, say, 100 feet or greater) such as on the hillside above the ISFSI pads, the strength of cemented sandstone and dolomite (jointed rock mass) is governed by a combination of both intact rock and discontinuities and is determined indirectly by laboratory data on intact rock samples, field observations of rocks at the surface and from borings, and field measurements of discontinuities, using the Hoek-Brown equations to derive strength envelopes (GEO.DCPP.01.19). For the sandstone and dolomite rock mass, a failure envelope with a friction angle of $\phi = 50$ degrees is observed to provide a lower bound to all Hoek-Brown envelopes (GEO.DCPP.01.19). These large failures are assumed to slide on clay beds or clay seams typically observed in the sandstone and dolomite rock mass. Clay bed drained strength is defined by a friction angle of $\phi = 22$ degrees as determined by laboratory tests on clay bed samples (GEO.DCPP.01.31). Similarly, clay bed undrained strength is defined by a friction angle of $\phi = 29$ degrees and a cohesion of 0 psf, or $\phi = 15$ degrees and a cohesion of 800 psf, whichever is lower for a given normal stress (GEO.DCPP.01.31). (The two undrained strength envelopes cross at about 2500 psf, or 18 feet of overburden.)

At the scale of much smaller sliding surfaces (with dimensions of, say, a few tens of feet or less) such as in the cutslopes surrounding the ISFSI pads, the strength of discontinuities within the jointed rock mass governs the failure. This strength is also determined indirectly by both laboratory and field data, using the Barton equations to derive strength envelopes (GEO.DCPP.01.20). For sandstone bedding planes, a straight-line failure envelope with a friction angle of $\phi = 31$ degrees is observed to approximate the mean curved envelope derived from the Barton equations at low overburden pressures (Figure 20-6 of GEO.DCPP.01.20). The mean curved failure

DCPP ISFSI

Calc. Number: GEO.DCPP.01.04 Rev. 1

envelope represents a sandstone bedding plane that in places (assumed up to half) is coated with clay film, with average roughness and strength. Similarly, a straight-line failure envelope with a friction angle of $\phi = 21$ degrees is observed to approximate the lower bound curved envelope derived from the Barton equations at low overburden pressures (Figure 20-6 of GEO.DCPP.01.20). The lower bound curved failure envelope represents a sandstone bedding plane completely coated with clay film, with lower bound (mean minus one sigma) roughness and strength. Because these clay films are very thin and unsaturated, these failure envelopes are valid for both drained and undrained loading. For dolomite bedding planes, the mean and lower bound failure envelope friction angles for similar bedding plane conditions are 33 and 18 degrees, respectively (Figure 20-3 of GEO.DCPP.01.20). It is noted that the lower bound friction angles are nearly the same as the value of 22 degrees derived for the drained strength of continuous clay beds within the dolomite (GEO.DCPP.01.31), providing increased confidence in the appropriateness of the clay bed value.

At an intermediate scale of potential sliding failure surfaces, such as beneath the ISFSI pads (with dimensions 68 by 105 feet from Klimczak, 9/27/01 (Drawing PGE-009-SK-001, page 11, attached)), the influence of discontinuities on the strength of the jointed rock mass may be greater than defined by the Hoek-Brown equations; that is, the friction angle at this scale may be less than 50 degrees. In this case, a friction angle weighted to account for the relative contribution of the different failure mechanisms may be more appropriate.

The strength of friable sandstone and dolomite (non-jointed rock mass) is governed by the intact rock as discontinuities have weathered and are no longer effective potential failure planes (GEO.DCPP.01.16). A representative failure envelope with a friction angle of $\phi = 50$ degrees is determined by laboratory tests of this material (GEO.DCPP.01.16).

2. The sliding resistance beneath the pads as a function of the failure envelopes described above is developed as follows:

The force per foot of pad width, S , resisting sliding beneath the pad is defined by:

DCPP ISFSI

Calc. Number: GEO.DCPP.01.04 Rev. 1

$$S = \text{tangent}(\phi) \cdot W \quad (1)$$

(Source: Peck and others, 1974, page 15, attached)

where: ϕ = representative friction angle along sliding surfaceW = weight of casks, pad, and any underlying rock above sliding surface
per unit pad width (minimally, take as weight of casks and pad only)

From the discussion above, for the condition where sliding within rock is controlled by failure through numerous smaller discontinuities and intact rock, a friction angle of 50 degrees applies. For the condition where sliding also involves a single bedding plane completely coated with clay film with a friction angle of 18 degrees (the lower of the values determined for bedding planes within sandstone and dolomite) and a maximum observed length of a few tens of feet, or at most about half the length of the pad (about 35 feet in shortest direction), then a friction angle weighted by relative length over which each mechanism is assumed effective to account for this combined sliding mechanism is calculated as follows:

$$\phi_{\text{weighted}} = \text{tangent}^{-1} \left(\frac{1}{2} \cdot \tan(18) + \frac{1}{2} \cdot \tan(50) \right) = 37, \text{ say, } 36 \text{ degrees.}$$

3. To ensure sliding occurs along rock bedding planes rather than along the clay beds (with an undrained strength of 29 degrees) identified in two areas beneath the pads (Figure 21-41 from GEO.DCPP.01.21), portions of the clay beds need to be removed. The depth of removal is determined by equating the sliding resistance along a clay bed, assumed continuous and horizontal for the entire length of the pad, and including the passive resistance required to break through the overlying rock along the edge of the pad, with the sliding resistance along a failure surface just beneath the pad within a combination of bedding plane and rock mass, as follows:

$$W_2 \cdot \text{tangent} \phi_{\text{clay}} + P_{\text{p rock mass}} \geq W_1 \cdot \text{tangent} \phi_{\text{weighted}} \quad (2)$$

where: ϕ = representative friction angle along sliding surface W_1 = weight of casks and pad W_2 = weight of casks, pad, and underlying rock above sliding surface P_p = passive force = $\tan^2(45 + \phi_{\text{rock mass}}/2) \cdot \gamma \cdot (H^2/2) \cdot L$
(from Peck and others, 1974, page 16, attached) γ = rock unit weight, pcf

DCPP ISFSI

Calc. Number: GEO.DCPP.01.04 Rev. 1

H = height of passive wedge (depth for clay bed removal)

L = length of exposed side of pad, 105 feet

and: weight of casks = $20 \cdot 360 \text{ k} = 7200 \text{ k}$ from Klimczak, 9/27/01, page 10, attached;

weight of interior pad $0.15 \cdot 105 \cdot 68 \cdot 7.75 = 8300 \text{ k}$, dimensions from Klimczak, 9/27/01 (Dwg PGE-009-SK-001, page 11, attached)

therefore, $W_1 = 7200 + 8300 = 15500 \text{ k}$.

$W_2 = 15500 + 0.14 \cdot 68 \cdot 105 \cdot H = 15500 + 1000H$.

$P_p = \tan^2 (45+50/2) \cdot 0.14 \cdot (H^2 / 2) \cdot 105 = 55.5 \cdot H^2$

substituting: $(15500 + 1000H) \cdot \tan 29 + 55.5 \cdot H^2 = 15500 \cdot \tan 36$

$(15500 + 1000H) \cdot 0.554 + 55.5 \cdot H^2 = 15500 \cdot 0.727$

$55.5 \cdot H^2 + 554H - 2669 = 0$

and solving: $H = 3.6 \text{ feet}$

Therefore, to obtain sufficient passive resistance to ensure sliding occurs on rock bedding rather than on a clay bed, the clay bed should be excavated to a depth of 3.5 feet beneath the proposed the pad base. This analysis is conservative in that it assumes the clay bed area remains constant, whereas the area is reduced as it is excavated, and actual resistance as a function of remaining clay bed and replacement material, will be higher. The analysis is also conservative in that H decreases slightly as the number of casks decreases, so the calculated value of H envelopes all pad loading conditions. This analysis is unaffected by changes in vertical acceleration, as any changes would apply equally to both sides of the above equation, thus canceling each other out. Replacing excavated material with a lean concrete mix will ensure engineering properties beneath the pad remain essentially the same as before excavation of the clay beds.

RESULTS

The sliding resistance within the rock beneath the pads is a function of the representative friction angle along the sliding surface in the rock mass. This angle varies between 50 degrees and 36 degrees, with the latter representing a very conservative lower bound. Thus, the force S in equation (1), above, varies between 1.2W and 0.7W. Clay beds beneath portions of the pads should be excavated to a depth of 3.5 feet beneath the pad

DCPP ISFSI

Calc. Number: GEO.DCPP.01.04 Rev. 1

base to ensure sliding occurs along rock bedding rather than along the beds, with an undrained friction angle of 29 degrees, and replaced with a lean concrete backfill..

CONCLUSIONS

The sliding resistance beneath the DCPD ISFSI pads is defined as a function of rock mass friction angle and pad weight for use by others in pad stability analyses. A range of values is provided for sensitivity studies.

REFERENCES

1. Bowles, J. E., 1988, Foundation Analysis and Design, 4th edition, McGraw-Hill.
2. Peck, R. B., Hanson, W. E., and Thornburn, T. H., 1974, Foundation Engineering, 2nd edition, John Wiley and Sons.
3. Geosciences calculation package GEO.DCPP.01.16, rev. 1, "Development of strength envelopes for non-jointed rock at DCPD ISFSI based on laboratory data."
4. Geosciences calculation package GEO.DCPP.01.19, rev. 1, "Development of strength envelopes for jointed rock mass at DCPD ISFSI using Hoek-Brown equations."
5. Geosciences calculation package GEO.DCPP.01.20, rev. 1, "Development of strength envelopes for shallow discontinuities at DCPD ISFSI using Barton equations."
6. Geosciences calculation package GEO.DCPP.01.21, rev. 0, " Analysis of Bedrock Stratigraphy and Geologic Structure at the DCPD ISFSI Site."
7. Geosciences calculation package GEO.DCPP.01.31, rev. 0, "Development of strength envelopes for clay beds at DCPD ISFSI based on field and laboratory data."
8. Witter (11/5/01): letter from Rob Witter to Rob White, entitled "Completion of Data Reports," dated 11/5/01, and accompanying Data Report I, Rock Laboratory Test Data, rev. 0.

DCPP-ISFSI

Calc. Number: GEO.DCPP.01.04 Rev. 1

9. Klimczak (9/27/01): letter from Richard Klimczak to Robert White, entitled "Transmittal of ISFSI Site and Vicinity Plans for the DCPD Used Fuel Storage Project," dated 9/27/01.
10. Geosciences Work Plan GEO 2001-03, Development of Engineering Properties for ISFSI and CTF Foundation Design, ISFSI Slope Analyses, and ISFSI Cut and Fill Slope Reinforcement Design for The DCPD ISFSI Site, rev. 1.

ATTACHMENTS

1. Klimczak (9/27/01): letter from Richard Klimczak to Robert White, entitled "Transmittal of ISFSI Site and Vicinity Plans for the DCPD Used Fuel Storage Project," dated 9/27/01, and Drawing PGE-009-SK-001, pages 10 and 11.
2. Bowles, J. E., 1988, Foundation Analysis and Design, 4th edition, McGraw-Hill, cover and page 551, pages 12 and 13.
3. Peck, R. B., Hanson, W. E., and Thornburn, T. H., 1974, Foundation Engineering, 2nd edition, John Wiley and Sons, cover and 419 and 426, pages 14 to 16.
4. Witter (11/5/01): letter from Rob Witter to Rob White, entitled "Completion of Data Reports," dated 11/5/01 (without attachments), pages 17 and 18.

GEO.DCPP.01.04 Rev.1

Memorandum

Date: September 27, 2001 File #: 72.10.05
To: Robert K. White Phone: (415) 973-0544
PG&E Geosciences Dept
From: Richard L. Klimczak, Project Engineer
Subject: Diablo Canyon Units 1 and 2
Transmittal of ISFSI Site and Vicinity Plans for the DCPD Used Fuel
Storage Project



**Pacific Gas and
Electric Company**

Dear Rob,

Attached are copies of three site plan drawings and a sketch of the cask transfer facility.

PG&E Drawing 471124 is a plant site plot plan. Fig. 2.1-2 is a site plan showing the ISFSI and Transport Route. UFSP-SK-004 is a sketch of the Cask Transfer Facility.

* PGE-009-SK-001 is the ISFSI site plot plan showing the cask storage pads, Cask Transfer Facility and the near vicinity of the ISFSI site. The drawing was prepared by Enercon Services Inc. Per Holtec calculation HI-2012618, Rev. 3, the weight of each loaded cask is 360,000 pounds.

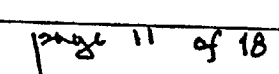
This transmittal is per requirements of DCPD Procedure CF3.ID17.

If you have comments or questions please contact me at (805) 595-6320 or A. Tafoya at (805) 595-6392.

Richard L. Klimczak
Project Engineer
Diablo Canyon Used Fuel Storage Project

Attachments: Dwg 471124, Fig. 2.1-2, PGE-009-SK-001, UFSP-SK-004

cc: LJStrickland	SLO B3	w/o	WPage	245 Market N4C 418B	w/o
BHPatton	SLO BB	w/o	DCPD RMS	DCPD 119/1	
NJahangir	DCPD 201/112	w/o	DCPD Chronological File		
AFTafoya	SLO B10		DCPD File No.72.10.05		



GEO.DC.PP.01.04 Rev.1

FOUNDATION ANALYSIS AND DESIGN

Fourth Edition

Joseph E. Bowles, P.E., S.E.

*Consulting Engineer; Software Consultant
Engineering Computer Software
Peoria, Illinois*

McGraw-Hill Book Company

New York St. Louis San Francisco Auckland Bogotá Caracas
Colorado Springs Hamburg Lisbon London Madrid Mexico Milan
Montreal New Delhi Oklahoma City Panama Paris San Juan
São Paulo Singapore Sydney Tokyo Toronto

GEO.DC.PP.01.04 Rev.1

MECHANICALLY STABILIZED EARTH AND CONCRETE RETAINING WALLS 551

slope angle β in the Rankine analysis and as some fraction of ϕ in a Coulomb analysis with 0.67ϕ commonly estimated for a concrete wall formed using plywood or metal forms so the backface is fairly smooth.

For the overall wall stability of Fig. 12-11b the angle β' may be taken as β for the Rankine method but if you use the Coulomb analysis take $\beta' = \phi$. This value then is used to obtain the horizontal component of P_a as shown. For the vertical friction component resisting overturning always take

$$P_{av} = P_{ah} \tan \phi$$

since the δ angle shown on the figure is always soil-to-soil.

For sliding stability one may take the friction angle between base and soil $\delta_s = \phi$ angle of the base soil (not backfill). The reason is that regardless of how smooth the base soil is compacted (and hopefully it is!), the wet concrete will adhere to it sufficiently that the effective friction resistance developed will be "soil-to-soil." The cohesion is usually somewhat reduced from contact with the wet concrete and it is usual to use a reduced value for adhesion c_a on the order of

$$c_a = 0.5 \text{ to } 0.7c$$

It is usual to use the Rankine value for K_p if passive pressure is included. If there is uncertainty that the full depth D is effective in resisting via passive pressure it is permissible to use a reduced value of D' as

$$D' = D - \text{uncertain depth}$$

The uncertain depth may be to the top of the base or perhaps the top 0.3 m depending on designer assessment of how much soil will remain in place over the toe of the wall. Note that some of this soil is backfill and must be carefully compacted when being replaced or full passive pressure resistance may not develop until the wall has slipped so far forward it has "failed."

Base Key

Where sufficient sliding stability is not possible—usually for walls with large H —a base key as illustrated in Fig. 12-13 has been used. There are different opinions on best location and value of a base key. It was common practice, until it was noted that the conditions of Fig. 12-13b were likely, to put the key beneath the stem as in Fig. 12-13a. This was convenient from the view of simply extending the stem reinforcement through the base and into the key. Later it appeared that the key was more effective located as in Fig. 12-13c and if one must use a key this is the author's recommended location.

Considering the labor involved with a key, a reinforced earth wall would probably be used if the wall were high enough to require a key. For the low cantilever wall in current practice a key should not be required since it would be

GEO:DCPP.01.04 Rev.1

Foundation Engineering

SECOND EDITION

RALPH B. PECK

Professor of Foundation Engineering
University of Illinois at Urbana-Champaign

WALTER E. HANSON

Consulting Engineer and Senior Partner
Hanson Engineers Incorporated, Springfield, Illinois

THOMAS H. THORNBURN

Professor of Civil Engineering
University of Illinois at Urbana-Champaign

JOHN WILEY & SONS

New York • Chichester • Brisbane • Toronto • Singapore

page 14 of 18

GEO.DC.PP.01.04 Rev. 1

426

26/Retaining Walls and Abutments

against the base can be determined by eq. 24.4.

Two useful criteria for proportioning soil-supported walls may be established from the preceding discussion: (1) the eccentricity of the resultant force, measured from the center line of the base, should not exceed one sixth the width of the base, and (2) the maximum pressure should not exceed the allowable soil pressure. One or the other of these two criteria commonly controls the width of the base.

On the other hand, retaining walls may be supported by rock, in which case the first criterion given above is commonly changed to permit larger eccentricities. However, in order to provide adequate safety against overturning, most designers prefer to limit the eccentricity to one fourth the width of the base. That is, the resultant force must intersect the plane of the bottom of the base within the middle half, even though the pressure at the toe may be considerably less than the allowable pressure for the rock. When the resultant lies outside the middle third, the maximum pressure at the toe must be computed by eqs. 24.5 and 24.6, because compression does not exist over the entire area of the base.

26.6. Forces Resisting Sliding

According to Fig. 26.1a, the horizontal component of the unfactored earth pressure P_A must be resisted by the shear between the soil and the base and by the passive earth pressure of the soil in contact with the front of the structure. The ratio between the resisting forces and the horizontal component of P_A is known as the *factor of safety against sliding*. This ratio should be not less than 1.5. Moreover, the passive earth pressure should be disregarded in computing the factor of safety unless local conditions permit reliable evaluation of its lower limiting value and unless the existence of the pressure is assured during the placing of the fill behind the wall.

The shearing resistance between the base and the soil is greatly influenced by the character of the soil. If the surface of contact between the concrete and soil is rough,

the maximum shearing strength of the soil can be counted on. Procedures for determining the shearing strength of soils of different types have been discussed in Chap. 4.

However, in the absence of tests, the total shearing resistance between the base and a soil that derives most of its strength from internal friction may be taken as the normal force ΣV times a coefficient of friction selected from the following values. For coarse-grained soil without silt, the coefficient of friction may be taken as 0.55; for coarse-grained soil with silt, 0.45; and for silt, 0.35. If the base of the retaining wall rests on clay, the shearing resistance against sliding should be based on the cohesion of the clay, which can be conservatively estimated as one half the unconfined compressive strength. If the clay is stiff or hard, its surface should be roughened before the concrete base is placed.

If the factor of safety against sliding is less than 1.5, the design should be revised. The resistance to sliding may be increased by the use of a key that projects into the soil below the base, as shown in Fig. 26.10, or the base may be widened to increase the surface of sliding. For the same volume of concrete, a key is ordinarily considered to be somewhat more effective than an increase in base width, but, on the other hand, the width of the base can usually be extended at less cost.

The effectiveness of short keys is often overestimated. Consideration of the equilibrium of the block of soil $bade$ (Fig. 26.10) leads to the conclusion that the total horizontal force acting on the key can be no larger than the sum of the force P_K and the shearing force S developed on the surface

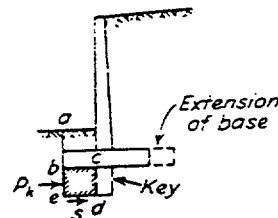


FIGURE 26.10. Horizontal forces resisting movement of key beneath retaining wall.

GEO.DC.PP.01.04 Rev. 1

Earth Pressure

419

Its value can be determined, from the geometry of Fig. 26.2b, as

$$p_A = k_A p_v = \frac{1 - \sin \phi}{1 + \sin \phi} p_v \quad 26.3$$

The coefficient

$$k_A = \frac{1 - \sin \phi}{1 + \sin \phi} \quad 26.4a$$

is known as the *coefficient of active earth pressure*. It may also be expressed, by trigonometric transformation, as

$$k_A = \tan^2 (45^\circ - \phi/2) = \frac{1}{\tan^2 (45^\circ + \phi/2)} \quad 26.4b$$

For a given sand at a given relative density, a definite strain $\Delta L_A/L$ is required to produce the active state (Terzaghi, 1934). For a dense sand it is on the order of 0.1 per cent; for a loose sand it is several times greater.

If the semiinfinite deposit of sand is compressed instead of being stretched, so that planes ab and $a'b'$ (Fig. 26.2d) are moved closer together, the horizontal pressure p_A increases while p_v remains constant. Consequently, the circle of stress becomes smaller (circle 4) and, when $p_A = p_v$, reduces to a point. As horizontal compression continues, the horizontal pressure exceeds the vertical pressure and becomes the major principal stress (circle 5). Eventually, the circle of stress touches the rupture lines and becomes the *rupture circle*, circle 6 in Fig. 26.2b. Failure then occurs within the deposit along two sets of planes corresponding to the points of tangency W and W' . According to the geometry of the rupture diagram, these planes are inclined at $45^\circ + \phi/2$ to the plane on which the major principal stress acts. Since the major principal stress now is the horizontal stress, the failure planes (Fig. 26.2d) are inclined at $45^\circ - \phi/2$ to the horizontal. Further compression of the deposit can cause only further slip along the failure planes because no circles of stress larger than circle 6 can exist if the minor principal stress is p_v . Hence, no larger horizontal pressure can occur at A

than that corresponding to the righthand extremity of the rupture circle 6. This maximum lateral pressure is known as the *passive earth pressure* p_P . Its value can be determined from the geometry of Fig. 26.2b, as

$$p_P = k_P p_v = \frac{1 + \sin \phi}{1 - \sin \phi} p_v \quad 26.5$$

The coefficient k_P is known as the *coefficient of passive earth pressure*. It may also be expressed as

$$k_P = \tan^2 (45^\circ + \phi/2) = 1/k_A \quad 26.6$$

For a given sand at a given relative density, a definite strain $\Delta L_P/L$ is required to produce the passive state. The magnitude of the necessary strain is several times larger than the tensile strain required to produce the active state.

According to eqs. 26.3 and 26.5, both the active and passive earth pressure increase in direct proportion to the depth below the surface. The total pressure on a unit width of a vertical plane extending from the surface to a depth H is, therefore,

$$P_A = \frac{1}{2} k_A \gamma H^2 \quad 26.7$$

or

$$P_P = \frac{1}{2} k_P \gamma H^2 \quad 26.8$$

The theory discussed in the preceding paragraphs was originally developed by Rankine (1857). Equation 26.7 has frequently been used to calculate the active earth pressure of a sand backfill with horizontal surface against a vertical retaining wall with height H . However, examination of Fig. 26.2c demonstrates that the state of stress associated with Rankine's theory for these conditions requires that there be no shearing stresses on vertical planes. Since the backs of real walls are rough and shearing stresses may develop, the Rankine theory can for most conditions provide only an approximation.

In reality no semiinfinite masses of sand exist. If, however, the active state of stress can be induced in a wedge-shaped zone such as CBD (Fig. 26.2c), the earth pressure against the vertical plane CD with height H is correctly given by eq. 26.7. The

WLA

William Lettis & Associates, Inc.

1777 Botelho Drive, Suite 262, Walnut Creek, California 94596
Voice: (925) 256-6070 FAX: (925) 256-6076

GEO.DCPR.01.04 Rev. 1

Mr. Robert White
Geosciences Department
Pacific Gas & Electric Company
245 Market Street, Rm. 421-N4C
San Francisco, CA 94105

November 5, 2001

Re: Completion of Data Reports (formerly appendices)

Dear Rob:

This letter transmits to Geosciences the following Diablo Canyon ISFSI Data Reports (formerly called appendices) that were prepared under the WLA Work Plan, Additional Geologic Mapping, Exploratory Drilling, and Completion of Kinematic Analyses for the Diablo Canyon Power Plant Independent Spent Fuel Storage Installation Site, Rev. 2 (11/28/00) using data collected under that Work Plan and a second WLA Work Plan, Additional Exploratory Drilling and Geologic Mapping for the ISFSI Site, Rev. 1 (9/21/01).

Diablo Canyon ISFSI Data Report A - Geologic Mapping in the Plant Site and ISFSI Site Areas, Rev. 0, November 5, 2001, November 5, 2001, prepared by J. Bachhuber, 42 p.

Diablo Canyon ISFSI Data Report B - Borings in ISFSI Site Area, Rev. 0, November 5, 2001, prepared by J. Bachhuber, 244 p.

Diablo Canyon ISFSI Data Report C - 1998 Geophysical Investigations at the ISFSI Site Area, (Agabian Associates and GeoVision), Rev. 0, November 5, 2001, prepared by J. Bachhuber, 84 p.

Diablo Canyon ISFSI Data Report D - Trenches in the ISFSI Site Area, Rev. 0, November 5, 2001, prepared by J. Bachhuber, 66 p.

Diablo Canyon ISFSI Data Report E - Borehole Geophysical Data (NORCAL Geophysical Consultants, Inc.), Rev. 0, November 5, 2001, prepared by C. Brankman, 303 p.

Diablo Canyon ISFSI Data Report F - Field Discontinuity Measurements, Rev. 0, November 5, 2001, prepared by J. Bachhuber and C. Brankman, 85 p.

Diablo Canyon ISFSI Data Report G - Soil Laboratory Test Data (Cooper Testing Laboratory), Rev. 0, November 5, 2001, prepared by J. Sun, 63 p.

Diablo Canyon ISFSI Data Report H - Rock Strength Data and GSI Sheets, Rev. 0, November 5, 2001, prepared by J. Bachhuber, 37 p.

GEO.DCPP.01.04 Rev. 1

WLA

Diablo Canyon ISFSI Data Report I - Rock Laboratory Test Data (GeoTest Unlimited), Rev. 0, November 5, 2001, prepared by J. Sun, 203 p.

Diablo Canyon ISFSI Data Report J - Petrographic Analysis and X-Ray Diffraction of Rock Samples (Spectrum Petrographics, Inc.), Rev. 0, November 5, 2001, prepared by J. Bachhuber, 204 p.

Diablo Canyon ISFSI Data Report K - Petrographic and X-Ray Diffraction Analyses of Clay Beds (Schwein/Christensen Laboratories, Inc.), Rev. 0, November 5, 2001, prepared by J. Bachhuber, 36 p.

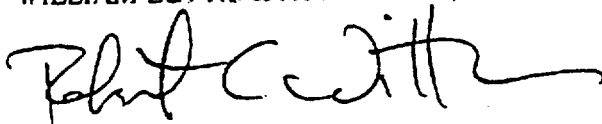
In addition to the revisions of those reports required under the various Work Plans, Mr. Scott Lindvall, the WLA ITR for the ISFSI project, has performed independent technical reviews of the Diablo Canyon ISFSI Data Reports as part of his review of Calculation Package GEO.DCPP.01.21, Analysis of Bedrock Stratigraphy and Geologic Structure at the DCPD ISFSI Site. He finds that the reports clearly and accurately compile and organize the data.

Mr. Albert Tafoya from the Diablo Canyon ISFSI Project Office in San Luis Obispo, Mr. Dale Marcum, NQS Technical Oversight for the project, and William Page of your office provided comments on the August versions of the Diablo Canyon ISFSI Data Reports (formerly called appendices) and their comments have been addressed.

These reports are submitted to you as per the PG&E Geosciences Department Calculation Procedure GEO.001, Rev. 04 (10/10/01).

We look forward to any comments you may have.

Sincerely,
WILLIAM LETTIS & ASSOCIATES, INC.



Robert C. Witter
Project Manager

CC: William Page

PG&E
Geosciences Department
Departmental Calculation Procedure
Attachment 5.2

Number: GEO.001
Revision: 04
Page: 1 of 1

Title: Design Calculation Cover Sheet

PACIFIC GAS AND ELECTRIC COMPANY
GEOSCIENCES DEPARTMENT
CALCULATION DOCUMENT

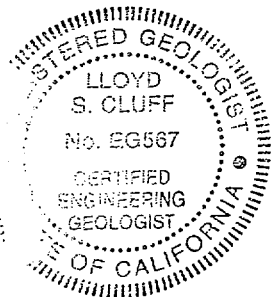
Calc Number GEO.DCPP.01.05
Revision 2
Date 11/6/01
Calc Pages: 18
Verification Method: A
Verification Pages: 1

TITLE: Determination of pseudostatic acceleration coefficient for use in DCPP ISFSI
cutslope stability analyses

PREPARED BY: Robert K White DATE 11/6/01
Robert K White Geosciences
Printed Name Organization

VERIFIED BY: Joseph Sun DATE 11/6/01
Joseph Sun Geosciences
Printed Name Organization

APPROVED BY: Lloyd Cluff DATE 11/7/01
Lloyd Cluff Geosciences
Printed Name Organization



pires 12/31/02

**Determination of pseudostatic acceleration coefficient for use in DCPD ISFSI
cutslope stability analyses
Calc Number GEO.DCPD.01.05**

Record of Revisions

Rev. No.	Reason for Revision	Revision Date
1	added attachments; clarified assumptions; added page reference to methodology step 6	10/15/01
2	revised assumption 2; revised input 1 and methodology step 1 from LTSP figure to SSER figure; changed reference and attachment from LTSP figure to SSER figure	11/6/01

DCPP ISFSI GEOTECHNICAL CALCULATION PACKAGE

Title: Determination of pseudostatic acceleration coefficient for use in DCP
ISFSI cutslope stability analyses
Calc Number: GEO.DCPP.01.05
Revision: Rev. 2
Author: Robert K. White
Date: November 6, 2001
Verifier: Joseph I. Sun

PURPOSE

As required by Geosciences Work Plan GEO 2001-03, Appendix K, derive a pseudostatic horizontal acceleration factor, or "seismic coefficient," as input to pseudostatic limit-equilibrium analyses of DCP ISFSI cutslope stability to be performed by others. This coefficient is derived from the design ground motion as described below.

ASSUMPTIONS

1. The maximum amplification determined along the profile through the powerblock to adjacent hillside overlooking the ISFSI site (PG&E, 1989, Response to Question 17a, page 8, attached) is appropriate for profile through the ISFSI site as well. This assumption is reasonable because the profiles are similar in terms of elevation gain and distance between low to high points.
2. The seismic coefficient determined herein is appropriate for use in near-face (20-foot deep or less) cutslope pseudostatic stability analyses. Overall stability analyses of the native slope above the cutslope involving clay beds will be modeled using dynamic methods.

DESIGN INPUTS

1. Peak acceleration from 84th percentile horizontal response spectrum obtained from U.S. Nuclear Regulatory Commission, 1991 (Figure 2.4, page 6, attached).
2. Topographic amplification factor from PG&E, 1989, Response to NRC Question 17a, Bases for the lack of topographic and directivity effects at the Diablo Canyon site, obtained from PG&E's Response to NRC Staff Questions (page 8, attached).

METHODOLOGY

The approach used to determine the seismic coefficient for limit-equilibrium analyses is based on EERC, 1994 (EERC Report 94/05), specifically pages 119, 120, 158, 173, 174, and 175 of that text (pages 12 to 18, including report cover, attached). Refer to Figure 7.11 (page 15, attached) from that report for a descriptive location of terms described below.

1. Determine the free field peak acceleration away from the toe of the cutslope (a_{ff}) by response analysis. In this case, the source is the DCPD LTSP response spectrum from U.S. Nuclear Regulatory Commission, 1991 (Figure 2.4, page 6, attached).
2. The peak acceleration in the free field on the hillside above the cutslope (a_{ffc}) is topographically amplified above the free field peak acceleration away from the toe of the cutslope (a_{ff}) by *up to* 10%, according to PG&E, 1989, Response to NRC Question 17a (page 8, attached).
3. The maximum acceleration at the cutslope crest (a_{max}) is amplified by 50 to 70% *above* the free field hillside acceleration (a_{ffc}), based on work by Ashford and Sitar described in EERC, 1994, the EERC report (page 16, attached).
4. The maximum average (also called the "peak average") seismic coefficient at any one time increment along cutslope face (k_{max}) is 30 to 50% of the maximum crest acceleration, based on work by Makdisi and Seed summarized in EERC, 1994, the EERC report (page 13, attached).
5. The average (also called the "equivalent maximum") seismic coefficient for any height along cutslope face (k_{av}) is 65 to 70% of the maximum average seismic coefficient, based on work by Seed and Martin summarized in EERC, 1994, the EERC report (page 14, attached).
6. The average seismic coefficient (k_{av}) derived can then be used for limit equilibrium stability analyses (page 18, attached).

SOFTWARE

No software is used to perform calculations.

ANALYSIS

1. a_{ff} (free field peak acceleration away from toe of cutslope) ≈ 0.83 g (scaled from Figure 2.4, page 6, attached).
2. a_{ffc} (free field peak acceleration away from crest of cutslope) $= 1.1 \cdot 0.83 = 0.91$ g (PG&E, 1989, Response to Question 17a, page 8, attached).
3. a_{max} (maximum acceleration at the cutslope crest) $= 1.7 \cdot 0.91 = 1.55$ g (EERC report, page 16, attached).
4. k_{max} (maximum average seismic coefficient) $= 0.5 \cdot 1.55 = 0.78$ g (EERC report, page 13, attached)
5. k_{av} (average seismic coefficient) $= 0.67 \cdot 0.78 = 0.52$ g, say 0.50 g (EERC report, page 14, attached)

CONCLUSION

The seismic coefficient appropriate for the pseudostatic limit-equilibrium analysis of DCPD ISFSI cutslope stability is determined to be 0.50 g, based on the 84th percentile ground motion developed for the DCPD site.

REFERENCES

1. EERC, 1994, Seismic Response of Steep Natural Slopes, by Scott Ashford and Nicholas Sitar, Report No. UCB/EERC-94/05, May.
2. U.S. Nuclear Regulatory Commission (1991). Safety Evaluation Report related to the operation of Diablo Canyon Nuclear Power Plant, Units 1 and 2, Docket Nos. 50-375 and 50-323, NUREG-0675, Supplement No. 34, June.
3. PG&E, 1989, Response to NRC Staff Questions on the Long Term Seismic Program Final Report, PG&E, February.

4. Geosciences Work Plan GEO 2001-03, Development of Engineering Properties for ISFSI and CTF Foundation Design, ISFSI Slope Analyses, and ISFSI Cut and Fill Slope Reinforcement Design for The DCPD ISFSI Site, rev. 1.

ATTACHMENTS

1. U.S. Nuclear Regulatory Commission (1991). Safety Evaluation Report No. 34, cover page and Figure 2.4, attached as pages 5 and 6.
2. PG&E, 1989, Response to NRC Question 17a, from Response to NRC Staff Questions on the Long Term Seismic Program Final Report, PG&E, February, attached as pages 7 to 11.
3. EERC, 1994, Seismic Response of Steep Natural Slopes, by Scott Ashford and Nicholas Sitar, Report No. UCB/EERC-94/05, May 1994, cover sheet, pages 119, 120, 158, 173, 174, and 175, attached as pages 12 to 18.

Safety Evaluation Report

related to the operation of
Diablo Canyon Nuclear Power Plant,
Units 1 and 2

Docket Nos. 50-275 and 50-323

Pacific Gas and Electric Company

11/85

U.S. Nuclear Regulatory Commission

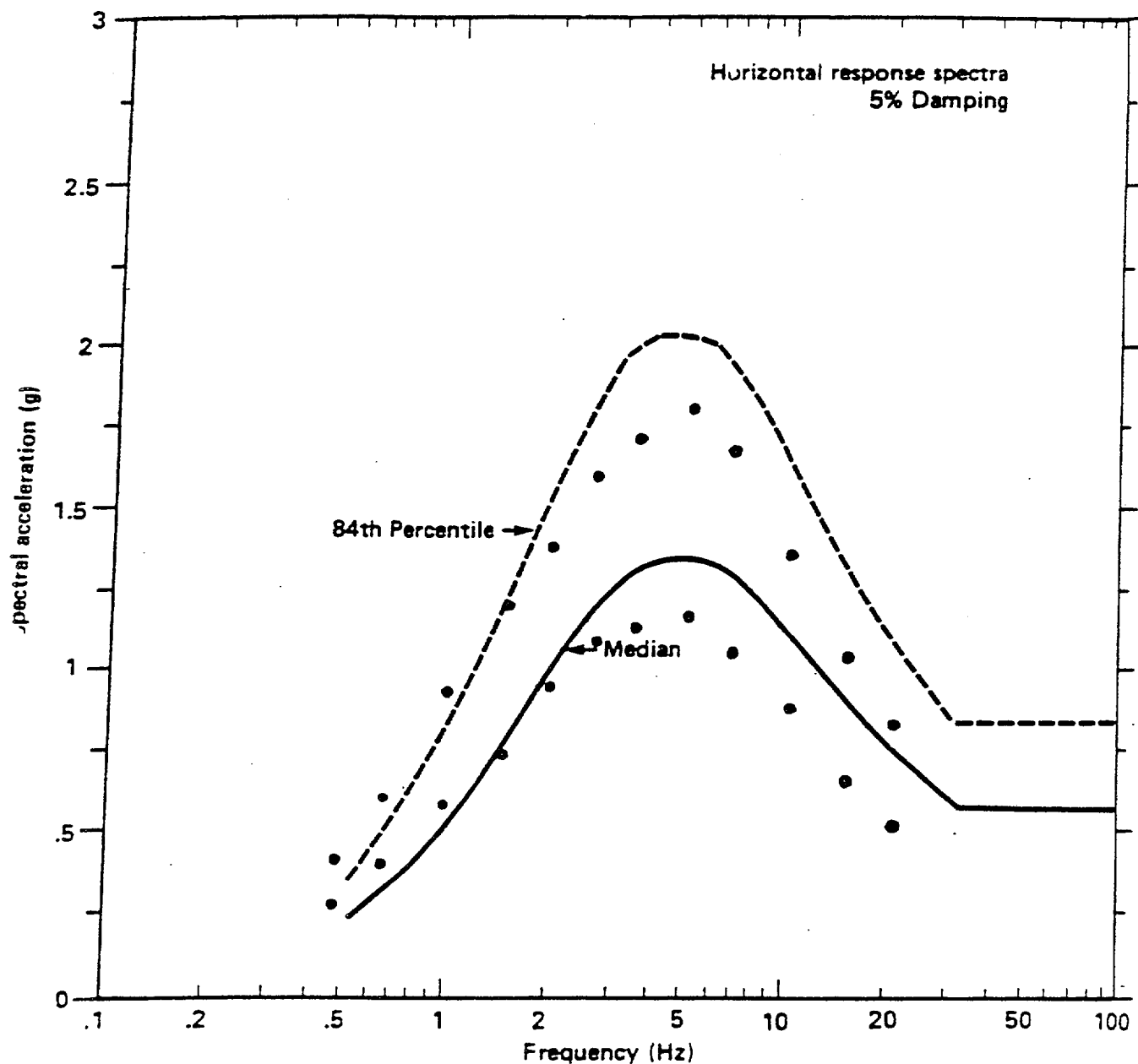
Office of Nuclear Reactor Regulation

June 1991



DIABLO
TSP
91

NUREG
675-34
V. 1



LTSP (lines) and staff's estimate based on Campbell (1990 and 1991b) (dots) median and 84th percentile horizontal acceleration response spectra for a magnitude 7.2 earthquake at 4.5 km.

Figure 2.4
Horizontal acceleration response spectra

Pacific Gas and Electric Company

778-1-1111
1111-1111
1111-1111
1111-1111

James C. Smith
Vice President
Pacific Gas and Electric Company

February 3, 1989

PG&E Letter No. DCL-89-029

RECEIVED
NRA

FEB 21 1989



U.S. Nuclear Regulatory Commission
ATTN: Document Control Desk
Washington, D.C. 20555

Re: Docket No. 50-275, OL-DPR-80
Docket No. 50-323, OL-DPR-82
Diablo Canyon Units 1 and 2
Response to NRC Staff Questions on the
Long Term Seismic Program Final Report

Gentlemen:

With reference to PG&E letter DCL-89-022 dated January 30, 1989,
enclosed are responses to NRC Staff questions 4-15, 17, 18, and 20 on
the Long Term Seismic Program Final Report.

Kindly acknowledge receipt of this material on the enclosed copy of this
letter and return it in the enclosed addressed envelope.

Sincerely,

J. D. Shiffer

J. D. Shiffer

cc w/enc.: J. B. Martin
H. Rood

cc w/o enc.: M. M. Mendonca

M. P. Narbut

B. P. Norton

B. B. H. Vogler

B. CPUC

Diablo Distribution

Diablo Distribution

RECEIVED

25185/0067K/DHO/1587

APR 21 '89

Receipt of the above material
is hereby acknowledged.

U.S. Nuclear Regulatory Commission

By

Date:

Rec'd 2/6/89
DCL

GEOSCIENCES
DEPARTMENT

LTSP

<u>LSC</u>	WUS	MKM	BDS
FWB	YBT	RLV	BES
JCG	PCW	YW	WHW
SJM	RKW	JAY	—

OFFICE FILES 1.3.1

LOG # LTSP 89-262

page 7 of 18

QUESTION 17a

What are the bases for:

- a. the lack of topographic and directivity effects at the Diablo Canyon site?*

* The topography in the Diablo Canyon region is shown in Figure Q17a-1. The effect of topography on ground motions at the site is estimated to be small, based on finite difference calculations summarized in Figure Q17a-2. The profile shown at the top of this figure is oriented along the crest of a ridge that lies east-southeast from the site to obtain an estimate of the maximum potential effect. The finite difference model is a two-dimensional half space having a boundary that undulates in one dimension, and thus projects the topography of the ridge into a slope of infinite horizontal extent. The seismograms for a plane SH wave arriving at an angle of incidence of 20 degrees to the left of vertical, approximating a source on the Hosgri fault zone, are shown below the topographic model. There is a tendency for stations near local ridge crests, such as stations 3, 10, and 12, to show amplification of 10 percent or less, whereas stations located at the foot of slopes, such as stations 2 and 9, show a minor amount of deamplification. The site itself, which is located between stations 5 and 7, is not significantly influenced by topography. We conclude that topographic amplification is not expected at the site, and that some modification or downweighting of strong motion recordings that are amplified by topographic effects is warranted when they are used to estimate site strong motions.

The effect of rupture directivity was tested by performing simulations for a unilateral strike-slip earthquake identical to those used for the estimation of the site-specific response spectrum, except that the spatially varying slip distribution was made uniform to isolate directivity effects from effects due to the variations in slip. The variation of peak acceleration with distance along the fault is shown in Figure Q17a-3. There is no trend for the peak acceleration to increase with distance away from the epicenter. The peak acceleration is large in the vicinity of the epicenter, due to the rapidly expanding rupture front in that region. We conclude that directivity effects at the Diablo Canyon site are not significant for peak accelerations.

page 8 of 18

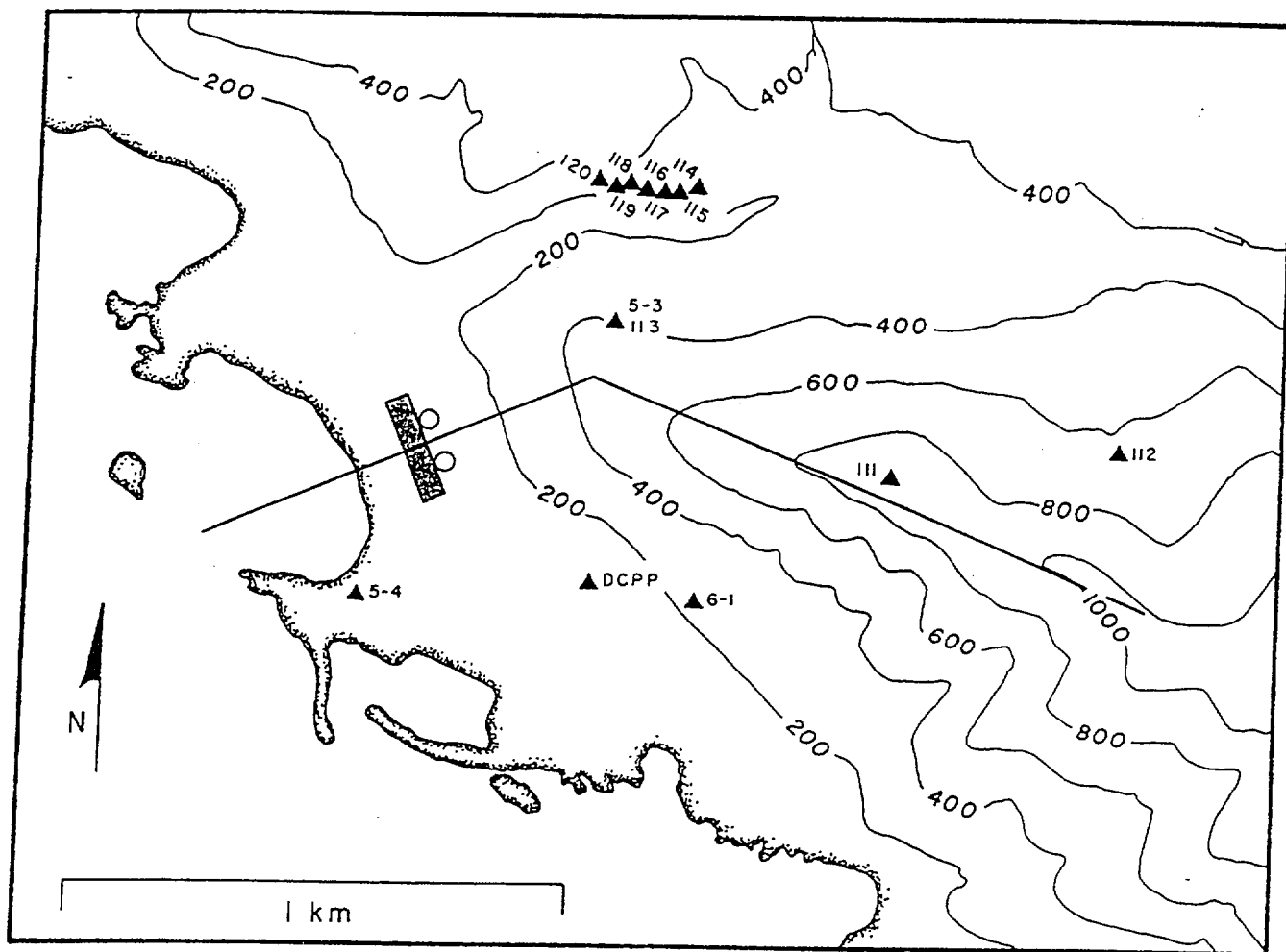


Figure 17a-1

Topography in the Diablo Canyon region shown elevation contours in feet above sea level.

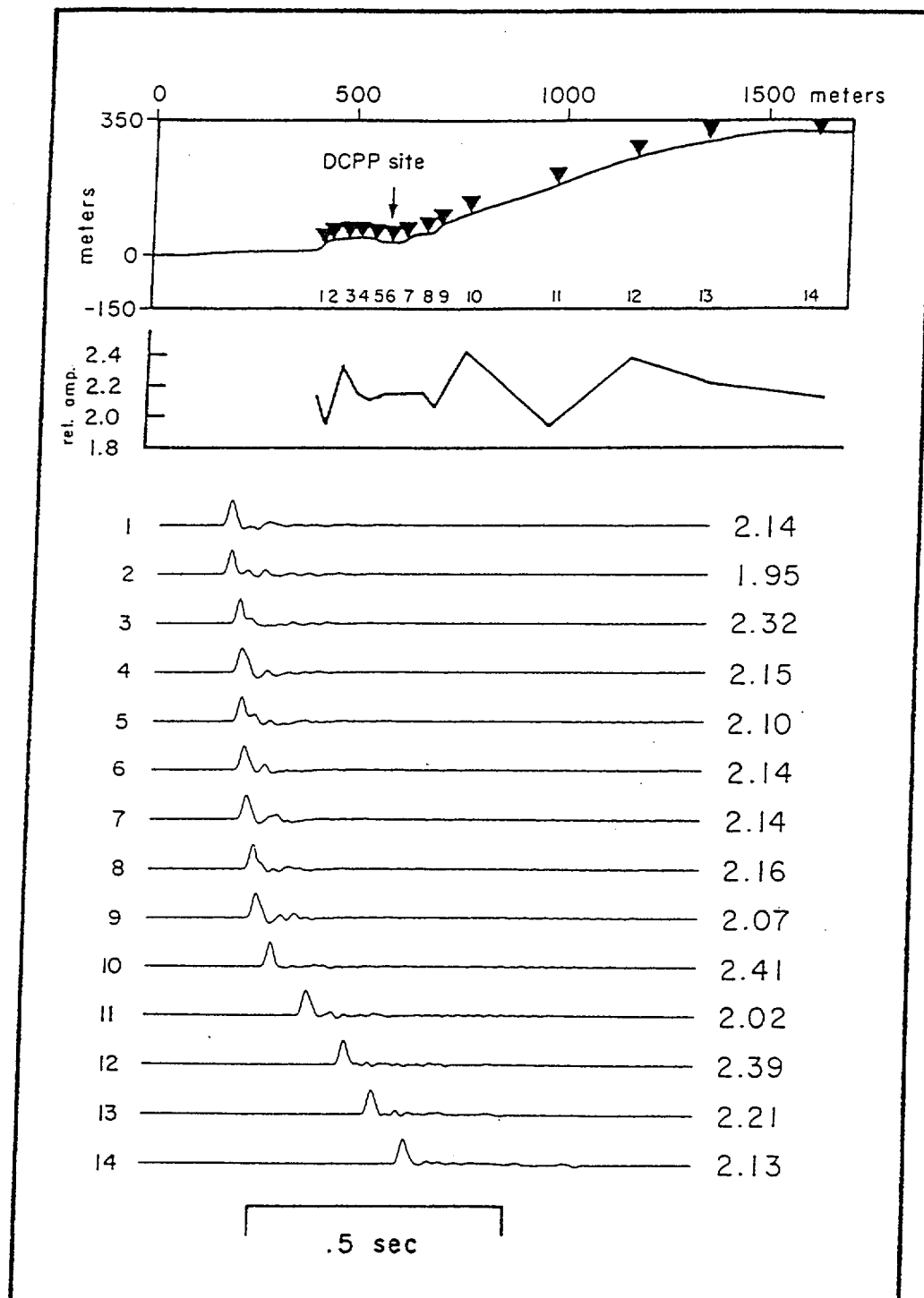


Figure Q17a-2

Finite difference modeling of topographic effects at the site. The topography along the profile shown in Figure Q17a-1 is shown together with station locations in the upper panel. The middle panel shows peak velocity across the profile derived from the seismograms in the lower panel.

page 10 of 18

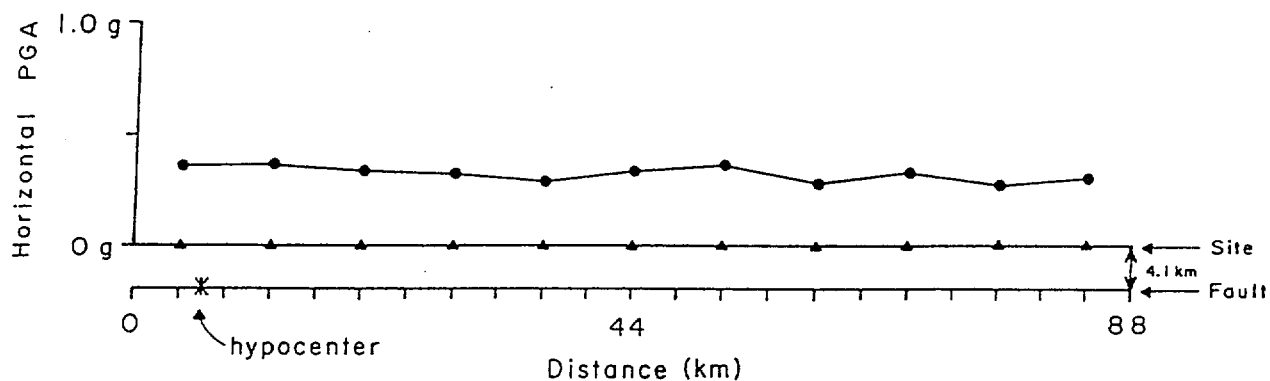


Figure Q17a-3

Illustration of the directivity effect for a unilateral strike-slip rupture on the Hosgri fault. The rupture segment and the line of stations parallel to the fault zone are shown in map view in the lower panel. The variation of peak ground acceleration along the line of stations is shown in the upper panel.

page 11 of 18

480.1
A73
1994
c.4

DISPLAY COPY

PLEASE DO NOT REMOVE

National Information Service
for Earthquake Engineering

REPORT NO.
UCB/EERC-94/05
MAY 1994

EARTHQUAKE ENGINEERING RESEARCH CENTER

*Return by
10/18*

**SEISMIC RESPONSE OF
STEEP NATURAL SLOPES**

by

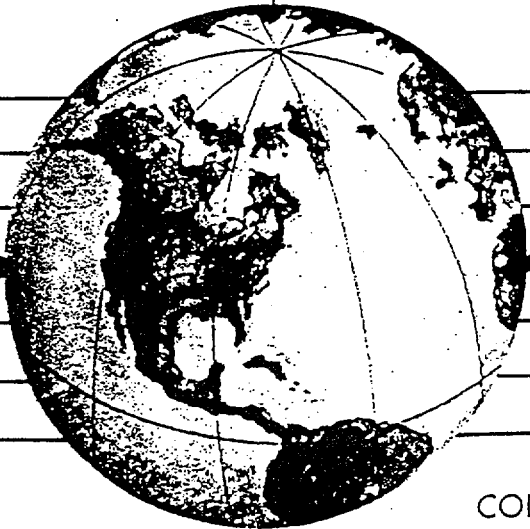
UNIVERSITY OF CALIFORNIA
Earthquake Engineering
Research Center

SCOTT A. ASHFORD
NICHOLAS SITAR

JUN 27 1994

LIBRARY

Final report on research sponsored by
the United States Geological Survey
under USGS Award Number 14-08-0001-G2127



COLLEGE OF ENGINEERING

UNIVERSITY OF CALIFORNIA AT BERKELEY

page 12 of 18

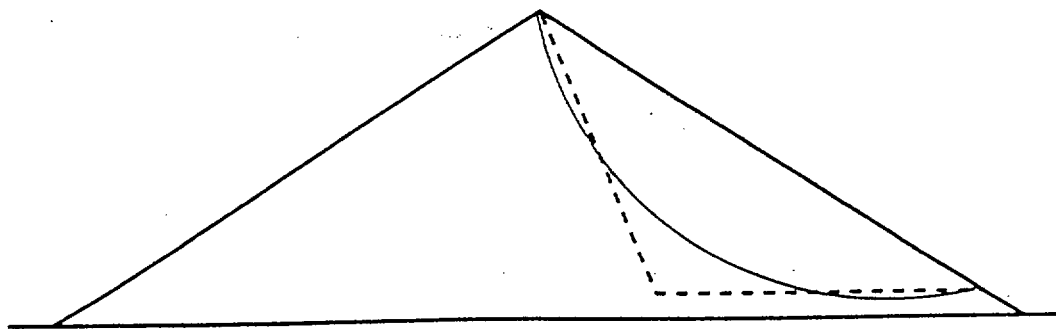


Figure 6.3: Assumed shape of potential sliding mass in Seed and Martin (1966).

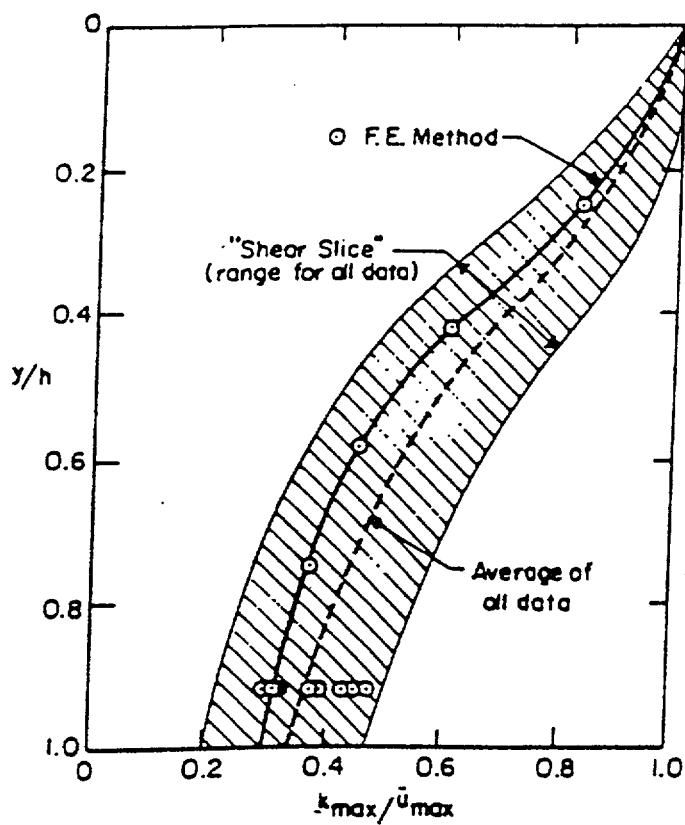


Figure 6.4: Relationship between k_{max}/\ddot{u}_{max} and depth of sliding mass (from Makdisi and Seed, 1978).

as shown in Equation 6.9. Also, by geometrical similarity, and by the assumptions in the shear slice method, the average seismic coefficient can be shown to be independent of the base width of the wedge and the inclination of the failure surface. As a result, this method is even more attractive due to its simplicity.

However, since the intent was to quantify the force that could be used in deformation analyses, simply selecting the maximum average seismic coefficient was already deemed over-conservative due to the short duration of the peak load. Therefore Seed and Martin (1966) proposed the concept of an "equivalent seismic force series". This involves judgement in selecting the average amplitude of significant force cycles, as well as period and duration, from the time history of the average seismic coefficient for a given depth of the dam. From the data presented in their study, the "equivalent maximum seismic coefficient" from the equivalent seismic force series was on the average 65 to 70 percent (range 50 to 85 percent) of the peak average seismic coefficient for any height in the dam.

Seed and Martin (1966) concluded that the height and composition of the dam played a significant role in calculating the seismic coefficient, and that the response is primarily due to the fundamental period of the dam. Though they believed that their procedure was a reasonable approach for the calculation of the dynamic force generated in a dam by an earthquake, they also stressed the limitations. The analyses assumed uniform shear along any horizontal slice through the dam, and preliminary analyses indicated that this assumption could be 25 to 30 percent conservative for failure surfaces extending only half way to the dam centerline. Also, the procedure

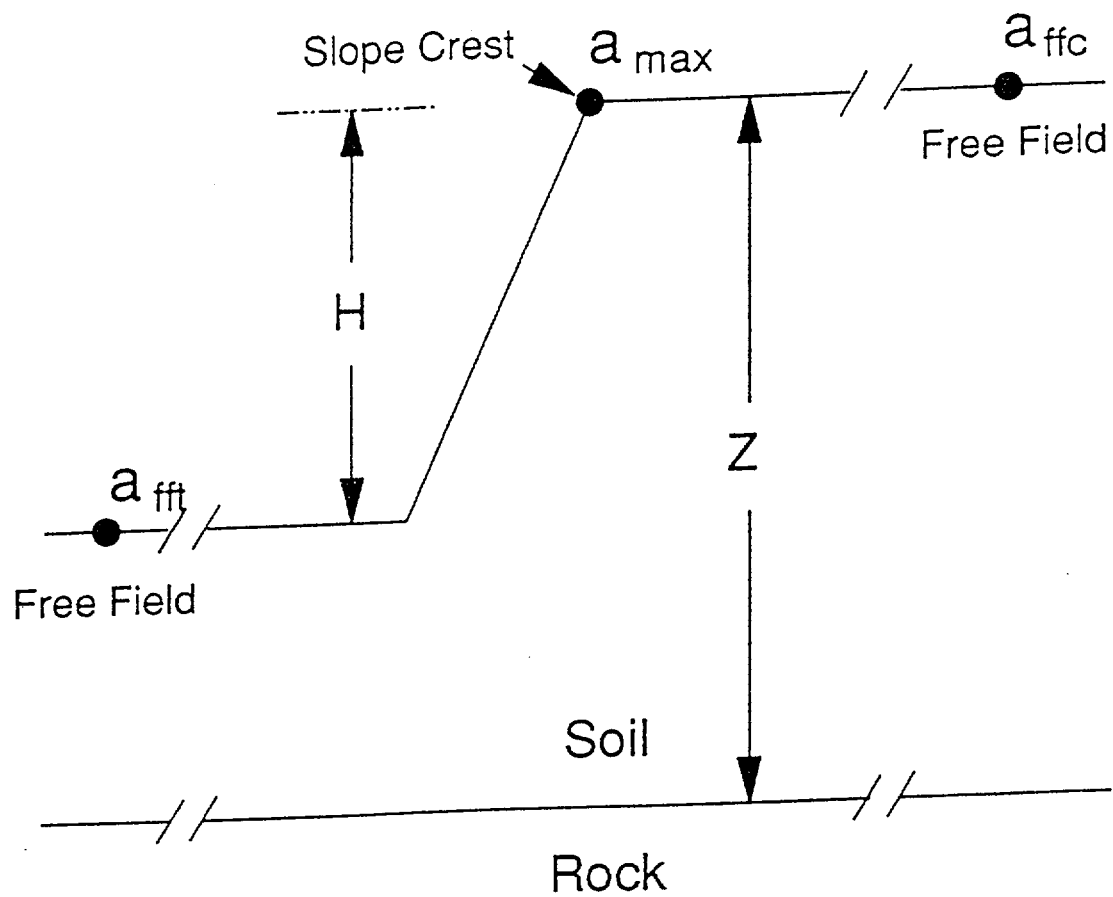


Figure 7.11: Acceleration locations calculated in study.

(Sitar and Clough, 1983). Their data show a 70 percent amplification at the crest when the predominant frequency of the earthquake is near the topographic frequency ($\omega_{eq} \approx 4.5$ Hz, $\omega_t \approx 4$ Hz, and $\omega_s \approx 2.5$ Hz), and a 40 percent amplification at the crest when the predominant frequency of the earthquake is closer to the natural frequency of the site ($\omega_{eq} \approx 4.5$ Hz, $\omega_t \approx 2.6$ Hz, and $\omega_s \approx 3.2$ Hz). Therefore, a reasonable estimate of the acceleration at the crest of the slope could be made by increasing the estimated free field motion behind the crest by about 50 percent, although in some cases, this simple adjustment could be somewhat unconservative. A conservative approach would be to select an input motion for the free field analysis that has a predominant frequency near the natural frequency of the profile behind the crest ($\omega_{eq} = \omega_s$). In such a case, increasing the computed free field motion by 50 percent would be amply conservative. *

The k_{max}/a_{max} profiles presented herein are of the same general shape, but cover a broader range, than the profiles developed by Makdisi and Seed (1978). Moreover, the k_{max}/a_{max} profiles vary with the frequency content of the earthquake and the slope angle. The ratio of k_{max}/a_{max} increases with slope angle, with the steepest slopes forming an upper bound. Thus, when selecting a value of k_{max}/a_{max} for a particular slope, it would seem appropriate to use the upper bound values for steep slopes (greater than 60 degrees); and average values for moderately steep slopes (less than 60 degrees).

The results of the analyses of inclined incident waves show that, even though the topographic amplification is greater for inclined waves, the magnitude of the acceleration at the crest (both horizontal and vertical) is greatest for the case of

vertically propagating waves. The ratio between the peak vertical and horizontal response in the time domain ranges from 0.3 to 0.5, and was observed to vary with incident angle and input motion.

7.6 IMPLICATIONS FOR STABILITY ANALYSES OF STEEP SLOPES

Though the study presented herein was carried out specifically for steep slopes in weakly cemented sands, the procedures used in the seismic response portion of the study are equally applicable to steep slopes in other materials. Therefore, based on the relationships between the peak acceleration at the crest and the maximum seismic coefficient, a procedure for incorporating the results of this study into the stability analysis of steep slopes can be suggested, as follows:

(1) The initial step should be a one-dimensional seismic site response analysis in the free field behind the crest of the slope (e.g. using SHAKE) using an input motion appropriate for the site under consideration. When considering topographic effects, ample conservatism can be obtained by selecting an input motion with a predominant frequency close to the natural frequency of the site.

e.g. Daly City site $a_{ff+} = 0.28$ $a_{ff-} = 0.48$

(2) To account for the effect of topography, the maximum ground surface acceleration obtained by the 1-D analysis should be increased by 50 percent to estimate the maximum acceleration at the crest of the slope.

e.g. Daly City site $a_{ff-} \times 1.5 = 0.72 \approx 0.75 = a_{max} (crest)$
174

(3) Normalized values of k_{\max} at various depths can be selected from the relationships presented in this study. Upper bound values should be used for steepest slopes, while average values should be used for shallower slopes. The values of k_{\max} should be multiplied by 0.65 (Seed and Martin, 1967) to get the k_{av} value to use for analysis.

e.g. for Daly City site, $\frac{k_{\max}}{a_{\max}} \approx 0.3$ for $h/H \approx 1$

(4) For steepest slopes, k_{av} can be used to estimate average tensile stress on failure plane and perform limit equilibrium analysis. For shallower slopes, k_{av} can be used in typical pseudo-static limit equilibrium analysis. For slopes in weakly cemented sands, static strengths can be used to estimate the dynamic strength of materials, based on results reported by Wang (1986) and Sitar (1990).

$$\text{so } k_{\max} = 0.3 (0.75) = 0.23$$

$$\text{and } k_{av} = 0.65 k_{\max} = 0.15$$

CF3.ID4
ATTACHMENT 7.2

TITLE: CALCULATION COVER SHEET

CALC No. 52.27.100.717, R0

RECORD OF REVISIONS

Rev No.	Status	Reason for Revision	Prepared By:	LBIE Screen	LBIE	Check Method*	LBIE Approval		Checked	Supervisor	Registered Engineer
		Remarks	Initials/ LAN ID/ Date	Yes/ No/ NA	Yes/ No/ NA		PSRC Mtg. No.	PSRC Mtg. Date	Initials/ LAN ID/ Date	Initials/ LAN ID/ Date	Signature/ LAN ID/ Date
0	F	Acceptance of Geosciences Calc. No. GEO.DCPP.01.07, Rev1. Calc. is in support of 10CFR72 DCP License Application (ISFSI Dry Cask) to the NRC prior to implementation. Note: Prepared per CF3.ID17 requirements	<i>NXJ</i> NXJ1/ 11/7/01	<input type="checkbox"/> Yes <input type="checkbox"/> No <input checked="" type="checkbox"/> NA	<input type="checkbox"/> Yes <input type="checkbox"/> No <input checked="" type="checkbox"/> NA	<input type="checkbox"/> A <input type="checkbox"/> B <input checked="" type="checkbox"/> C	N/A	N/A	<i>AFT</i> 11/13/01 AFT2/	<i>LJS</i> LJS2/ 11/13/01	<i>LJS</i> LJS2/ 11/13/01
				<input type="checkbox"/> Yes <input type="checkbox"/> No <input type="checkbox"/> NA	<input type="checkbox"/> Yes <input type="checkbox"/> No <input type="checkbox"/> NA	<input type="checkbox"/> A <input type="checkbox"/> B <input type="checkbox"/> C					
				<input type="checkbox"/> Yes <input type="checkbox"/> No <input type="checkbox"/> NA	<input type="checkbox"/> Yes <input type="checkbox"/> No <input type="checkbox"/> NA	<input type="checkbox"/> A <input type="checkbox"/> B <input type="checkbox"/> C					

*Check Method: A: Detailed Check, B: Alternate Method (note added pages), C: Critical Point Check



SUBJECT Development of Coefficient of Subgrade Reaction for DCPD ISFSI Pad Stability Checks

MADE BY Nxj1 DATE 11/7/01 CHECKED BY KL DATE 11/13/01

Table of Contents:

Section	Type	Title	No. of Pages
1	Index	Cross-Index (For Information Only)	1 - 4
Attachments	"A"	Development of Coefficient of Subgrade Reaction for DCPD ISFSI Pad Stability Checks (GEO Sciences # GEO.DCPD.01.07 Rev. 1)	14



SUBJECT _ Development of Coefficient of Subgrade Reaction for DCPD ISFSI Pad Stability Checks
MADE BY NXJ1 DATE 11/7/01 CHECKED BY KFT2 DATE 11/07/01

1- Cross reference between Geo Sciences calculation Numbers and DCPD (Civil Group's) Calculation Numbers: This section is For Information Only.

Cross-Index

(For Information Only)

Item No.	Geosciences Dept. Calc. No.	Title	DCPD, Civil Calc. No.	Comments
1	GEO.DCPD.01.01	Development of Young's Modulus and Poisson's Ratios for DCPD ISFSI Based on Field Data	52.27.100.711	
2	GEO.DCPD.01.02	Determination of Probabilistically Reduced Peak Bedrock Accelerations for DCPD ISFSI Transporter Analyses	52.27.100.712	
3	GEO.DCPD.01.03	Development of Allowable Bearing Capacity for DCPD ISFSI Pad and CTF Stability Analyses	52.27.100.713	
4	GEO.DCPD.01.04	Methodology for Determining Sliding Resistance Along Base of DCPD ISFSI Pads	52.27.100.714	
5	GEO.DCPD.01.05	Determination of Pseudostatic Acceleration Coefficient for use in DCPD ISFSI Cutslope Stability Analyses	52.27.100.715	
6	GEO.DCPD.01.06	Development of Lateral Bearing Capacity for DCPD CTF Stability Analyses	52.27.100.716	
7	GEO.DCPD.01.07	Development of Coefficient of Subgrade Reaction for DCPD ISFSI Pad Stability Checks	52.27.100.717	
8	GEO.DCPD.01.08	Determination of Rock Anchor Design Parameters for DCPD ISFSI Cutslope	52.27.100.718	
9	GEO.DCPD.01.09	Determination of Applicability of Rock Elastic Stress-Strain Values to	52.27.100.719	Calculation to be replaced by letter



SUBJECT _ Development of Coefficient of Subgrade Reaction for DCPD ISFSI Pad Stability Checks
MADE BY NXJ1 DATE 11/7/01 CHECKED BY AFT2 DATE 11/07/01

Cross-Index

(For Information Only)

Item No.	Geosciences Dept. Calc. No.	Title	DCPD, Civil Calc. No.	Comments
		Stress-Strain Values to Calculated Strains Under DCPD ISFSI Pad		
10	GEO.DCPD.01.10	Determination of SSER 34 Long Period Spectral Values	52.27.100.720	
11	GEO.DCPD.01.11	Development of ISFSI Spectra	52.27.100.721	
12	GEO.DCPD.01.12	Development of Fling Model for Diablo Canyon ISFSI	52.27.100.722	
13	GEO.DCPD.01.13	Development of Spectrum Compatible Time Histories	52.27.100.723	
14	GEO.DCPD.01.14	Development of Time Histories with Fling	52.27.100.724	
15	GEO.DCPD.01.15	Development of Young's Modulus and Poisson's Ratio Values for DCPD ISFSI Based on Laboratory Data	52.27.100.725	
16	GEO.DCPD.01.16	Development of Strength Envelopes for Non-jointed Rock at DCPD ISFSI Based on Laboratory Data	52.27.100.726	
17	GEO.DCPD.01.17	Determination of Mean and Standard Deviation of Unconfined Compression Strengths for Hard Rock at DCPD ISFSI Based on Laboratory Tests	52.27.100.727	
18	GEO.DCPD.01.18	Determination of Basic Friction Angle Along Rock Discontinuities at DCPD ISFSI Based on Laboratory Tests	52.27.100.728	



SUBJECT: Development of Coefficient of Subgrade Reaction for DCPD ISFSI Pad Stability Checks
MADE BY NXJ1 DATE 11/7/01 CHECKED BY KAF2 DATE 11/07/01

Cross-Index

(For Information Only)

Item No.	Geosciences Dept. Calc. No.	Title	DCPD, Civil Calc. No.	Comments
19	GEO.DCPD.01.19	Development of Strength Envelopes for Jointed Rock Mass at DCPD ISFSI Using Hoek-Brown Equations	52.27.100.729	
20	GEO.DCPD.01.20	Development of Strength Envelopes for Shallow Discontinuities at DCPD ISFSI Using Barton Equations	52.27.100.730	
21	GEO.DCPD.01.21	Analysis of Bedrock Stratigraphy and Geologic Structure at the DCPD ISFSI Site	52.27.100.731	
22	GEO.DCPD.01.22	Kinematic Stability Analysis for Cutslopes at DCPD ISFSI Site	52.27.100.732	
23	GEO.DCPD.01.23	Pseudostatic Wedge (SWEDGE) Analyses of DCPD ISFSI Cutslopes	52.27.100.733	
24	GEO.DCPD.01.24	Stability and Yield Acceleration Analysis of Cross-Section I-I'	52.27.100.734	
25	GEO.DCPD.01.25	Determination of Seismic Coefficient Time Histories for Potential Sliding Masses Along Cut Slope Behind ISFSI Pad	52.27.100.735	
26	GEO.DCPD.01.26	Determination of Potential Earthquake-Induced Displacements of Potential Sliding Masses on DCPD ISFSI Slope	52.27.100.736	
27	GEO.DCPD.01.27	Cold Machine Shop Retaining Wall Stability	52.27.100.737	
28	GEO.DCPD.01.28	Roadway Capacity with Transporter	52.27.100.738	



SUBJECT Development of Coefficient of Subgrade Reaction for DCPD ISFSI Pad Stability Checks
MADE BY NXJ1 DATE 11/7/01 CHECKED BY AFT2 DATE 11/07/01

Cross-Index

(For Information Only)

Item No.	Geosciences Dept. Calc. No.	Title	DCPD, Civil Calc. No.	Comments
29	GEO.DCPD.01.29	Determination of Seismic Coefficient Time Histories for Critical Slides on DCPD ISFSI Transport Route	52.27.100.739	
30	GEO.DCPD.01.30	Determination of Potential Earthquake-Induced Displacements of Critical Slides Along DCPD ISFSI Transport Route	52.27.100.740	
31	GEO.DCPD.01.31	Development of Strength Envelopes for Clay Beds	52.27.100.741	
32	GEO.DCPD.01.32	Verification of Computer Program SPCTLR.EXE	52.27.100.742	
33	GEO.DCPD.01.33	UTEXAS3 Computer Program Verification	52.27.100.743	
34	GEO.DCPD.01.34	Verification of Computer Code QUAD4M	52.27.100.744	
35	GEO.DCPD.01.35	Verification of Computer Program DEFORMP	52.27.100.745	
36	GEO.DCPD.01.36	Determination of Design Parameters for ISFSI Fill Slope	52.27.100.746	Calculation to be delayed – retaining wall to be shown on drawing
37	GEO.DCPD.01.37	Development of Freefield Ground Motion Storage Cask Spectra and Time Histories for the Used Fuel Storage Project	52.27.100.747	

PG&E
Geosciences Department
Departmental Calculation Procedure
Attachment 5.2

Number: GEO.001
Revision: 03
Page: 1 of 1

Title: Design Calculation Cover Sheet

PACIFIC GAS AND ELECTRIC COMPANY
GEOSCIENCES DEPARTMENT
CALCULATION DOCUMENT

Calc Number GEO.DCPP.01.07
Revision 1
Date 10/15/01
Calc Pages: 12
Verification Method: A
Verification Pages:

(NOT ATTACHED)
SEE GEOSCIENCES
ORIGINAL FILES
AL. 0
"

TITLE: Development of coefficient of subgrade reaction for DCPD ISFSI pad stability checks

PREPARED BY:

Joseph Sun

DATE 10/15/01

Joseph Sun

Printed Name

Geosciences

Organization

VERIFIED BY:

Robert K White

DATE 12/15/01

Robert K White

Printed Name

Geosciences

Organization

APPROVED BY:

Lloyd S. Cluff

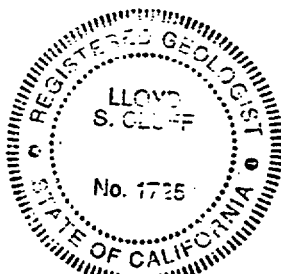
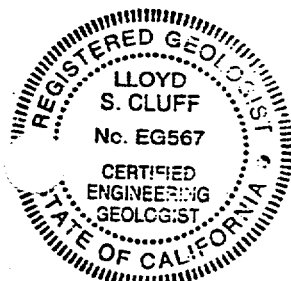
DATE 10/15/01

Lloyd Cluff

Printed Name

Geosciences

Organization



Expires 12/31/02

Expires 12/31/02

Development of coefficient of subgrade reaction for DCPD ISFSI pad stability
checks
Calc Number GEO.DCPD.01.07

Record of Revisions

Rev. No.	Reason for Revision	Revision Date
1	revised assumptions to clarify basis and reasonableness; updated input values from revised GEO.DCPD.01.01	10/15/01

DCPP ISFSI GEOTECHNICAL CALCULATION PACKAGE

Title: Development of coefficient of subgrade reaction for DCPD ISFSI pad stability checks
Calc Number: GEO.DCPP.01.07
Revision: Rev. 1
Date: October 15 2001
Author: Joseph I. Sun
Verifier: Robert K. White

PURPOSE

As required by Geosciences Work Plan GEO 2001-03, Appendix E, this calculation package documents the development of equivalent Winkler spring constants (coefficient of subgrade reaction) for the DCPD ISFSI pad foundation rock. These constants are to be used for an independent check of pad stresses and strains, to be performed by others. The values were developed for both harder rock (hard dolomite and cemented sandstone) and softer rock (friable sandstone) to bracket the likely variation of foundation rock expected under the pad.

ASSUMPTIONS

1. The foundation rock beneath the ISFSI pads varies between dolomite/cemented sandstone and friable sandstone. This is based on the 2001 field investigation results as documented in Calculation Package GEO.DCPP.01.21 Figure 21-41. Rock elastic properties are derived from measured in-situ wave velocities as documented in Calculation Package GEO.DCPP.01.01.
2. Elastic properties will generally vary between that measured for hard dolomite/cemented sandstone and friable sandstone. This is based on the interpretation of in-situ shear wave velocities where the high and low shear wave velocity measurements corresponded to the hard dolomite/cemented sandstone and friable sandstone from the boring logs. Should very localized zones have elastic properties lying below those stated in GEO.DCPP.01.01, they will either encompass too limited a volume to influence the individual pads, or, if extensive, the soft zones will be subexcavated during construction. This is based on about 100-ft spacing

DCPP ISFSI

Calc. Number: GEO.DCPP.01.07, Rev. 1

borings drilled within the pad footprint area that showed no consistent soft zones extending across multiple borings, and based on common construction practice and expecting PG&E to have QA engineers on site during construction.

3. The harder foundation material will not undergo significant non-linear stress-strain behavior under pad design loads. This assumption was subsequently verified by a review of the pad stability analysis results which showed strain levels are sufficiently small such that non-linear behavior is not expected (White, 10/15/01).
4. Simplifications made in the governing equation, below, are appropriate for the level of detail required and appropriate for the uncertainties associated with the inputs (Young's modulus and Poisson's ratio) used in the calculation. This assumption is considered reasonable based on a review of the equation, and was also recommended in the reference (Bowles, 1988) provided below.

INPUTS

1. Values of Young's modulus and Poisson's ratio from PG&E Geosciences Department Calculation Package GEO.DCPP.01.01.
2. Pad width of 68 feet from Klimczak, 9/27/01 (Drawing PGE-009-SK-001, page 8, attached).

METHODOLOGY AND EQUATIONS

1. Based on the equation developed by Vesic (1961) and presented in Bowles (1988), page 7, attached; calculate coefficient of subgrade reaction using elastic properties of the foundation material as follows:

$$k'_s = 0.65 \times [(E_s \times B^4) / (E_f \times I_f)]^{1/12} \times E_s / (1 - \mu^2) \quad (1)$$

in which k'_s = coefficient of subgrade reaction

E_s = Young's modulus of foundation soil/rock

E_f = Young's modulus of footing

B = width of footing

I_f = moment of inertia of footing

μ = Poisson's ratio of foundation soil/rock

DCPP ISFSI

Calc. Number: GEO.DCPP.01.07, Rev. 1

And using the procedure as presented in Bowles (1988), page 10, attached:

2. Substitute $k_s = k'_s / B$ into equation (1)
3. Observe that $0.65 \times [(E_s \times B^4) / (E_f \times I_f)]^{1/12}$ approaches 1 for any values because of the 12th root.
4. Simplify equation (1) accordingly as follows:

$$k_s = E_s / B \times [1 / (1 - \mu^2)] \quad (2)$$

SOFTWARE

No software is used to perform calculations.

CALCULATION

1. Based on calc package GEO.DCPP.01.01, the elastic properties for the hard dolomite/cemented sandstone and friable sandstone are as follows:

Foundation Material	Young's Modulus	Poisson's Ratio
Hard dolomite and cemented sandstone	2.1×10^6 psi	0.37
Friable sandstone	0.2×10^6 psi	0.31

2. Use 68 feet as width (B) for ISFSI pad in equation (2).
3. Compute coefficient of subgrade reaction for hard dolomite/cemented sandstone:

$$\begin{aligned}
 k_s &= (2.1 \times 10^6 \text{ lb/in}^2) * (144 \text{ in}^2/\text{ft}^2) / (68 \text{ ft}) \times [1 / (1 - 0.37^2)] \\
 &= 5,152,426 \text{ lb/ft}^3 \\
 &\text{or } 5,152 \text{ kips/ft}^3
 \end{aligned}$$

4. Compute coefficient of subgrade reaction for friable sandstone:

$$\begin{aligned}
 k_s &= (0.2 \times 10^6 \text{ lb/in}^2) * (144 \text{ in}^2/\text{ft}^2) / (68 \text{ ft}) \times [1 / (1 - 0.31^2)] \\
 &= 468,558 \text{ lb/ft}^3 \\
 &\text{or } 469 \text{ kips/ft}^3
 \end{aligned}$$

DCPP ISFSI

Calc. Number: GEO.DCPP.01.07, Rev. 1

RESULTS AND CONCLUSION

For dolomite and cemented sandstone (hard rock), for E_s of 2.1×10^6 psi under very small strain ($10^{-4}\%$), Poisson's Ratio of 0.37, and a foundation width of 68 ft, the computed coefficient of subgrade reaction (k_s) is: 5,152 kips/ft³ (2.98 k/in³). This harder rock is not expected to undergo significant non-linear behavior even during large earthquakes.

For altered sandstone (soft rock), for E_s of 0.2×10^6 psi under very small strain ($10^{-4}\%$), Poisson's Ratio of 0.31, and a foundation width of 68 ft, the computed k_s is: 469 kips/ft³ (0.28 k/in³). This value, according to DM-7, 1986 (page 12, attached), corresponds to dense sands or very stiff clay. This material has the potential to experience non-linear behavior under large earthquakes. If the material is strained to higher levels, the Young's modulus could drop below the value measured at small strain ($10^{-4}\%$), and so would the coefficient of subgrade reaction.

The coefficient of subgrade reaction (k_s) is in units of $F(\text{force})/L(\text{length})^3$ or kips/ft³. To convert this to a nodal spring constant with units of F/L , each node spring k_s must be multiplied by the contributing area of the analytical element to get units in kips/in.

REFERENCES

1. Bowles, Joseph E., 1988, Foundation Analysis and Design, 4th edition.
2. DM-7, 1986, Naval Facilities and Engineering Command, Foundations and Earth Structures, Design Manual 7.02 ("DM-7"), September.
3. Vesic, A.S., 1961, "Beams on Elastic Subgrade and the Winkler Hypothesis", Proceedings, 5th International Conference on Soil Mechanics and Foundation Engineering, Vol. 1, pp. 845-850.
4. Geosciences Work Plan GEO 2001-03, Development of Engineering Properties for ISFSI and CTF Foundation and ISFSI Cut and Fill Slope Reinforcement for The DCPD ISFSI Site, rev. 0.
5. Geosciences calculation package GEO.DCPP.01.01, rev. 1, "Development of Young's Modulus and Poisson's ratio for DCPD ISFSI based on field data."
6. Geosciences calculation package GEO.DCPP.01.21, rev. 0, "Analysis of Bedrock Stratigraphy and Geologic Structure at the DCPD ISFSI Site."

DCPP ISFSI

Calc. Number: GEO.DCPP.01.07, Rev. 1

7. White, (10/15/01): letter report from Robert White to Richard Klimczak, entitled "Determination of applicability of rock elastic stress-strain values to calculated strains under DCPP ISFSI pad," dated 10/15/01.
8. Klimczak (9/27/01): letter from Richard Klimczak to Robert White, entitled "Transmittal of ISFSI Site and Vicinity Plans for the DCPP Used Fuel Storage Project," dated 9/27/01.

ATTACHMENTS

1. Klimczak (9/27/01): letter from Richard Klimczak to Robert White, entitled "Transmittal of ISFSI Site and Vicinity Plans for the DCPP Used Fuel Storage Project," dated 9/27/01, and Drawing PGE-009-SK-001, pages 6, 7, and 8.
2. Bowles, J. E., 1988, Foundation Analysis and Design, 4th edition, McGraw-Hill, cover and page 407, pages 9 and 10.
3. DM-7, 1986, Naval Facilities and Engineering Command, Foundations and Earth Structures, Design Manual 7.02 ("DM-7"), September, cover and page 7.1-129, pages 11 and 12.

GEO. DUTP. 01-07 Rev. 1

Memorandum

Date: September 27, 2001 File #: 72.10.05
To: Robert K. White Phone: (415) 973-0544
PG&E Geosciences Dept
From: Richard L. Klimczak, Project Engineer
Subject: Diablo Canyon Units 1 and 2
Transmittal of ISFSI Site and Vicinity Plans for the DCPD Used Fuel
Storage Project



**Pacific Gas and
Electric Company**

Dear Rob,

Attached are copies of three site plan drawings and a sketch of the cask transfer facility.

PG&E Drawing 471124 is a plant site plot plan. Fig. 2.1-2 is a site plan showing the ISFSI and Transport Route. UFSP-SK-004 is a sketch of the Cask Transfer Facility.

PGE-009-SK-001 is the ISFSI site plot plan showing the cask storage pads, Cask Transfer Facility and the near vicinity of the ISFSI site. The drawing was prepared by Enercon Services Inc. Per Holtec calculation HI-2012618, Rev. 3, the weight of each loaded cask is 360,000 pounds.

This transmittal is per requirements of DCPD Procedure CF3.ID17.

If you have comments or questions please contact me at (805) 595-6320 or A. Tafoya at (805) 595-6392.

Richard L. Klimczak

Richard L. Klimczak
Project Engineer
Diablo Canyon Used Fuel Storage Project

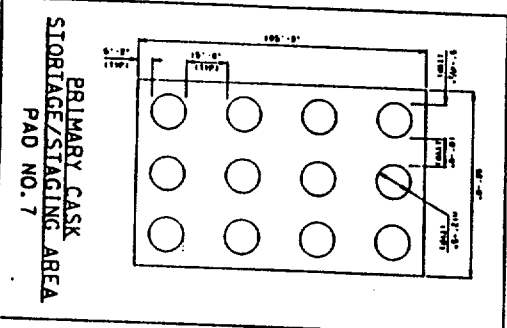
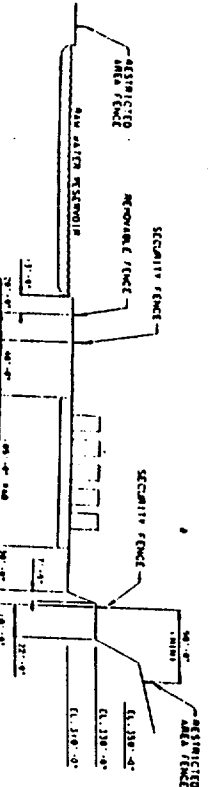
Attachments: Dwg 471124, Fig. 2.1-2, PGE-009-SK-001, UFSP-SK-004

cc: LJStrickland	SLO B3	w/o	WPage	245 Market N4C 418B	w/o
BHPatton	SLO BB	w/o	DCPD RMS	DCPD 119/1	
NJahangir	DCPD 201/112	w/o	DCPD Chronological File		
AFTafoya	SLO B10		DCPD File No.72.10.05		

GEO. DCP. 01.07 Rev. 1

<u>DWG. NO.</u>	<u>REVISION</u>	<u>TITLE</u>
471124	1	Plot Plan
Fig. 2.1-2	D	Plan Drawing of the ISFSI Site
PGE-009-SK-001	0	Site Plot Plan, ISFSI Cask Storage Pad, Cask Transfer Facility
UFSP-SK-004	A	Cask Transfer Facility Structure (Schematic)

SECTION A-A
N.T.S.



PRIMARY CASK
STORAGE/STAGING AREA
PAD NO. 7

- NOTES:
1. EXISTING TOWER ROAD WILL BE RE-ROUTED TO BE RE-ROUTED TO FACILITATE INSTALLATION OF THE RESTRICTED AREA FENCE.

REVISIONS:

1. CORRECTION SECTION NO. 400-54-102, ELECTRICAL, SITE PLAN
2. CORRECTION SECTION NO. 400-54-110, ELECTRICAL, SITE PLAN
3. CORRECTION SECTION NO. 400-54-110, CASE STORAGE FACILITY
4. CORRECTION SECTION NO. 400-54-110, DRAINAGE SYSTEM
5. CORRECTION SECTION NO. 400-54-110, FENCE LAYOUT/STAGING
6. CORRECTION SECTION NO. 400-54-110, FENCE LAYOUT/STAGING
7. CORRECTION SECTION NO. 400-54-110, FENCE LAYOUT/STAGING

THIS DRAWING IS APPROVED AS SHOWN BY THE SIGNATURE OF THE DESIGNER.

DATE: 11/11/01
BY: [Signature]
CHECKED BY: [Signature]

PG&E/DIABLO CANYON

SITE PLAN

ISFSI CASK STORAGE PAD

CASK TRANSFER FACILITY

NO.	DESCRIPTION	DATE	BY	CHECKED
1	11/11/01	11/11/01	11/11/01	11/11/01
2	11/11/01	11/11/01	11/11/01	11/11/01
3	11/11/01	11/11/01	11/11/01	11/11/01
4	11/11/01	11/11/01	11/11/01	11/11/01
5	11/11/01	11/11/01	11/11/01	11/11/01
6	11/11/01	11/11/01	11/11/01	11/11/01
7	11/11/01	11/11/01	11/11/01	11/11/01
8	11/11/01	11/11/01	11/11/01	11/11/01
9	11/11/01	11/11/01	11/11/01	11/11/01
10	11/11/01	11/11/01	11/11/01	11/11/01

GEO. DEPT. 01.07 Rev. 1

FOUNDATION ANALYSIS AND DESIGN

Fourth Edition

Joseph E. Bowles, P.E., S.E.

*Consulting Engineer/Software Consultant
Engineering Computer Software
Peoria, Illinois*

McGraw-Hill Book Company

New York St. Louis San Francisco Auckland Bogotá Caracas
Colorado Springs Hamburg Lisbon London Madrid Mexico Milan
Montreal New Delhi Oklahoma City Panama Paris San Juan
São Paulo Singapore Sydney Tokyo Toronto

page 9 of 12

From Bowles, Foundation
Analysis and Design, 1988

GEO.DCAPP.01.07 Rev. 1

SPECIAL FOOTINGS AND BEAMS ON ELASTIC FOUNDATIONS 407

For footings on clay:

$$k_s = k_1 B \quad (9-3)$$

For footings on sand (including size effects):

$$k_s = k_1 \left(\frac{B+1}{2B} \right)^2 \quad (9-4)$$

For a rectangular footing on sand of dimensions $B \times mB$:

$$k_s = k_1 \frac{m+0.5}{1.5m} \quad (9-5)$$

In these equations k_s = desired value for full-sized footings and k_1 = value from a 1×1 ft square plate load test.

Vesic (1961a, 1961b) proposed that the modulus of subgrade reaction could be computed using the stress-strain modulus E_s as

$$k_s = 0.65 \sqrt{\frac{E_s B^4}{E_f I_f}} \frac{E_s}{1 - \mu^2} \quad (9-6)$$

where E_s, E_f = modulus of soil and footing, respectively, in consistent units

B, I_f = footing width and its moment of inertia based on cross section (not plan) in consistent units

One can obtain k_s from k'_s as

$$k_s = \frac{k'_s}{B}$$

Since the twelfth root of any value $\times 0.65$ will be close to 1, for all practical purposes the Vesic equation reduces to

$$k_s = \frac{E_s}{B(1 - \mu^2)} \quad (9-6a)$$

One may rearrange Eq. (5-16a) and using $E'_s = (1 - \mu^2)/E_s$ as in Eqs. (5-18) and (5-19) obtain

$$p^{2.57} \Delta H = \Delta q B E'_s I_f$$

and since k_s is defined as $\Delta q / \Delta H$ we obtain

$$k_s = \frac{\Delta q}{\Delta H} = \frac{1}{B E'_s I_f} \quad (9-7)$$

but carefully note the definition of E'_s . Now we can correctly incorporate the size effects which are a major concern—particularly for the mat foundations of the next chapter. As for Eqs. (5-18) and (5-19) we can write a k_s ratio from Eq. (9-7) as follows:

$$\frac{k_{s1}}{k_{s2}} = \frac{B_2 E'_{s2} I_{f2}}{B_1 E'_{s1} I_{f1}} \quad (9-8)$$

Naval Facilities Engineering Command

200 Stovall Street
Alexandria, Virginia 22332-2300

UNCLASSIFIED//FOR OFFICIAL USE ONLY



GE0-DC PP.01.01 Rev. 1

Foundations & Earth Structures

DESIGN MANUAL 7.02
REVALIDATED BY CHANGE 1 SEPTEMBER 1981

page 11 of 12

GEO. DEPT. 01.07 Rev. 1

From NAVFAC, Foundation and Earth Structures, 1986

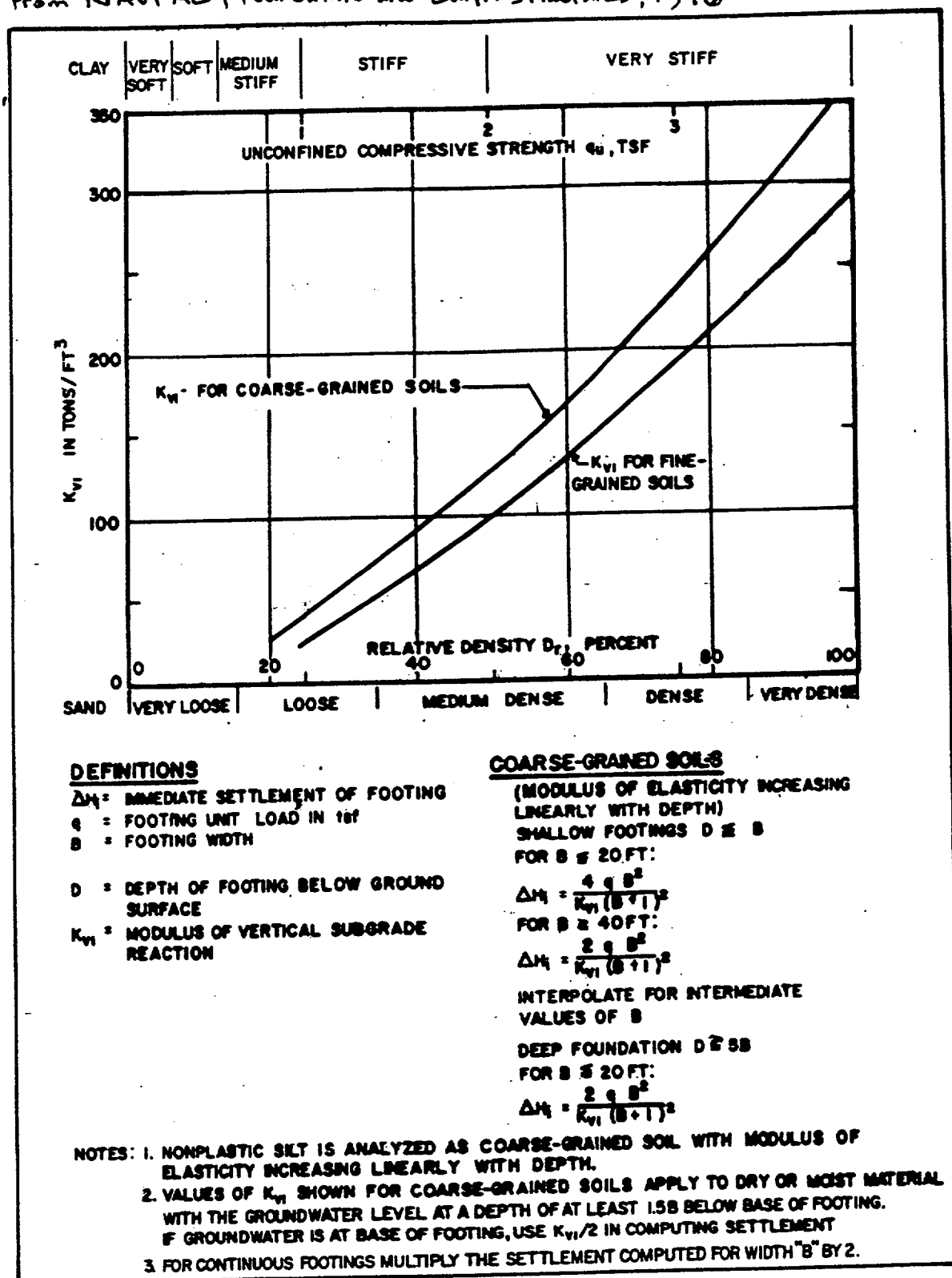


FIGURE 6
 Instantaneous Settlement of Isolated Footings on Coarse-Grained Soils

7.1-219